



TECHNISCHE
UNIVERSITÄT
DARMSTADT



Developing a Protocol for *In Vitro* Characterization of Circulating Cancer Stem Cell-like Cells

**Vom Fachbereich Biologie der Technischen Universität Darmstadt
zur Erlangung des Grades Doctor rerum naturalium (Dr. rer. nat.)
Dissertation von Martina Quartieri
Tag der Einreichung: 15.09.2023, Tag der Prüfung: 30.10.2023
Darmstadt, 2023**

Erstgutachter: Prof. Dr. Marco Durante

Zweitgutachter: Prof. Dr. Gerhard Thiel

Quartieri, Martina: Developing a protocol for *In Vitro* characterization of Circulating Cancer Stem Cell-like cells

Darmstadt, Technische Universität Darmstadt

Jahr der Veröffentlichung der Dissertation auf TUprints: 2023

Tag der mündlichen Prüfung: 30.10.2023

Veröffentlicht unter CC BY-SA 4.0 International

<https://creativecommons.org/licenses/>

GSI Helmholtzzentrum für Schwerionenforschung GmbH
Technische Universität Darmstadt

**Developing a Protocol for *In Vitro*
Characterization of Circulating Cancer Stem
Cell-like Cells**

Vom Fachbereich Biologie der Technischen Universität Darmstadt zur
Erlangung des akademischen Grades eines *Doctor rerum naturalium*
vorgelegte Dissertation von

Martina Quartieri

1. Referent: Prof. Dr. Marco Durante
2. Referent: Prof. Dr. Gerhard Thiel

Tag der Einreichung: 15.09.2023

Tag der mündlichen Prüfung: 30.10.2023

Darmstadt 2023

Zusammenfassung

Krebs ist weltweit die häufigste Todesursache, und trotz der in den letzten Jahrzehnten erzielten Therapieverbesserungen sind Tumorrezidive und Metastasen nach wie vor das größte Problem für den Therapieerfolg. Tumore zeichnen sich durch eine heterogene Zellpopulation aus, die auf die sich rasch entwickelnde dynamische Mikroumgebung des Tumors zurückzuführen ist. Die Blutgefäße, die sich während der Tumorbildung bilden, weisen eine desorganisierte Struktur auf, die zur Entwicklung einer hypoxischen Umgebung im Tumor beiträgt. Eine solche Mikroumgebung führt zur Entwicklung einer Subpopulation von Tumorzellen, die einen mesenchymalen Phänotyp aufweisen und in das Blut und die Lymphgefäße einwandern können. Bei diesen Zellen handelt es sich um die zirkulierenden Krebsstammzellen (CCSCs), die strahlenresistent sind und folglich für die Metastasenbildung verantwortlich sind. CCSCs verfügen über Marker, die für die Migration und Stammzelleneigenschaft (CD133), die Resistenz gegen Anoikis (Trk B), den programmierten Zelltod, und die Immunabwehr (CD47) entscheidend sind. Die Hypoxie trägt dazu bei, die Stammzellenkapazität zu simulieren und die Subpopulation der CD133-positiven Zellen zu selektieren. Darüber hinaus sind diese Zellen strahlenresistent und eine weitere Selektion ist möglich, nachdem sie ionisierender Strahlung ausgesetzt wurden. Idealerweise würde ihre Isolierung, Kultivierung und Charakterisierung *in vitro* die Möglichkeit bieten, das Wissen über die für die Metastasenbildung verantwortlichen Mechanismen zu erweitern. Es ist jedoch technisch äußerst anspruchsvoll, sie im Blutkreislauf zu identifizieren, da sie nur in geringer Zahl im Blutkreislauf vorhanden sind. Zu diesem Zweck haben wir in dieser *In-vitro*-Studie unter Verwendung von Hypoxie (akut und chronisch) und ionisierender Strahlung (4 Gy Röntgenstrahlung) Zellen mit einem CCSC-ähnlichen Phänotyp für die weitere Charakterisierung ausgewählt. Wir haben versucht, diese Zellen *ex vivo* aus dem Blut der Tiere zu isolieren und zu charakterisieren. Dabei untersuchten wir die Expression der CD133- und CD47-Marker zwischen Primärtumor und Metastasen durch histologische Analyse von Proben, die im *In-vivo*-Mausexperiment gewonnen wurden.

Abstract

Cancer is the leading cause of death worldwide and despite the treatment improvements that have been done in the past decades, tumor recurrence and metastasis still remain the main concern for therapy success. Tumors are characterized by a heterogeneous population of cells because of the dynamic tumor microenvironment that evolves rapidly. The blood vessels that generate during tumor formation display a disorganized structure contributing to developing a hypoxic environment in the tumor. Such microenvironment induces the development of a subpopulation of tumor cells that exhibit a mesenchymal phenotype and that can migrate into the blood and the lymphatic vessels. Such cells are the Circulating Cancer Stem Cells (CCSCs), which are radioresistant and subsequently responsible for metastasis formation. CCSCs have markers critical for migration and stemness (CD133), resistance to *anoikis* (Trk B), the programmed cell death that usually occurs after cell intravasation in the blood circulation, and immune evasion (CD47). Hypoxia contributes to simulating cells' stemness capacity and to selecting the subpopulation of positive cells for CD133. Moreover, these cells are radioresistant and a further selection is possible after exposing them to radiation. Ideally isolating, culturing and characterizing them *in vitro* would give the possibility to increase the knowledge about the mechanisms responsible for metastasis formation. However, identifying them in circulation is challenging since they are present only in a few numbers in the bloodstream. For this purpose, in this *in vitro* study, we select using hypoxia (acute and chronic) and radiation (4 Gy X-rays) cells with a CCSC-like phenotype for further characterization. We tried to isolate and characterize *ex vivo* these cells from the animals' blood. We investigated the expression of CD133 and CD47 markers between primary tumor and metastasis, through histological analysis of samples obtained from *in vivo* mice experiment.

Contents

1. Introduction.....	1
1.1 Motivation.....	1
1.2 Osteosarcoma.....	2
1.3 Metastatic cascade.....	4
1.4 Tumor Hypoxia.....	8
1.5 Cancer Stem Cells (CSCs).....	14
1.6 Circulating Tumor Cells (CTCs).....	18
1.7 Radiotherapy.....	22
1.8 Aim of the project.....	24
2. Materials and methods.....	25
2.1 Cell culture.....	25
2.2 U2OS Migration Assay.....	25
2.3 U2OS hanging drop.....	26
2.4 Photon irradiation.....	26
2.5 Clonogenic Survival Assay (CSA).....	26
2.6 LM8 immunocytochemistry (ICC) staining.....	27
2.7 LM8 Sphere formation and migration assay.....	28
2.8 Western blot.....	29
2.9 CD133 cell sorting.....	31
2.10 CD133+ FACS analysis.....	32
2.11 LM8 injection in mice.....	32
2.12 CTC extraction from mice blood with magnetic beads.....	32
2.13 Cryostat sample preparation.....	33
2.14 Immunohistochemistry (IHC) staining.....	33
2.15 Statistical analysis.....	34
3. Results.....	35
3.1 Migration ability and sphere formation capacity: preliminary results using the U2OS cells.....	35
3.2 Clonogenic Survival Assay: a comparison between normoxia and acute hypoxia.....	38
3.3 Hypoxia influences morphology of LM8 cells.....	39
3.4 Investigating the hypoxia inducible factor status of LM8 cells under hypoxia.....	41
3.5 Hypoxia increases CD133 expression.....	42

3.6	Hypoxia increases the subpopulation of cells expressing TrK B.....	43
3.7	Hypoxia and radiation influences sphere formation, size and cluster.....	45
3.8	CD133 influence on radioresistance, sphere and cluster formation.....	47
3.9	Hypoxia influences the migration capacity of LM8 cells.....	50
3.10	CD47 expression in CD133+ LM8 cells	53
3.11	CTC isolation <i>ex vivo</i>	55
3.12	CD133 and CD47 expression in primary tumor and metastasis	56
4.	Discussion	59
4.1	Initial characterization of U2OS cell line.....	59
4.2	Initial characterization of LM8 cell line	61
4.3	Prolonged hypoxia influence on LM8 cells.....	62
4.4	Influence of hypoxia and radiation in sphere formation, size and cluster.....	63
4.5	LM8 migration capacity	64
4.6	Hypoxia-induced expression of CD47	64
4.7	CTC isolation from mice blood.....	65
4.8	IHC analysis of CD133 and CD47 expression in primary tumor and metastasis.....	66
4.9	Conclusions.....	67
4.10	Future perspectives.....	68
	Appendix	70
	Bibliography	76
	Curriculum Vitae	102
	Acknowledgements	103
	Ehrenwörtliche Erklärung	105

List of figures

Figure 1. Normal osteogenesis and osteosarcomagenesis: schematic procedure and genes involved.	3
Figure 2. Scheme of Epithelial-to-Mesenchymal transition	5
Figure 3. Scheme of signals that regulate proliferating and dormant tumor cells.....	7
Figure 4. Invasion-metastasis cascade	8
Figure 5. Hypoxia signaling pathway.....	9
Figure 6. HIF1 α and HIF2 α behaviour at different oxygen concentrations and under different duration of hypoxic exposition.....	10
Figure 7. Oxygen Enhancement Ratio (OER).....	11
Figure 8. Effects on radiation comparing normoxia and hypoxia: the oxygen fixation hypothesis...	12
Figure 9. TGF β and SMAD pathway: differences between normoxia and hypoxia	13
Figure 10. Pathways activated by hypoxia.....	14
Figure 11. Cells and factors that compose the Cancer Stem Cell niche in tumor	16
Figure 12. Scheme of CD133 structure.....	17
Figure 13. Characteristics of single CTC in comparison with CTC cluster.....	18
Figure 14. BDNF/Trk B pathway in cancer	20
Figure 15. CD47 structure.....	21
Figure 16. Direct and indirect damage caused by ionizing radiation.	23
Figure 17.	
Figure 18. Figure 18. Western Blot analysis of E-cadherin and N-cadherin.....	36
Figure 19. Sphere formation with U2OS.....	38
Figure 20. Clonogenic Survival Assay (CSA) of LM8 cell line: comparison between normoxia (21% O ₂) and hypoxia (1% O ₂).....	39
Figure 21. Morphological analysis of LM8 cells..	40
Figure 22. Western Blot analysis of E-cadherin and N-cadherin expression in LM8 murine osteosarcoma cell line.	41
Figure 23. HIF1 α expression levels in LM8 cells	42
Figure 24. CD133 expression after hypoxia (acute and chronic) and radiation.....	43
Figure 25. TrkB expression on LM8 cells.	44
Figure 26. LM8 whole cell population: representative picture of the spheres, sphere formation efficiency, area of the spheres, number of cells forming spheres and number of spheres cluster. ...	47

Figure 27. Clonogenic Survival Assay (CSA) of LM8 cell line: comparison between LM8 full population and CD133+ subpopulation.	48
Figure 28. LM8 CD133+ cell population: representative picture of the spheres, sphere formation efficiency, area of the spheres, number of cells forming spheres and number of spheres cluster. ...	50
Figure 29. Sphere migration in collagen of LM8 whole population.	52
Figure 30. Sphere migration in collagen of CD133+ sorted LM8.	53
Figure 31. CD47 expression in CD133+ cells, comparing normoxia, acute hypoxia and chronic hypoxia.....	54
Figure 32. CTC isolation from blood of mice: comparison between sham control and irradiated samples.....	55
Figure 33. Western Blot analysis of primary tumor vs metastasis.	56
Figure 34. Tumor growth and immunohistochemical analysis of CD133 and CD47 expression between primary tumor and lung metastasis.....	58

List of tables

Table 1: Solutions and antibodies used for immunocytochemistry.....	28
Table 2: 10X RIPA compounds	30
Table 3: Details of RIPA buffer	30
Table 4: List of primary antibodies used.	30
Table 5: List of secondary antibodies used.	31
Table 6: Solutions used for magnetic beads.....	33
Table 7. Solutions used for IHC staining.....	34

List of Graphical Abstracts and Experimental Design

Graphical Abstract 1: Hypoxia and radiation in selecting Circulating Cancer Stem Cell-like phenotype.	24
Experimental Design 2: LM8 sphere formation efficiency workflow.....	29
Experimental Design 3: CD133 cell sorting workflow.....	31
Experimental Design 4: LM8 injection in mice workflow created with BioRender.....	32

1. Introduction

1.1 Motivation

Cancer is the second leading cause of death globally and it can affect people regardless of their wealth or social status. Statistical data show that in 2023, 20 million people worldwide were affected by cancer, and 10 million died (Siegel et al., 2023). Together with surgery and chemotherapy, radiation therapy is one of the most important and standard treatments for cancer applied to almost 50% of all cancer patients (Baskar et al., 2012; Debela et al., 2021). Radiotherapy can be employed as a standalone therapeutic option, where focused radiation is directed precisely at the tumor site. Alternatively, it can complement other treatment modalities, such as surgery or chemotherapy, amplifying the overall impact on cancerous cells. Furthermore, in cases where the disease is advanced or incurable, radiotherapy serves a vital role as a palliative measure, alleviating symptoms and improving the quality of life for patients. Despite its remarkable efficacy in targeting and destroying cancer cells, radiotherapy encounters challenges when facing certain tumors exhibiting high radioresistance. As a result, eradicating such radioresistant cancer cells can be more difficult (Fukui et al., 2022). While a certain dose of radiation may fail to completely eradicate the tumor, excessively escalating the dosage is not viable due to the risk of causing damage to the surrounding healthy tissues near the tumor site (Kim et al., 2014).

More than 100 different types of cancer have been identified because of their heterogeneity. All of these forms show a different treatment response, aggravating the decision of the therapeutic approach (Potdar et al., 2015). Among these, osteosarcoma is one of the most common types of cancer (Kashima et al., 2003; De Luca et al., 2018). The first-line treatment for osteosarcoma in the early stages is neoadjuvant chemotherapy, followed by surgical resection of the primary tumor and adjuvant chemotherapy again after surgery, showing a relevant rise in the survival rate of the patients (Isakoff et al., 2015). Despite this, osteosarcoma nowadays still has a poor prognosis because of its capacity to metastasize to the lungs and bones and because of its ability to relapse even after 5 years, drastically decreasing the overall survival from 70% to 30% (De Luca et al., 2018; Huang et al., 2019; Riggio et al., 2021). Metastases can develop simultaneously with the primary tumor or even years after treatment. This occurs when cancer cells break away from the original tumor and enter the bloodstream becoming circulating tumor cells (CTCs) (Deng et al., 2022; Banyard et al., 2015; Pei et al., 2019). Identifying these CTCs is difficult because they are present in meager numbers. These

cells are able to survive a programmed cell death and escape from the immune system control. For this reason, they can easily disseminate in distant organs, originating metastases and becoming the principal cause for cancer-related death (Gao et al., 2017; Parker et al., 2022). Treating a patient with several metastases multiple times is not advised, because the damage provoked to the subject is higher than the benefits obtained by the treatment (Sosa et al., 2014). Nowadays, there is still no understanding of the signals that allows the cells to migrate, to extravasate to distal organs becoming quiescent, and then “waking up” forming metastases even 5 years after (Pradhan et al., 2018). To shed light on such mechanisms it is important to study these CTCs. In my thesis, I investigated an *in vitro* protocol for characterizing and isolating cells with CTC-like phenotype.

1.2 Osteosarcoma

Osteosarcoma (OS) is one of the most common primary tumors of bone, with an annual incidence rate of 3.1 per million (Valery et al., 2015; Harris et al., 2022). It is mainly diffused among children and young adults with an incidence of 4.2 per million, with a second peak of incidence in adults over 50s (Kansara et al., 2014; Choong et al., 2011; Shao et al., 2022). It develops primarily in the tissues at the extremities of long bones (tibia, humerus, femur) and it is characterized by malignant osteoblasts that produce immature bone tissue (Mutsaers et al., 2014). Multiple hypotheses are at the base of osteosarcoma generation: the most common is the osteoblast origin (Tataria et al., 2006). This assumption claims that osteosarcoma derives from defective differentiation of osteoblast cells (Lin et al., 2017). During a normal osteogenesis, bone cells differentiate from mesenchymal stem cells (MSCs). These non-hematopoietic precursors reside in the bone marrow and contribute to maintaining and regenerating bone tissues (Yang et al., 2020). During this process, markers for osteoblastic progenitors (COL1A and ALP), for mature osteoblasts (PTH1R and BGLAP) and for osteocytes (FGF23 and MEPE) are expressed. Germline mutations such as mutation of p53 and Rb1 (both tumor suppressor proteins) and sporadic mutations might occur in the normal osteogenic process, resulting in osteoblasts or osteocytes that are not completely differentiated, with the consequence of uncontrolled proliferation in cells, giving rise to osteosarcoma (Figure 1). This process is called “osteosarcomagenesis”. (Lin et al., 2017; de Azevedo et al., 2020).

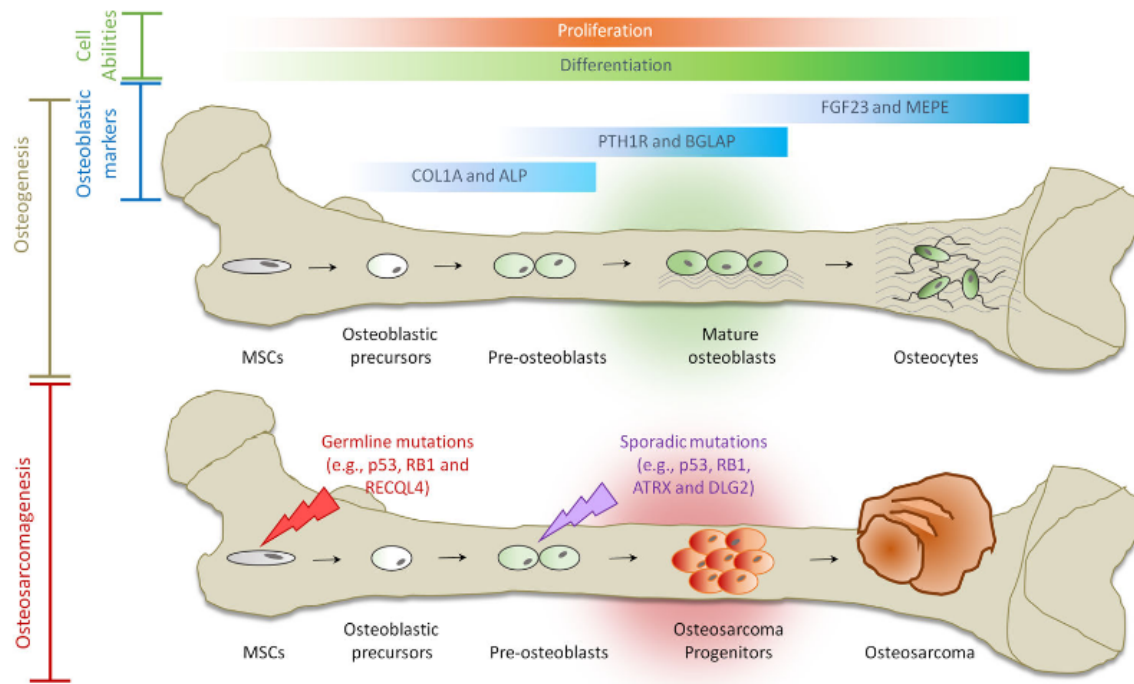


Figure 1. Normal osteogenesis and osteosarcomagenesis: schematic procedure and genes involved (Lin et al., 2017)

Tumoral microenvironment of osteosarcoma is composed of bone cells (osteoblasts, osteoclasts and osteocytes), stromal cells (mesenchymal stem cells and fibroblasts), vascular cells, immune cells and cells of the extracellular matrix; all of these cells interact each other's facilitated by the environmental signals like extracellular vesicles, cytokines, chemokines and soluble growth factors (Mutsaers et al., 2014). Also characterized by tumor heterogeneity, almost 25% of bone tumor displays clustered chromosome rearrangements, while most osteosarcomas are characterized by a chromosomal instability that leads to losses or gains of chromosomes and of tumor suppressor genes such as p53 or RB (Kansara et al., 2014; Lorenz et al., 2015). This active microenvironment, together with high tumor heterogeneity makes difficult to design and validate new therapies to treat osteosarcoma, as well as to understand the mechanisms at the base of its recurrence and identifying which cell type generates this neoplasia (Schiavone et al., 2019; Corre et al., 2020). The main approach to treat osteosarcoma is surgery, with the aim to remove the tumor part and its surrounding normal tissue to avoid local recurrence (Rothzerg et al., 2022). Surgery can be used in combination with radiation or chemotherapy, applied before or after tumor resection to prevent metastatic formations (Mutsaers et al., 2014). Despite these therapy approaches, approximately 20% of patients affected by osteosarcoma develop metastases, particularly in the lungs (Silva et al., 2022; Kim et al., 2022). Osteosarcoma is a high metastatic neoplasia, with pulmonary metastases as primary cause of death. Its metastatic ability

is based on a complex cell-cell or cell-matrix interaction, as well as to gene alterations and epigenetic regulations, both leading to epithelial-mesenchymal transition (EMT) (Odri et al., 2022). Osteosarcoma cells are able to produce matrix components through cell-surface receptors. The main receptor proteins are the integrins that are involved in cell signaling and activate pathways involved in cell migration (Luo et al., 2007). Ezrin protein, which also plays a role in cell-cell interaction, usually functions as a linker between actin cytoskeleton and the plasma membrane by forming dynamic domains including lamellipodia and filopodia (Song et al., 2020). Since this protein mediates numerous signal transduction in tumorigenesis, when overexpressed it might lead to metastasis formation (Khanna et al., 2004). At the beginning of metastasis formation, cells escape from primary site invading the surrounding tissues by extracellular matrix (ECM) degradation underlined by the overexpression of matrix metalloproteinases (MMPs) (Sheng et al., 2021). These proteinases are important also for angiogenesis because they remodel the blood vessels creating a leaky vascular network that grants tumor cell intravasation in the blood vessels (Oh et al., 2001). Primary tumor produces factors such as growth factors and cytokines that travel inside extracellular vesicles (EVs) influencing metastatic niches; they also interact with the resident cells contributing to make OS cells migrating and disseminating to the lungs (Odri et al., 2022). Such EVs are the result of the interplay between MSCs and OS cells: these vesicles carry a membrane-associated form of TGF- β and stimulate interleukins (IL-6) expression in MSCs, thus activating STAT3, a mediator of cell growth and apoptosis, and facilitating lung metastasis formation as well as an increase in drug resistance for OS (Yang et al., 2020). In MSCs, tumor cells are also able to induce oxidative stress through production of ROS and this triggers the aerobic glycolysis and lactate production, stimulating migration capacity of cancer cells (Cortini et al., 2017). Moreover, hypoxia might influence MSC-tumor interplay by promoting pro-angiogenic factors and by triggering metabolism, cell growth and differentiation (Yang et al., 2020).

1.3 Metastatic cascade

Cancer cells disseminating from the primary tumor undergo to a multi-step process, also known as “invasion-metastasis cascade” (Giancotti., 2013). These cancer cells go through a phenotypical change called “Epithelial-To-Mesenchymal Transition” (EMT), which makes them able to detach from the primary tumor, increasing their motility (Kashima et al., 2003; Guarino et al., 2007). During this process, polarized epithelial cells lose their epithelial integrity because of the loss of cell-cell junctions (tight junctions, gap junctions, adherens junctions and desmosomes). A remodeling of the cytoskeleton and a decrease in the expression of proteins such as E-cadherin, an adherens junction

protein that is involved in the maintenance of cell polarity, cell differentiation, and migration (Chen et al., 2014; Loh et al., 2019) follows the process. The downregulation of E-cadherin is balanced by an upregulation of the transmembrane protein N-cadherin, thus conferring the cells a more mesenchymal phenotype (Figure 2) (Kalluri et al., 2009). Moreover, N-cadherin mediates the collective cell migration, an extremely efficient process that makes the epithelial cells pass through the tumor microenvironment, promoting metastases (Mrozik et al., 2018). This phenomenon, known as “cadherin switch”, is crucial for the metastatic cascade (Gonzalez et al., 2021).

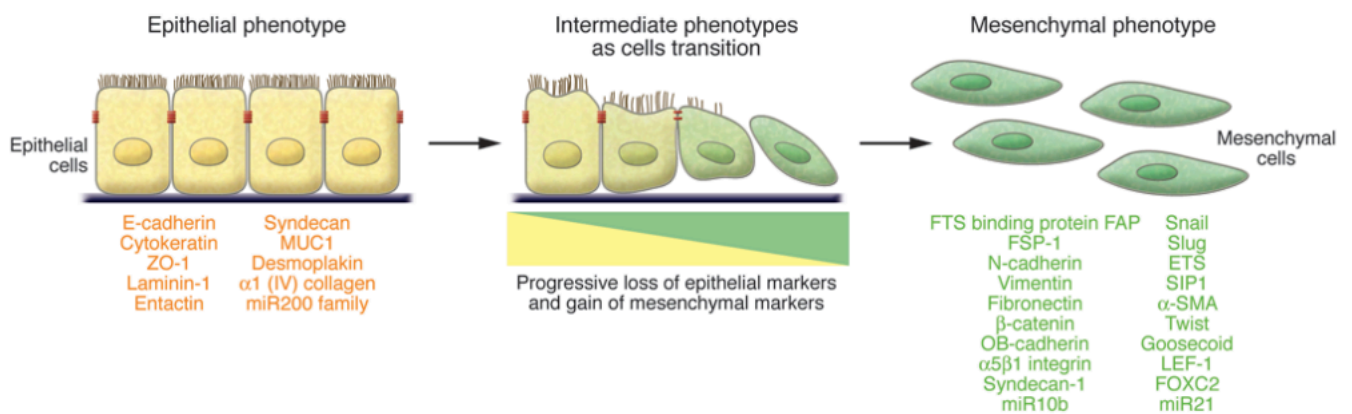


Figure 2. Scheme of Epithelial-to-Mesenchymal transition (Kalluri et al., 2009)

Cadherin switch is also regulated by Wnt/ β -catenin pathway. This pathway is composed by a group of proteins that are relevant for embryonic development and adult tissue homeostasis and when deregulated often leads to cancer diseases (Lin et al., 2021). More in detail, β -catenin binds E-cadherin in the cytoplasm forming a complex that stabilizes cell-cell contacts; loss of E-cadherin and phosphorylation of Wnt protein result in a release of β -catenin that moves to the nucleus, allowing the expression of genes involved in cell proliferation, survival and migration (Mylavarapu et al., 2019; Liu et al., 2022). EMT is not only responsible for an increased cell migration, but it also influences the stemness capacity of the cells, suppresses immune response and confers radiotherapy resistance to cells (Zijl et al., 2011). After EMT occurs, cells disseminate from the primary tumor and intravasate inside of the blood circulation (Doujon et al., 2021). Within the blood vessels, these cells are subjected to stress generated by the change in the oxygen concentration and in the pressure of the blood flow, they might be detected by the immune system and they might undergo to a programmed cell death called “anoikis” (Wang et al., 2018). Anoikis is a crucial mechanism that might be induced by death receptors and mitochondria-mediated apoptotic pathways: death receptors are able to

activate caspase-8 (involved in the programmed cell death) that activates its downstream protein caspase-3 by cleavage and triggers the apoptotic response. An inhibitor for anoikis is tropomyosin receptor kinase B (TrK B) that contributes to metastasis formation. Moreover, in some cell lines anoikis resistance is conferred by hyperactivation of STAT3 signalling (pancreatic cancer cell lines) or loss of E-cadherin (breast cancer cell lines) (Shen et al., 2020). Only a specific subpopulation of these EMT cells is able to survive to this stress and are the ones that retain metastatic capacity, the Circulating Tumor Cells (CTCs) (Chiang et al., 2016; Tinganelli et al., 2020). These cells circulate in the blood vessels until they reach favorable niche, known as pre-metastatic niche; at this point they revert their phenotype through the “Mesenchymal-to-Epithelial transition” (MET) and going back to the cell adhesion ability, they adhere to the wall of capillaries and extravasate, giving rise to metastasis at distant sites (Potdar et al., 2015; Patel et al., 2012; Franken et al., 2012). During extravasation, cancer cells begin to show motile phenotype and express matrix metalloproteinases (MMPs), that digest the ECM rich in laminin and collagen (Wirtz et al., 2011). Once the cancer cells disseminate from the blood circulation, they are called Disseminating Tumor Cells (DTC) and they can enter in a quiescent state or dormancy, where they show a prolonged growth or arrest without displaying an increase in cell death (Dasgupta et al., 2017). Dormancy could be induced at a cellular level when the cells, due to the lack of growth factors and adhesion signalling, undergo to G0-G1 arrest exiting the cell cycle (Aguirre-Ghiso., 2007). Nevertheless, tumor cell dormancy can also be caused by cell-depleting events such as cell apoptosis; these two types of dormancies could be correlated and DTCs need to overcome them in order to progress towards metastases (Dasgupta et al., 2017). Moreover, dormant tumor cells could result from stress signals that have been produced by a niche that is favourable to quiescence; on the other side, there are tumor cells able to remodel a microenvironment that allows cell expansion, thus resuming the growth of such quiescent cells (Figure 3) (Aguirre-Ghiso., 2007).

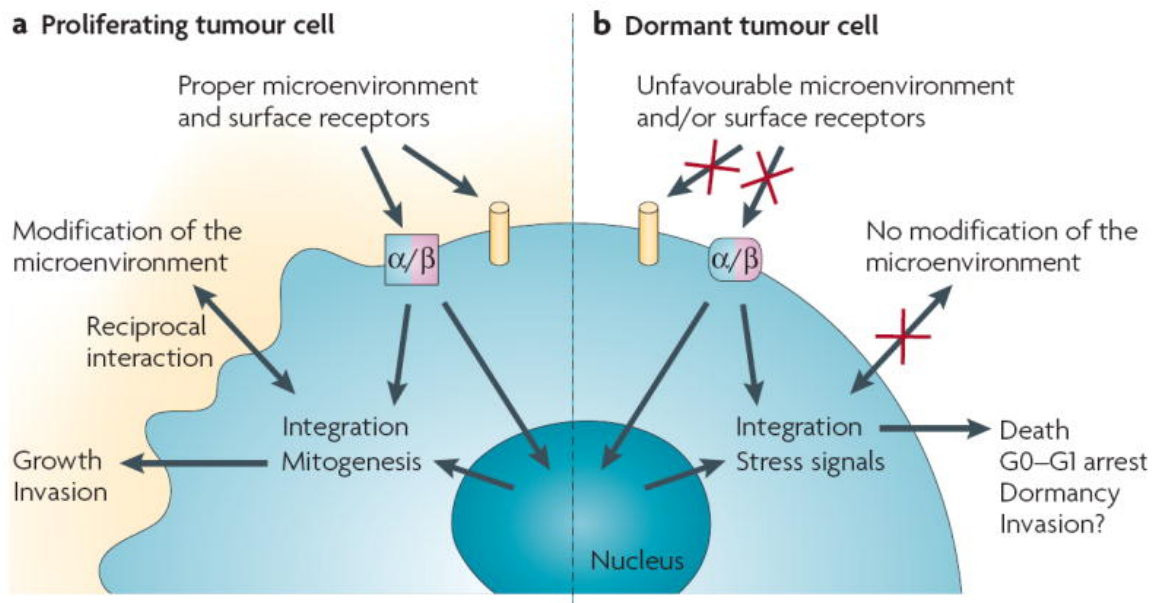


Figure 3. Scheme of signals that regulate proliferating and dormant tumor cells (Aguirre-Ghiso., 2007)

Indeed, these cells go undetected for years or decades, after which they can “wake up” and form metastases (Gomis et al., 2017). At the base of this mechanism is the crosstalk between cancer cells and the surrounding extracellular matrix: by reaching distant organs, these cells enter contact with new ECM produced by the stromal cells of the area. Afterwards, binding membrane receptors on dormant cells activate various signalling cascades promoting the cell cycle and making the cells “waking up” from their dormancy state (Park et al., 2020). An Extracellular signal-regulated kinase (ERK) plays an important role in regulating cancer cell proliferation and dormancy. ERK is activated in proliferating cancer cells, allowing G0-G1-S phase transition; during proliferation, high levels of p38 mitogen-activated protein kinase, usually responsive to stress stimuli and involved in cell differentiation, apoptosis and autophagy, inhibits ERK inducing G0-G1 arrest leading to senescence and apoptosis (Park et al., 2020). In addition, extracellular factors can trigger tumor cell dormancy: hypoxia for instance is able to induce cell dormancy through the production of Tumor Growth Factor beta (TGF- β), as well as by increasing the expression of anti-angiogenic factors (tombospondin) or decreasing the expression of angiogenic signals (VEGF), thus limiting the amount of nutrients that tumor needs for its growth (Todd et al., 2020; Butturini et al., 2019). Intrinsic factors as well contribute to tumor cell dormancy, such as pathways involved in metabolic processes (PI3K/Akt pathway) and cell cycle regulators (p21/p27, Rb-E2f pathways) (Damen et al., 2021). These series of events that compose the metastatic cascade help to understand better the complex mechanisms that is behind the metastasis formation from the primary tumor (Figure 4) (Dasgupta et al., 2017).

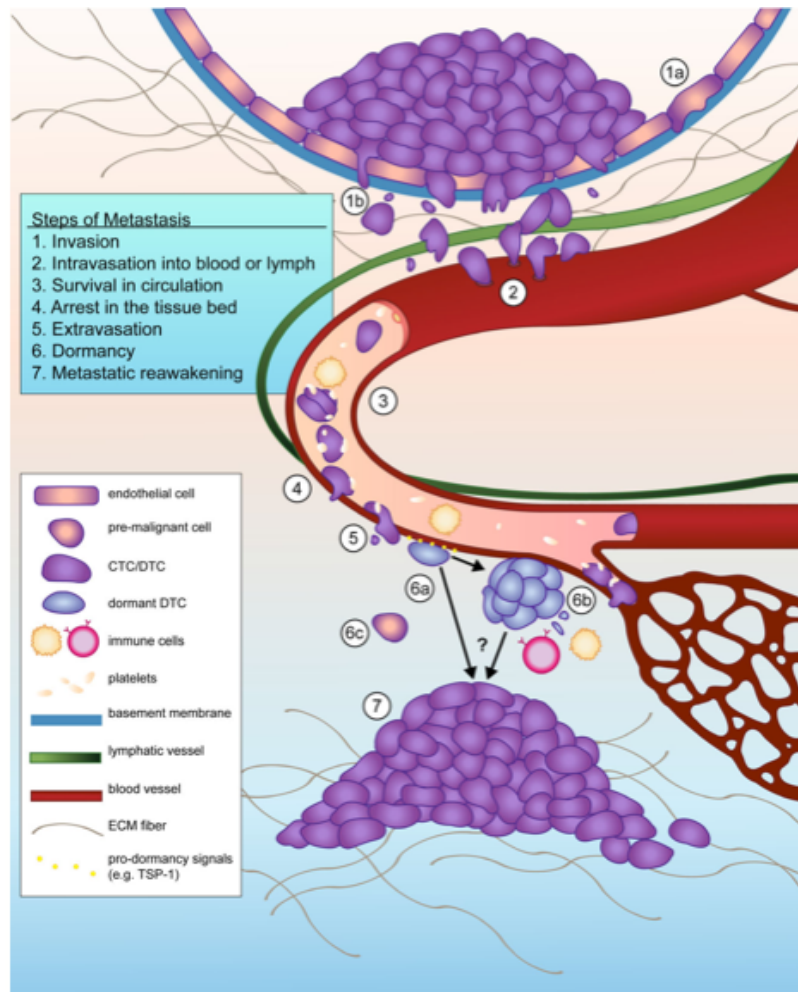


Figure 4. Invasion-metastasis cascade (Dasgupta et al., 2017).

1.4 Tumor Hypoxia

In biological experiments, “normoxia” refers to normal experimental *in vitro* conditions (21% O₂). However, this differs from the average level of oxygen that is present in healthy body tissues, where the oxygen levels range from 9.5% to 4.6%, depending on the organ vascularization and metabolic activity; this oxygen concentration is known as “physoxia” (McKeown., 2014). Oxygen level might drop to 1-2% or below, and in this case the condition is called “hypoxia”, a phenomenon that usually occurs in malignant tumors (Muz et al., 2015). During the growth of the tumor, cells acquire nutrients through angiogenesis; as the tumor becomes bigger, cells grow faster than the blood supply, resulting in an inefficient tumor vascular system that is not able to provide enough oxygen and nutrients, resulting in hypoxia formation (Li et al., 2021). Hypoxia is considered to be one of the hallmarks of tumor microenvironment and cancer cells are able to respond to such stress by showing a genetic instability; therefore, they increase their invasiveness and metastatic capacity, and might become resistant to treatments, such as chemotherapy or radiotherapy (Ezkiimir., 2015).

The hypoxic response is mediated by Hypoxia Inducible Factors (HIFs), involved in angiogenesis, anaerobic metabolism, and apoptosis resistance (Saxena et al., 2019). HIFs are heterodimers characterized by three different oxygen dependent HIF α subunits (HIF1 α , HIF2 α and HIF3 α) that are expressed in the cytoplasm, and a HIF-1 β subunit that is expressed in the nucleus. Oxygen and iron dependent enzymes known as HIF-prolyl hydroxylase domain (PHD1-3) (Koh et al., 2012) subsequently stabilize HIF α . In a normoxic condition, PHD hydroxylates the HIF α subunit, and then binds to the Von Hippel-Lindau tumor suppressor protein (pVHL), resulting in a HIF ubiquitination and proteasomal degradation (Marxsen et al., 2004). On the other side, hypoxia suppresses PHDs resulting in a HIF α translocation in the nucleus, where it binds to HIF-1 β subunit resulting in the transcriptional upregulation of the hypoxia-responsive elements (HRE) (Figure 5) (Vito et al., 2020).

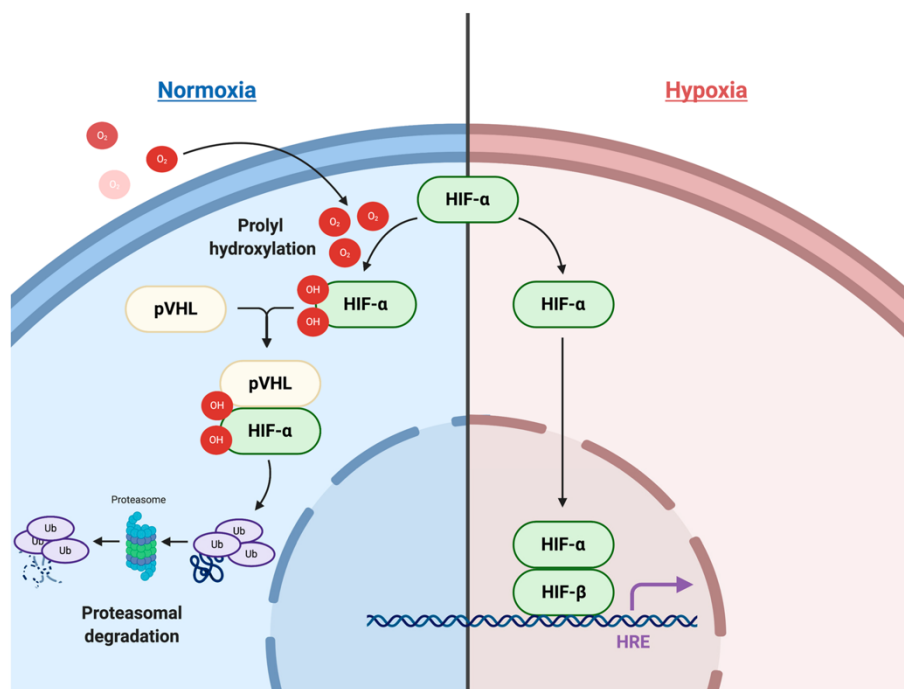


Figure 5. Hypoxia signaling pathway (Vito et al., 2020).

Cells response to hypoxia is mediated by HIF1 α and HIF2 α , depending on the oxygen level: HIF2 α appears to be more stable compared to HIF1 α at higher oxygen concentration (e.g.: 5% O₂) (Figure 6: A). HIF1 complex induces the expression of pro-angiogenic genes, while HIF2 α is specifically expressed in endothelial cells, and facilitates the expression of matrix metalloproteinases (MMPs) as well as it is required for initiation of the vascular network (Jaskiewicz et al., 2022). HIF1 α and HIF2 α also behave differently depending on the duration of hypoxia (Lin et al., 2011). HIF1 α protein levels reach a peak around 4h to 8h of hypoxic condition, and subsequently decrease after 24h, creating a condition called “acute hypoxia” (Reiterer et al., 2019). This “short-period” stability of HIF1 α might

be due to the upregulation of PHD2 that hydroxylates HIF1 contributing to its degradation (Butturini et al., 2019). HIF2 α protein expression instead is more stable, it starts to be expressed during the acute hypoxia condition and it remains stable also after 24h of hypoxic exposition, when HIF1 α decreases (Figure 6: B) (Saxena et al., 2019). This transition from HIF1 α to HIF2 α is known as “HIF switch”.

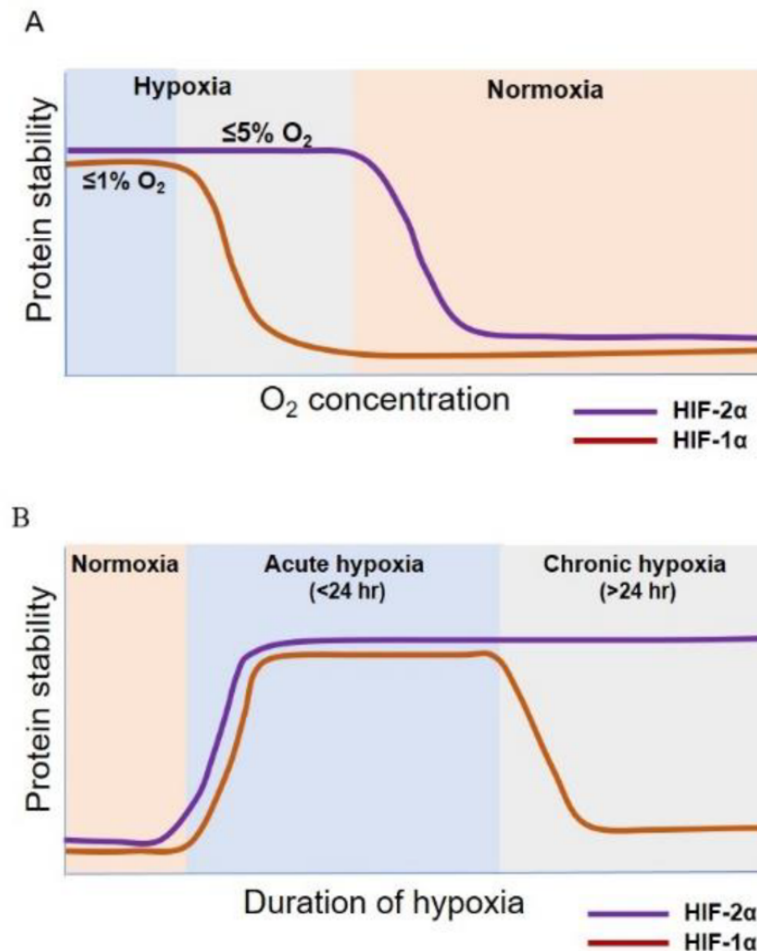


Figure 6. HIF1 α and HIF2 α behaviour at different oxygen concentrations (A) and under different duration of hypoxic exposition (B) (Saxena et al., 2019).

HIFs are involved in metabolic activity of the cells. In normoxic condition, oxidative phosphorylation that occurs in mitochondria produces ATP that gives energy to the cells. When the oxygen amount is limited, HIFs intervene and adjust the production of ATP enhancing the expression of metabolic enzymes that display HIF1 isoform specificity. Such enzymes regulate the glucose usage and reduce the metabolic reliance on oxygen (Taylor et al., 2022). Moreover, HIF1 α expression appears to increase in the hematopoietic stem cells, by decreasing their metabolic activity, activating genes essential to maintain the cells in a dormant state (Takubo et al., 2010). In addition, HIF2 α is reported to promote epithelial-to-mesenchymal transition and activates genes responsible for tumor invasion

and aggressiveness (Zhang et al., 2017). HIF1 α and HIF2 α are also involved in tumor immune-evasion. HIF1 α increases the expression of Programmed Cell Death Ligand 1 (PDL1), a transmembrane protein that inhibits the immune response, thus making the cells more resistant to the apoptosis induced by the immune system. In a limited way, also HIF2 α plays a role in tumor immune escape: when expressed, it reduces the number of tumor-infiltrating immune cells by activating downstream pathways, resulting in evasion from immune surveillance (Wu et al., 2022).

Hypoxia is also involved in resistance to therapy resulting in a restraining factor for tumor control in radiotherapy, leading up to three times radioresistance (Tinganelli et al., 2015). The increase of radioresistance is represented by a factor called Oxygen Enhancement Ratio (OER) (Figure 7), that is the ratio between the radiation doses delivered under hypoxia (D_{hypox}) and the ones in normoxic condition (D_{normox}), in order to obtain the same biological endpoint (Telarovic et al., 2021; Boulefour et al., 2021).

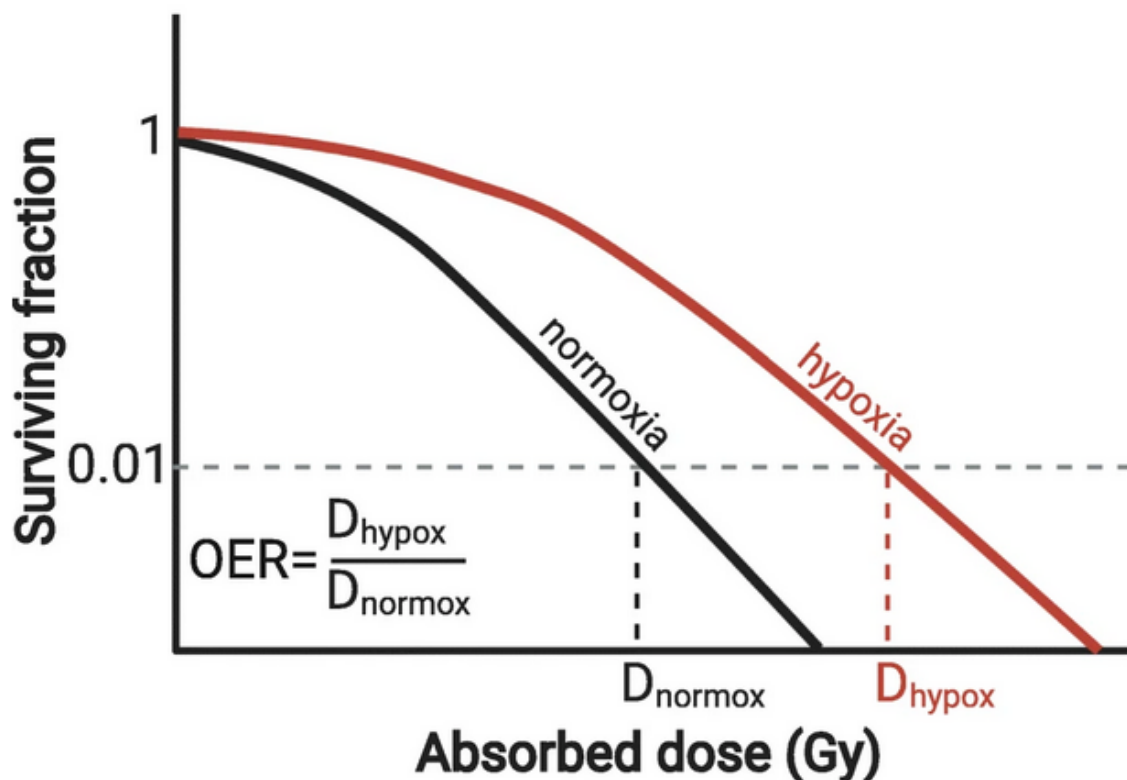


Figure 7. Oxygen Enhancement Ratio (OER) (Telarovic et al., 2021).

Different mechanisms can explain hypoxic radioresistance; the more diffused one is the oxygen fixation hypothesis: radiation interacts with other molecules in the cells, in particular water, and it

produces free radicals such as hydrogen atoms (H^+), hydroxyl groups (HO) and superoxide radical anion (O_2^-) that interacts with the DNA damaging it and causing DNA strand breaks. When oxygen interacts with these radicals, it contributes to make the damage permanent. In the presence of a low level of oxygen, the DNA radicals are reduced by sulfhydryl groups (SH groups) that repair the DNA, so that it comes back to its original form (Figure 8) (Wang et al., 2019).

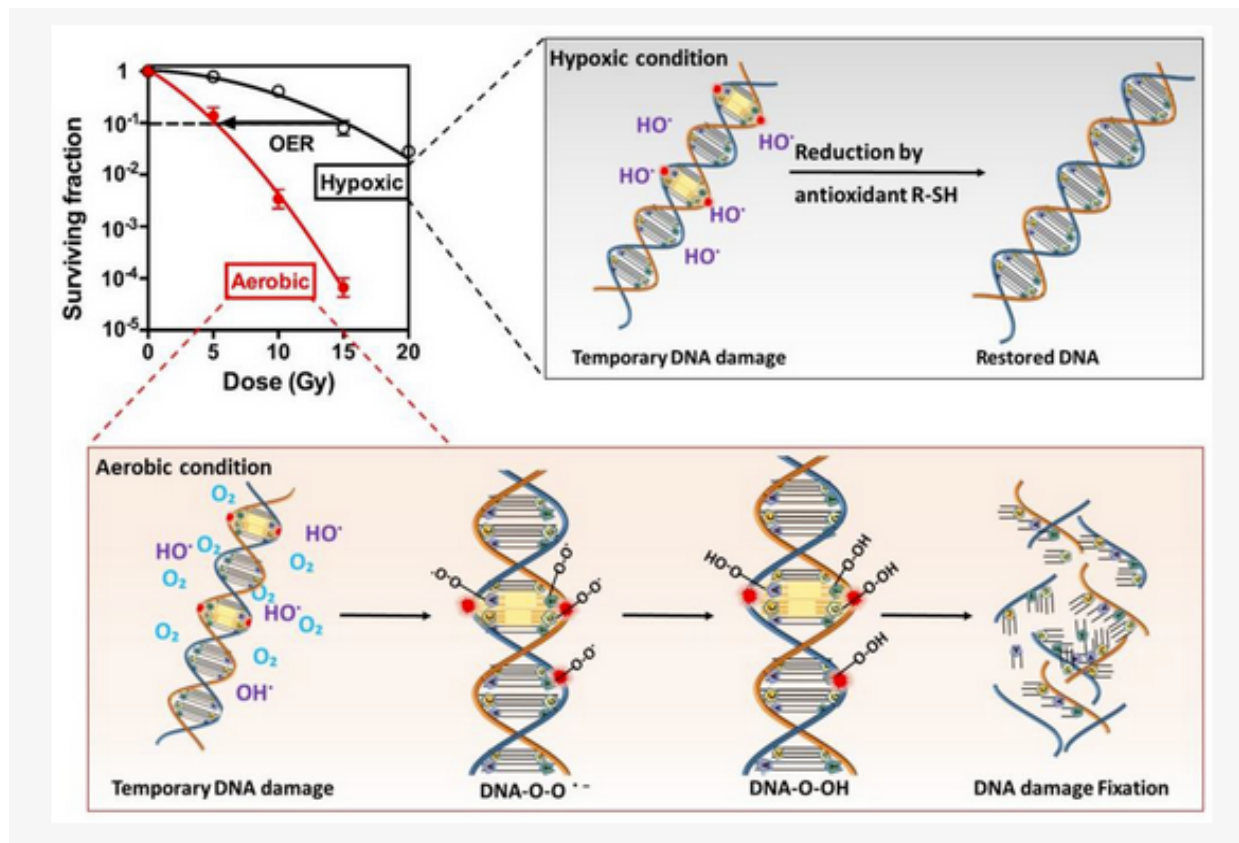


Figure 8. Effects on radiation comparing normoxia and hypoxia: the oxygen fixation hypothesis (Wang et al., 2019).

Hypoxia influence on EMT transition and on cancer stemness is the main cause for metastasis formation (Wiechec et al., 2022). Hypoxia triggers TGF- β and Notch signalling pathways: TGF- β is involved in tumor cell motility and invasion by activating SMADs cytoplasmic receptors by phosphorylation (Jiang et al., 2011). SMADs translocate in the nucleus, thus regulating the transcription of genes involved in cell proliferation, migration and EMT transition (Hao et al., 2019; Brochu-Gaudreau et al., 2022). Under hypoxia, HIF-1 complex and TGF- β might cooperate and can cause EMT either by activating SMAD2 proteolysis and increasing the levels of SMAD3 (Figure 9), or by decreasing the protein levels of PHD2 (HIF-1 α -associated prolyl hydroxylase) through SMAD signalling pathway (Minguyan et al., 2018). Hypoxia triggers EMT also by increasing the

transcriptional activity of the Notch intracellular domain, that moves in the nucleus after cleavage of the cytoplasmic tail of Notch transmembrane receptor (Tam et al., 2020). This interplay between HIF-1 α and Notch is also important for stemness of cancer cells (Pistollato et al., 2010).

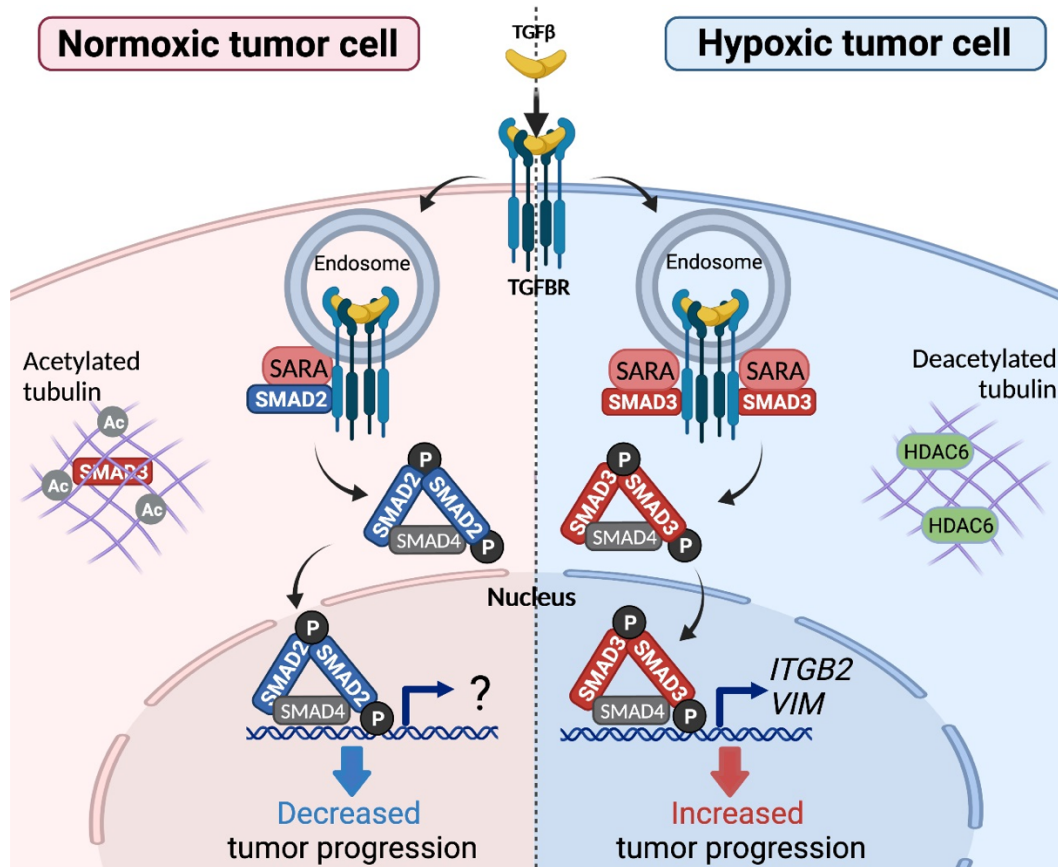


Figure 9. TGF β and SMAD pathway: differences between normoxia and hypoxia (Brochu-Gaudreau et al., 2022).

It is reported an influence of hypoxia on the function and activity of cancer stem cells, in fact it contributes to enhance their self-renewal capacity and preserves their undifferentiated state (Gustaffson et al., 2005). Together with EMT markers, low level of oxygen contributes to activation of cancer stemness markers such as Oct4, Sox2 and Nanog, leading to an increased tumor aggressiveness, invasion, metastatic capacity and resistance to therapy (Figure 10) (Bao et al., 2012). In addition, HIF1 binds directly to the “do not eat me” CD47 marker, helping to escape phagocytosis of the cells preserving their stemness capacity (Ohnishi et al., 2013). Moreover, HIF1 α and HIF2 α regulate CSC phenotype by upregulating the CSC marker CD133 (Yun et al., 2014; Bar., 2011; Simsek et al., 2010; Iida et al., 2012). Hypoxia also seems to influence CTCs formation, in particular it contributes to the generation of CTC clusters that are endowed with a high metastatic potential and seeding capability compared to the normoxic ones (Donato et al., 2020).

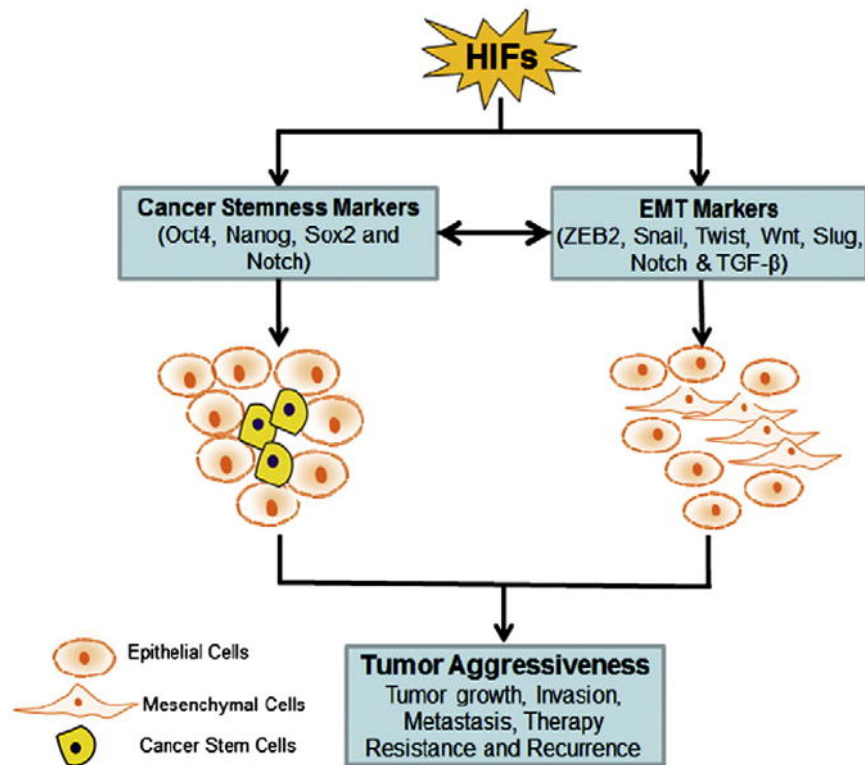


Figure 10. Pathways activated by hypoxia (Bao et al., 2012).

1.5 Cancer Stem Cells (CSCs)

Not all cancer cells can disseminate and form metastasis; metastasis in fact is a process that displays less than 0.1% of cells able to metastasize, in preclinical settings (Celia-Terrassa et al., 2020). A heterogeneous population of cells composes tumor, and among them, the ones that are responsible for malignancy and for tumor initiation and that retain stem-like properties are called “Cancer Stem Cells” (CSCs) (Ayob et al., 2018; Albini et al., 2015). CSCs are characterized by self-renewal capacity, the ability to differentiate, and resist to therapies including ionizing radiation (Lim et al., 2021). These cells reside in niches, that are regions within the tumor microenvironment, important for protecting the cells maintaining their stemness capacity (Plaks et al., 2015; Zijl et al., 2014). CSCs are protected against radiation effects due to a series of factors, such as an upregulated DNA damage reaction: as a response to radiation, checkpoint-pathways in the cell cycle are activated, resulting in a delayed cell cycle progression that allows the repairs to the damage in the DNA (Schulz et al., 2019; Arnold et al., 2020). Furthermore, CSCs seem to have more pronounced pro-survival pathways that preserve these cells from apoptosis (Arnold et al., 2020). Moreover, radiation resistance can be acquired because of tumor heterogeneity that promotes clonal evolution, leading to more

resistant, aggressive and invasive tumors (Arnold et al., 2020). These cells are also involved in tumor proliferation, display a poor clinical outcome, and are able to form tumors when injected in animal host (Yu et al., 2012). Furthermore, CSCs also possess the capacity to form spheres when cultivated in an *in vitro* culture (Bahmad et al., 2018; Morrison et al., 2012).

Many authors propose that CSCs originate from normal stem cells: such cells are can differentiate into different cell types (multipotency), and are characterized by a high proliferation capacity and the ability to self-renew. These cells might encounter genetic mutations, thus generating tumors (Walcher et al., 2020). Another theory claims CSCs arise from committed progenitor cells that acquire stemness capacity. The combination of these two theories makes up the characteristics of CSCs that can be considered a rare population of stem-like cells that help the initiation and progression of tumors, contributing to its heterogeneity (Flaherty et al., 2012). Cancer Stem Cells play a role as initiators of the metastatic cascade by showing an EMT phenotype with a subsequent increase in the migration capacity, needed to disseminate from the primary tumor (Shiozawa et al., 2013). Multiple cells signaling pathways link EMT to CSCs; the most relevant are TGF- β and Wnt/ β -catenin (Tanabe et al., 2020). TGF- β , a multifunctional cytokine, influences the production of tumor-initiating stem cells (TISCs) by upregulation of Nanog, a transcription factor important for cell stemness capacity (Celia-Terrassa et al., 2020). Wnt/ β -catenin pathway regulates cell self-renewal and EMT process: nuclear β -catenin induces its downstream target CD44, which is a critical regulator of CSC stemness and self-renewal, as well as is involved in tumor initiation (Wang et al., 2018). CSCs reside in a specific microenvironment niche, usually composed by stromal cells, endothelial cells, ECM, immune cells, signaling molecules and blood vessels; these niches are important for cell renewal and for maintaining tumor malignancy and are also reported to be responsible for CSC radioresistance (Figure 11) (Ju et al., 2022).

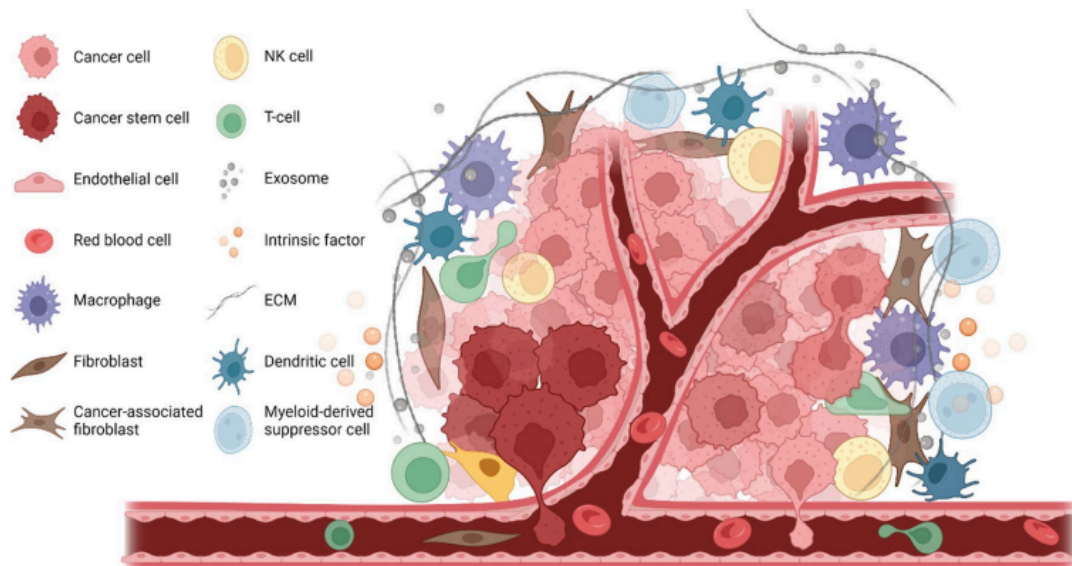


Figure 11. Cells and factors that compose the Cancer Stem Cell niche in tumor (Ju et al., 2022).

Cells that reside in CSC niches produce factors that stimulate CSC self-renewal, tumor cell invasion and metastasis (Oskarrson et al., 2014). CSCs are also present in hypoxic niches, where hypoxia contributes to maintain their undifferentiated status by activating various signaling pathways and promoting their EMT process (Ju et al., 2022; Yun et al., 2014; Zhang et al., 2022). Hypoxia keeps the CSCs in a slow cell cycle, and it contributes to protect cells from DNA damage caused by oxidative stress (Carnero et al., 2016). Low oxygen level of 1% O₂ also contributes to the pluripotency of stem cells, and to maintaining CSC phenotype (Ju et al., 2022). Hypoxia also increases the expression of CSCs surface markers, like the CD133, useful for their identification and isolation (Yang et al., 2015). Also known as prominin-1, CD133 is a transmembrane protein containing three extracellular domains (EC), five transmembrane domains (TM) and three intracellular domains (IC) (Figure 12) (Glumac et al., 2018).

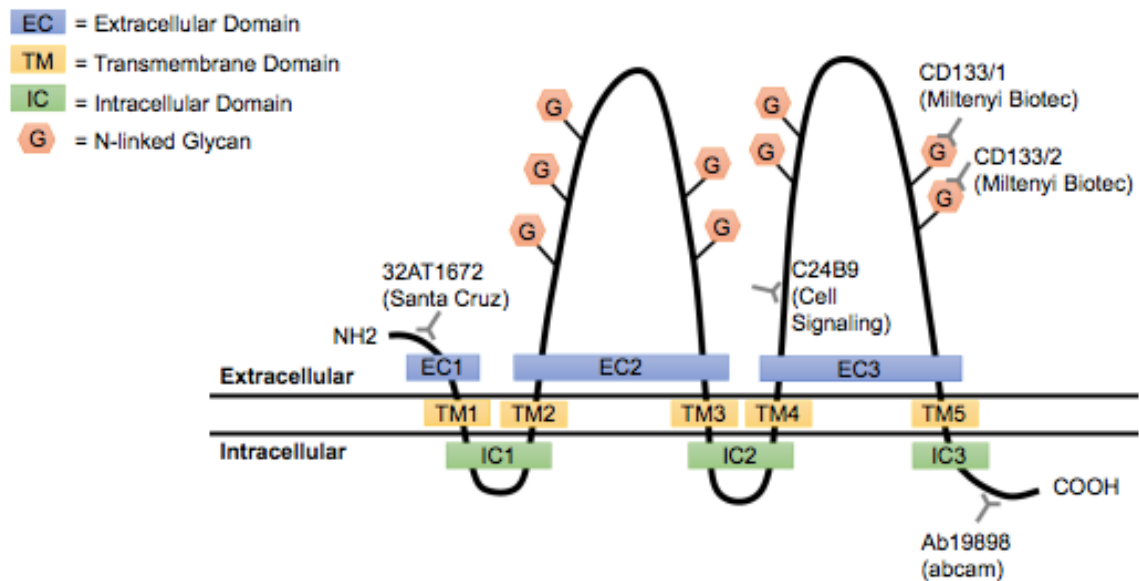


Figure 12. Scheme of CD133 structure (Glumac et al., 2018).

CD133 is localized on the protrusions of the plasma membrane, it is involved in membrane organization and can bind to cholesterol-based lipid micro-domains participating in different signaling cascades (Ferrandina et al., 2009). This protein is also able to polarize, and because of this capacity it might be involved in cell migration (Ferrandina et al., 2009).

CD133 binds Akt, thus activating its downstream pathway PI3K/Akt, related to tumorigenesis (Yoon et al., 2021). CD133 also interacts with EGFR, a receptor tyrosine kinase involved in proliferation and migration (Jang et al., 2017); in addition, it is involved in the induction and activation of Wnt/ β -catenin signaling pathway, that regulates the stemness capacity of these cells and confers resistance to radiation therapy (Behrooz et al., 2021). When activated, these cells become more invasive and able to form metastasis and start their EMT process (Behrooz et al., 2021). It is also documented in the literature that hypoxia in the stem cell niches promotes the expression of CD133 by upregulating HIFs (Glumac et al., 2018). In literature, HIF1 α promotes CD133⁺ colon and pancreatic CSCs through Oct4 and Nanog, both transcriptional factors that confer pluripotency state in stem cells. Furthermore, CD133 boosts HIF1 α expression contributing to its nuclear translocation and gene transcription, and increases the cells self-renewal capacity, migration and invasion ability (Zhang et al., 2021; Maeda et al., 2016).

1.6 Circulating Tumor Cells (CTCs)

A portion of CSCs disseminate from the primary tumor because of the EMT process, intravasate and enter blood circulation. This subpopulation is called Circulating Tumor Cells (CTCs) (Lin et al., 2021). It is challenging to isolate these cells due to the low amount of them in the blood circulation which is approximately 1 to 10 CTCs per mL of blood (Liu et al., 2021; Akpe et al., 2020). Once in the blood, they are subjected to different types of flow: in arterial vessels where the pressure is higher, an increase in the shear stress leads to cell disaggregation, cell cycle arrest and cell death. Once the CTCs reach the capillaries where the blood pressure decreases, they become able to arrest thanks to cell adhesion. In veins instead, where the blood flow is slow, CTCs interact with other blood cell components and develop systems to escape from their control, thus promoting colonization to organs at distant sites (Follain et al., 2020). CTCs circulate in the blood vessels as single cells or in clusters (Micalizzi et al., 2017). The clusters are composed of cells with different genotype and phenotype (Tinganelli et al., 2020). It is documented in literature that CTC clusters have a stronger metastatic potential compared to single CTCs, because they display an increased expression of proteins involved in adherens junctions and desmosomes, such as plakoglobin that mediates cell-cell adhesion, thus maintaining the aggregation status of CTCs (Chen et al., 2022; Hurtado et al., 2023). Moreover, CTC clusters grant stemness properties to the cells by overexpressing cell surface markers such as CD44 glycoprotein, commonly up-regulated in Cancer Stem Cells, and by showing an increase in the stemness-associated transcription factors OCT4, SOX2 and NANOG (Figure 13) (Amintas et al., 2020).

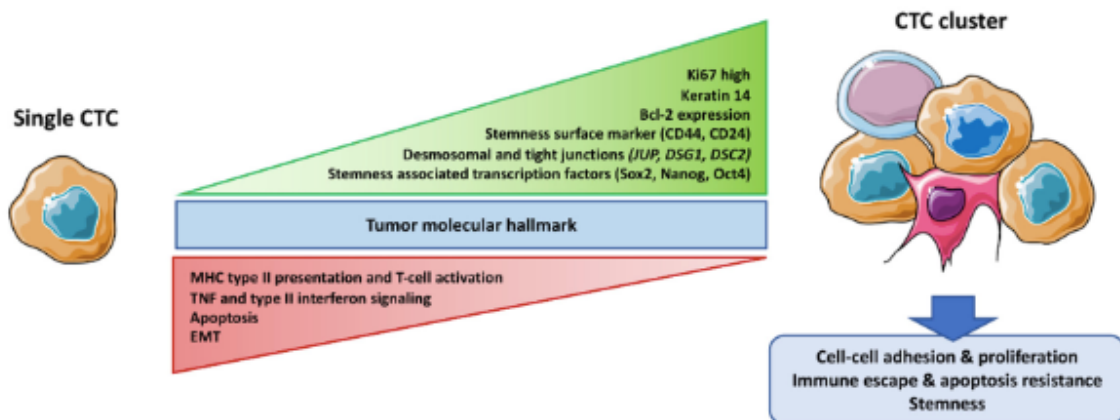


Figure 13. Characteristics of single CTC in comparison with CTC cluster (Amintas et al., 2020).

Thanks to their increased cell-cell adhesion capacity, the CTCs clusters can easily resist cell-detachment-induced apoptosis. Since they have a downregulation of multiple pathways, such as type II interferon and TNF signaling pathway, they support the capability of evading the immune-system

control (Amintas et al., 2020). In general, due to the stress they are subjected to inside the blood circulation, cancer cells are oriented to die because of a programmed cell death called “anoikis” (Guarino et al., 2007; Wang et al., 2018). This type of apoptosis acts as a physiological barrier to cancer progression by depriving the cells of adhesion signals necessary for cancer cell advancement (Geiger et al., 2005). Cells have achieved different strategies for anoikis resistance. One way involves a change of the integrin receptors that are usually involved in cell-matrix contacts to boost cell survival enabling the cells to invade (Taddei et al., 2012). Another approach is the oxidative stress: the production of ROS prevents tumor cells from anoikis by activating Src protein, which is important for cell migration (Giannoni et al., 2008). EMT as well is a crucial step: during EMT, E-cadherin is downregulated, thus resulting in a decrease of cell-cell contact, increased angiogenesis and anoikis resistance (Cavallaro et al., 2004). Hypoxia can also contribute to the pro-survival role of cancer cells because of its ability to induce EMT and produce ROS (Adeshakin et al., 2021). Furthermore, anoikis resistance might be conferred by specific markers such as TrK B (Receptor tyrosine kinase B), a transmembrane protein that works as a receptor for brain-derived neurotrophic factor (BDNF) (Geiger et al., 2005; Yuan et al., 2018; Douma et al., 2004). Upregulation of the BDNF/TrK B signal transduction pathway is able to activate the downstream PI3K/Akt pathway, which is relevant for regulating cell proliferation and malignancy in cells (Figure 14) (Serafim et al., 2020). By cooperating with other signaling pathways like TGF- β or Wnt/ β -catenin, it promotes EMT process, enhancing migration and invasion of CTCs and their resistance to apoptosis (Hemmings et al., 2012; Xu et al., 2015; Yuan et al., 2018).



Figure 14. BDNF/TrK B pathway in cancer (Serafim et al., 2020).

Circulating Tumor Cells can also evade immune system detection by displaying a high amount of CD47 protein (Chao et al., 2012). CD47 is a cell surface protein with an extracellular N-terminal IgV domain, five transmembrane domains and a short C-terminal cytoplasmic tail (Eladl et al., 2020). This protein is normally expressed in cells and it binds to its extracellular ligands such as signal regulatory proteins (SIRPs) and to integrins (α IIB β 3 integrins), thus inducing a phosphorylation and blocking cell phagocytosis, providing a “do not eat me” signal that spares cells from the immune detection (Figure 15) (Lian et al., 2019; Eladl et al., 2020). CD47 expression can also be triggered by hypoxia: in literature it is reported that HIFs activate the transcription of the CD47 gene, while a knockdown of HIF activity or CD47 leads to an increase in phagocytosis following death of the cells (Zhang et al., 2015).

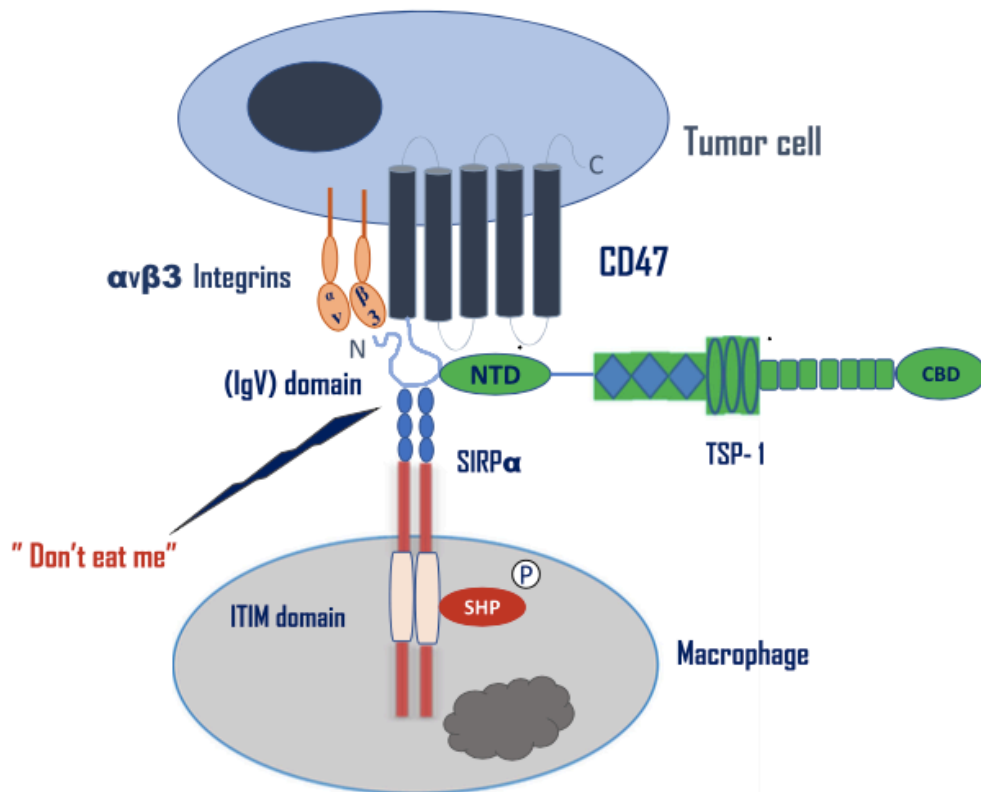


Figure 15. CD47 structure (Eladl et al., 2020).

Only a small subset of CTCs are able to survive to the stress in the blood circulation and they are called Circulating Cancer Stem Cells (CCSCs) (Papaccio, 2020). There are two known hypotheses at the base of CCSCs formation: one hypothesis claims that such cells originate in primary tumor as CSCs and they have features that allows them to detach, enter in blood vessels and survive, initiating metastases (Shiozawa et al., 2013). Another hypothesis believes that CCSCs originate secondly from disseminated tumor cells that, after detaching from primary tumor, escape from a state of dormancy (Yang et al., 2015). The first hypothesis is considered the most probable (Hardin et al., 2017). Additionally to their stemness capacity, CCSCs also display an increased fucosylation, a type of glycosylation characterized by the attachment of a fucose sugar to glycolipids (Tinganelli et al., 2020). Fucosylation of proteins regulates adhesion molecules and growth factors receptors (Miyoshi et al., 2008). An *in vitro* study showed that an increase of fucose sugar in the cells affects sphere formation and invasion ability of such circulating cancer stem cells, as well as promotes their migration and metastatic dissemination (Yang et al., 2015).

1.7 Radiotherapy

Radiotherapy is the less invasive and one of the most widely used cancer treatments, with more than 50% of the cancer patients treated with it (Delaney et al., 2005). It can be used alone, or in combination with other treatment modalities such as surgery, chemotherapy or immune therapy. Radiotherapy can be applied before surgery as neoadjuvant therapy in order to shrink the tumor prior to its treatment. It can also be performed after surgery with the intention of destroying any cancer cell that might persist after the treatment reducing their chance of relapse; in this case, it is known as adjuvant therapy (Baskar et al., 2012). The most common types of radiation used to treat patients in radiotherapy are Ionizing radiations (IR), consisting of photons such as X-rays and gamma rays, that by generating ions cause genetic changes in the cancer cells, killing them (Carlos-Reyes et al., 2021). Different organs and tissues show different radiation tolerance, depending on the tissue proliferative rate: if low, tissues show a higher tolerance (Barnett et al., 2009). Radiation dosage is measured using Gray (Gy), defined as the absorption of one joule of radiation energy per kilogram of matter (Van Assendelft et al., 1973).

There are different ways for administering the dose in radiation therapy: fractionation is the most common procedure used in clinic, in which the total amount of radiation required for treatment can be applied by using smaller once-daily doses, in order to minimize the damage to the healthy tissue (Boria et al., 2019). Fractionated RT is administered on a ~2 Gy daily dose, bringing benefits to cancer treatments: for example, hypoxic cells are reoxygenated during fractionation and become radiosensitive (Kepka et al., 2021). Furthermore, fractionation bases on the survival advantage of normal tissue over cancer cells, because normal cells display a slower proliferation rate as opposed to cancer cells, therefore having time to repair the damage before replication starts (Torgovnick et al., 2015). Ionizing radiations (IR) cause direct and indirect damages to the cells. In the direct damage, radiation interacts with the DNA straight away, disrupting the molecular structure by the production of DNA double strand breaks (DSB) (Hur et al., 2017). This change to the DNA leads to cell damage and cell death. Despite this, some cells that are radioresistant are able to survive to this damage and might be able to produce tumor eventually. On the other hand, in the indirect damage radiation hits molecules of water that makes up the most part of the cells and other parts of the cells thus resulting in production of free radicals and reactive oxygen species (ROS) (Desouky et al., 2015). The free radicals produced have a very reactive unpaired electron in the composition, and they react with the DNA causing a damage in its molecular structure, generating DSB or single strand breaks (SSB). Hydrogen peroxide (H_2O_2) is also toxic for the DNA resulting in cell death. Together with

these water radiolysis products, also reactive nitrogen species (RNS) are able to damage the DNA (Figure 16) (Wardman., 2009; Hur et al., 2017).

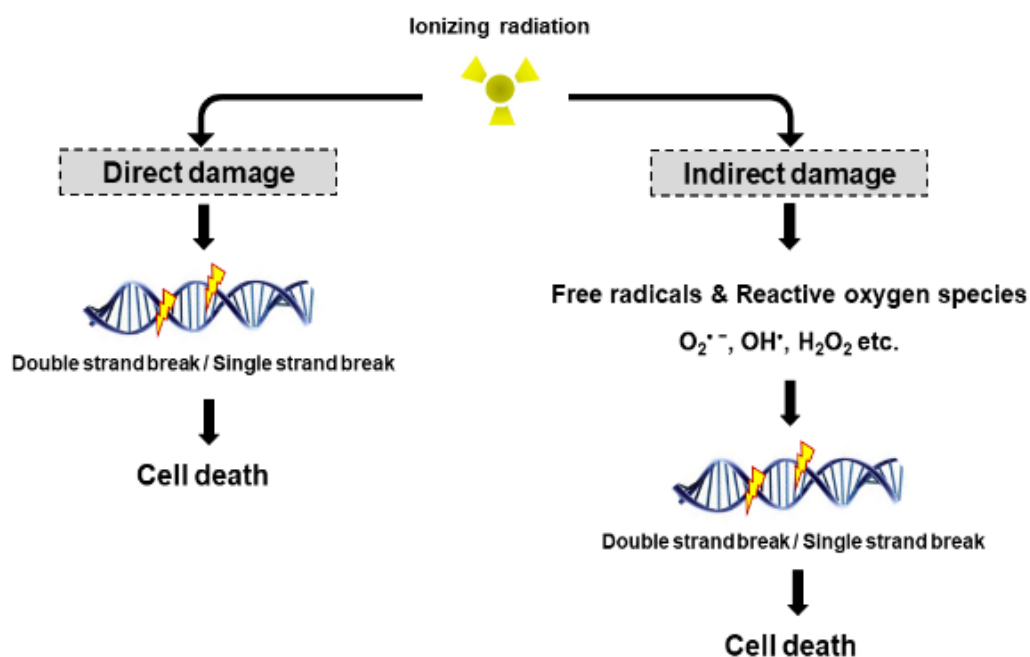


Figure 16. Direct and indirect damage caused by ionizing radiation (Hur et al., 2017).

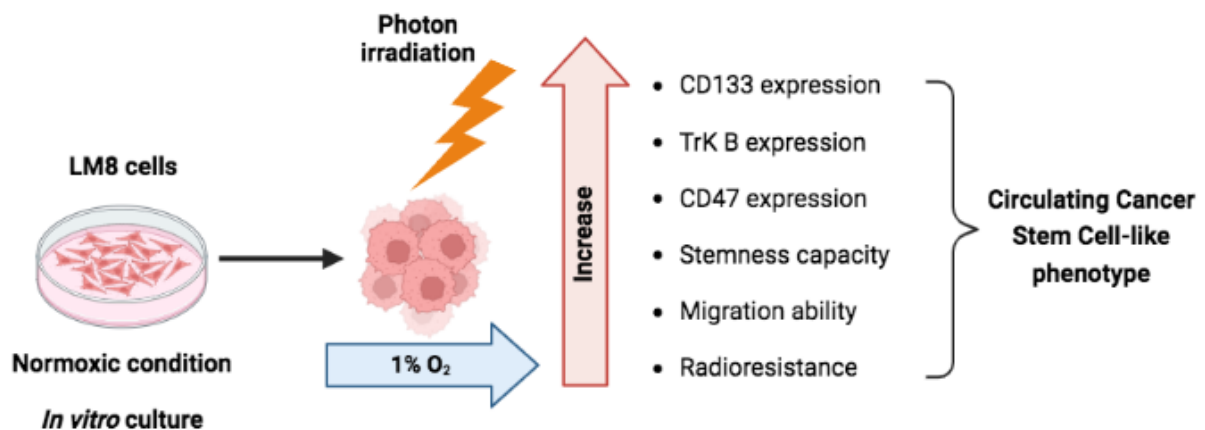
Even though IR is commonly used as treatment for malignancies, it can also promote tumor recurrence and metastasis (Kawamoto et al., 2012; Klopp et al., 2007). It influences the actin reorganization in the cytoskeleton and decreases cell-cell adhesion by downregulation of E-cadherin and upregulation of N-cadherin, thus stimulating EMT process (Kim et al., 2016). IR can induce ROS that activates the EMT process, as well as it activates Snail that is crucial in IR-induced EMT, migration and invasion (Li et al., 2020).

In vitro studies report an increase in cellular migration following irradiation (Panzetta et al., 2020). A good candidate to stimulate cell movement and pre-metastatic niche formation are the exosomes, vesicles released in intracellular space and derived from the fusion of endosomal multivesicular bodies (MVB) with the plasma membrane (Tinganelli et al., 2020). Such vesicles can interact with cells either by ligand-receptor interaction triggering intracellular signalling pathways or they can be incorporated by endocytosis (Thomas et al., 2013). Radiation can induce changes in the amount of these vesicles thus rendering the cells more radioresistant and affecting the migratory potential, local tumor recurrence and metastasis (Mutschelknaus et al., 2017). Moreover, by changing the amount of the exosomes, it increases the number of vesicles that activate Akt pathway that, by triggering MMPs, is involved in cell motility and invasion (Tinganelli et al., 2020). Moreover, IR is able to induce stemness and metabolic alterations in cancer cells: it can enhance the expression of matrix

metalloproteinases (MMPs), in particular MMP-2 and MMP-9 that are relevant for cell invasion and metastasis (Park et al., 2006). MMPs secretion leads to degradation of proteins that compose the ECM, so that the cells loose interaction with ECM and increase in the migration (Moncharmont et al., 2014). Additionally, HIF1 is involved in IR-induced EMT: irradiation increases HIF1 accumulation in the nucleus, and it also induces vascular damage that causes hypoxia (Lee et al., 2017). By disrupting tumor vasculature, IR can cause the release of the viable CTCs in the blood circulation, generating metastasis in distant sites (Koonce et al., 2017). Another cause for tumor relapse might be related to tumor cell’s dormancy. Malignant tumors are composed of dormant cells that possess cancer stem cell features and stay in a quiescent state (Tinganelli et al., 2020). These cells not only are insensitive to ionizing radiation because they are dormant, but also are able to “wake up” after radiation stress, and initiate proliferation and differentiation (Liu et al., 2020).

1.8 Aim of the project

Circulating Cancer Stem Cells are responsible for tumor recurrence and metastasis formation. However, the isolation of these cells *in vivo* is challenging because they are present in low amounts in the circulation. Therefore, in this study, we wanted to isolate the Circulating Cancer Stem Cell-like phenotype with an *in vitro* protocol. Our hypothesis is that stressors such as hypoxia (1% O₂) and radiation (X-rays) contribute to the selection of a subpopulation of cells positive for CD133, with an increased TrK B and CD47 expression, higher stemness capacity, migration activity and radioresistance (Graphical abstract 1). We exposed murine osteosarcoma LM8 cells to 1-week hypoxia (acute hypoxia) and 2-weeks of hypoxia (chronic hypoxia), because we hypothesized that different hypoxic exposition times influence different steps of CCSCs selection.



Graphical Abstract 1: Hypoxia and radiation in selecting Circulating Cancer Stem Cell-like phenotype (created with BioRender).

2. Materials and methods

2.1 Cell culture

Human osteosarcoma cells U2OS (ATCC HTB-96) and highly metastatic murine osteosarcoma cell line LM8 (Cell Bank Riken BioResource Research Center) were used to perform the experiments outlined in this work. Both cell lines were cultivated in Dulbecco's Modified Eagle Medium (DMEM 1X + GlutaMAX-I, Gibco, Bleiswijk, The Netherlands), supplemented with 10% fetal bovine serum (FBS superior, Sigma, Brazil) and 1% Penicillin-Streptomycin (10,000 U/ml Penicillin, 10 mg/ml Streptomycin, Pan Biotech, Aidenbach, Germany). The cells are cultivated in a humidified 5% CO₂ incubator at 37° C. Normoxic cells were maintained at 21% O₂ concentration (74% N₂, 1L of H₂O for humidification and 5% CO₂ composition), while hypoxic cells were cultured under 1% O₂ concentration inside of a hypoxic working station In VivO₂ 400 (Baker Ruskin, United Kingdom). The specific parameters for the incubator setup were 94% N₂, 1% O₂ and 5% CO₂, with 65% humidity and at 37°C. Cells were exposed to hypoxia for one week (acute hypoxia) and two weeks (chronic hypoxia). The cells continuously maintained inside the hypoxic working station to avoid sample reoxygenation. For the passage, the cells have been washed with Dulbecco's Phosphate Buffered Saline (Sigma Aldrich, United Kingdom), trypsinized with 1 mL of Trypsin-EDTA (0.05%/0.02%, Pan Biotech, Aidenbach, Germany) and reseeded with a dilution of 1:20.

2.2 U2OS Migration Assay

To investigate the migration capacity of U2OS, a scratch wound analysis was used. Cells were seeded in 60 mm petri dishes (TPP Techno Plastic Products, Switzerland) at a density of 400.000 cells for Normoxia and 600.000 cells for hypoxia. When the cells reached confluence, they were treated for 24h with 400 µg/ml of Mytomycin-C, an antineoplastic antibiotic that, by inhibiting DNA synthesis, is used to reduce the cell proliferation (Grada et al., 2017). Thereafter, centrally placed wounds were created by streaking the plastic tip of a pipette across the cell monolayer, and pictures of the scratch were taken at intervals of 0h, 4h, 6h and 24h, with the Motic AE31 microscope (camera: Moticam 3+ 3.0 MP; ocular lenses: WFPL 10×; objective lenses: 4×/ 0.10 ∞/- WD 23.5). The scratch was analyzed by measuring the wound's width at different time points. Three replicates were performed for the experiment, with 5 photos analysed for each scratch.

2.3 U2OS hanging drop

We used the hanging drop technique to investigate the U2OS capacity of forming spheres (Berens et al., 2015). Cells were detached from the flasks, centrifuged at 200xg for 5 minutes and the pellet was resuspended in 2 ml of complete medium. Afterwards, cell count was performed with the Biorad cell counter TC20 (Biorad, Berkley California) and cells were diluted to obtain a density of 4 million cells/ml. 10 drops of 10 ml of volume were seeded in the inside of the lid of a 60 mm petri dish, while 5 ml of Phosphate Buffered Saline (PBS) was placed at the bottom of the dish. The lid with the drops was then flipped and the closed petri dish was kept respectively in normoxic and hypoxic conditions for 6 days. Three replicates were performed for this experiment. Pictures were taken daily, using Motic AE31 microscope (camera: Moticam 3+ 3.0 MP; ocular lenses: WFPL 10×; objective lenses: 4×/ 0.10 ∞/- WD 23.5). Moreover, U2OS sphere formation was also tested with ultra-low attachment plates, whose protocol can be found in paragraph 2.6.

2.4 Photon irradiation

Photon irradiations were performed using an X-ray generator Isovolt DSI (Seifert, Ahrensberg), 7 mm beryllium, 1 mm aluminum and 1 mm copper filter system, operating at 250 kV and 16 mA. The dose rate was determined by an ionization chamber (SNA4, PTW Freiburg, Germany). To perform the experiments we used a dose rate of 2 Gy/min. Irradiation in hypoxia was performed by putting the flasks inside a CondoCell box (Baker Ruskinn, United Kingdom) allowing them to preserve the hypoxic environment (1% O₂) for the entire irradiation time.

2.5 Clonogenic Survival Assay (CSA)

The CSA was performed with LM8 murine osteosarcoma cells. LM8 were seeded at a density of 250.000 cells in T25 flasks and maintained in incubators (21% O₂ and 1% O₂) for 48 hours. The cells were irradiated with X-rays doses of 0 Gy, 2 Gy, 4 Gy, 6 Gy and 10 Gy under normoxia and hypoxia conditions. Three replicates for the experiment were performed. For hypoxic irradiation, flasks were transported and irradiated inside a CondoCell hypoxic isolation box (Baker Ruskinn, United Kingdom). After irradiation, cells were counted and re-seeded in triplicate in T25 flasks and kept in a 21%O₂ incubator for ten days to allow the formation of colonies. Colony staining was performed with methylene blue and only colonies with more than 50 cells were counted. For the analysis, the Plating Efficiency (PE) was considered according to the following equation:

$$PE = \frac{\text{number of colonies formed}}{\text{number of cells seeded}} \times 100\%$$

The survival (S) was then calculated:

$$S = \frac{(\text{Average number of colonies formed})}{\frac{\text{number of cells} \times \text{volume to seed}}{1000}}$$

To plot the graph, the ratio between Survival and Plating Efficiency was calculated, normalizing the values on the control dose (0 Gy).

2.6 LM8 immunocytochemistry (ICC) staining

50.000 LM8 cells were seeded in coverslips and maintained respectively in normoxic and hypoxic incubators. At the end of experiment, the medium was removed from the coverslips, and 4% PFA solution (Roth, Karlsruhe, Germany) was added for sample fixation and left in incubation for 20 minutes. Followed by adding Triton X-100 0,01% (Roth, Karlsruhe, Germany) in PBS for 15 minutes, and after the Triton is removed, a solution of 3% BSA in PBS (PanReac Applichem, Darmstadt, Germany) is added for one hour, to block the unspecific binding. Subsequently Rhodamine Phalloidin antibody (Invitrogen, USA, dilution 1:500) is applied to the coverslips for staining the cytoskeleton of the cells and left to incubate for one hour at room temperature in a dark place. We used DAPI (Sigma Life Science, Germany, dilution 1:1000) for counter staining of the cells. After the incubation, coverslips are washed and are applied on the glass slides (Star Frost microscope slides, 76x26 mm), followed by PermaFluor mounting medium (Thermo Scientific, USA). 6 pictures of the cells, with three replicates, were taken using Leica DMI 4000B confocal microscope (ocular lenses: HC PLAN 10×; objective lenses: ∞/-/D ACS APO 20×/ 0.60 IMM). Pictures were analyzed with LASX 1.4.4 software. A detailed description of the material used for ICC can be found in Table 1.

Table 1: Solutions and antibodies used for immunocytochemistry

Paraformaldehyde (PFA): 37% Stock solution, Roth, Karlsruhe, Germany.
Triton X-100: Roth, Karlsruhe, Germany.
BSA Albumin Fraction V (pH 7), PanReac Applichem, Darmstadt, Germany.
Rhodamine Phalloidin (F-actin) antibody R415, 1:500, Invitrogen, USA, RRID:AB_2572408.
DAPI: D9542-1 MG, 1:1000, Sigma Aldrich, Germany.
Mountant PermaFluor, Thermo Scientific, USA.

2.7 LM8 Sphere formation and migration assay

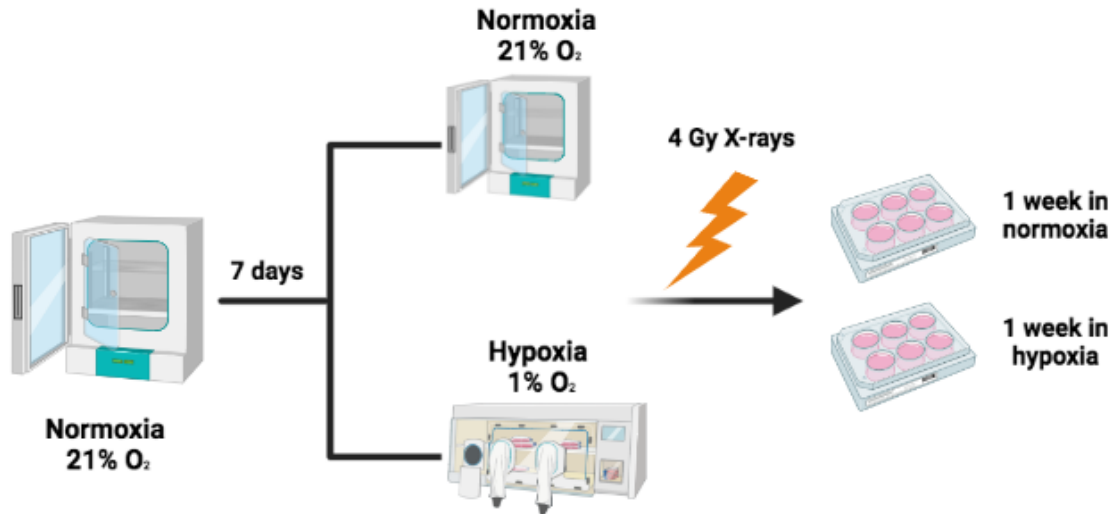
LM8 cells were cultured in normoxia for one week, then irradiated with 4 Gy X-rays dose, counted with a cell counter (Beckman Coulter, USA) and 30.000 cells were seeded in triplicate in each well of ultra-low attachment 6-well plates (Greiner Bio-one, Germany). After seeding, the plates were maintained for one week respectively in incubators at 21% O₂ and 1% O₂ (acute hypoxia), to allow the cells to form floating spheres. In parallel with this setup, LM8 were also cultivated in hypoxia for one week, irradiated in hypoxic environment, seeded in plates and kept for another week in 1% O₂ environment (Chronic Hypoxia). Afterwards, sphere formation efficiency was evaluated according to the following equation:

$$\text{Sphere formation efficiency (\%)} = \frac{\text{Number of spheres}}{\text{Total number of cells}} \times 100$$

To investigate migration capacity, spheres were embedded in collagen (Collagen I, rat tail, Enzo Life Sciences), with 6 samples analysed for each of the three independent experiments, and pictures were taken after 24h and 48h timepoints using Motic AE31 microscope (camera: Moticam 3+ 3.0 MP; ocular lenses: WFPL 10×; objective lenses: 4×/ 0.10 ∞/- WD 23.5). The following formula was used for the analysis:

$$\text{Area of migration} = \text{External area of migration} - \text{Internal area of the sphere}$$

A visual description of the experiment is presented in Experimental Design 2.



Experimental Design 2: LM8 sphere formation efficiency workflow (created with BioRender).

2.8 Western blot

Cells (U2OS and LM8) were irradiated with 4 Gy X-rays and maintained respectively in T75 flasks and ultra-low attachment six well plates, at 21% O₂ and 1% O₂. 1 week after, cells were harvested on ice with 200 µL of RIPA-buffer (Table 2-3). Sham controls have been made for comparison. Scraped cells are collected in 1,5 ml Eppendorf tubes and incubated for 30 minutes on ice, followed by 15 minutes of centrifugation at 14.000 rpm. Afterward, the supernatant is collected for protein quantification and further experiments. Protein quantification was performed with the DC protein Assay Kit from BioRad (Bio-Rad DC Protein Assay Kit 2, USA, N° 5000112). Equal amounts of protein (15–25 µg/lane) were subjected to SDS-PAGE and transferred to Immobilon-P polyvinylidene difluoride membranes (Merck Millipore). The membranes were incubated with primary and secondary antibodies (Table 4-5) and peroxidase activity was detected using chemiluminescence reagents (Pierce ECL western Blotting Substrate, Thermo Scientific, Rockford, USA) then visualized with image analyzer Fusion software (Fusion FX Vilber Lourmat, Peqlab).

Table 2: 10X RIPA compounds

1,752g NaCl, Sigma Aldrich, Germany
2 ml Triton-X-100, Carl Roth, Germany
1g deoxycholic acid, Sigma Aldrich, Germany
1 ml 20% SDS, Applichem, Germany
6,67 ml 1,5M Tris pH 8,0, Carl Roth, Germany
Fill to 20 ml with ddH ₂ O

Table 3: Details of RIPA buffer

1×RIPA (compounds can be found in Table 2).
1× Halt Protease Inhibitor, Thermo Scientific, Germany
1mM Na-Orthovanadat, Alfa Aesar, Massachusetts, USA
2 mM Na-Fluorid, Sigma Aldrich, Germany
ddH ₂ O to bring to the volume needed

Table 4: List of primary antibodies used.

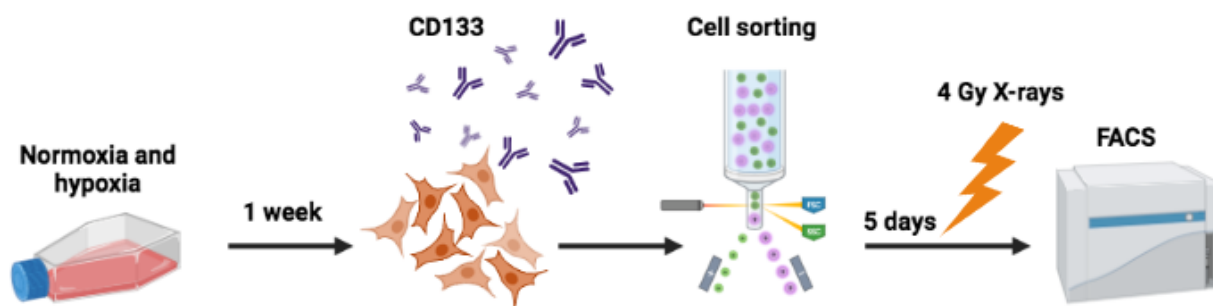
CD 133, Prominin 1 antibody, 1:1000, Abcam, RRID: AB_470302.
CD47 Polyclonal Antibody, 1:1000, Invitrogen, RRID: AB_2899620.
HIF1a Polyclonal Antibody, 1:1000, Bethyl laboratories, USA, RRID: AB_2117114.
E-cadherin Monoclonal Antibody, 1:500, Invitrogen, USA, RRID: AB_86564.
N-cadherin monoclonal antibody, 1:500, Cell Signaling Technology, RRID: AB_2687616.
Monoclonal Anti-β-Actin Antibody, 1:10000, Sigma-Aldrich, RRID: AB_476744.
Anti-GAPDH antibody, 1:5000, Sigma-Aldrich, RRID: AB_796208.

Table 5: List of secondary antibodies used.

Goat Anti-Mouse IgG (H L)-HRP Conjugate antibody 1:3000, Bio-Rad, RRID:AB_11125547.
Goat Anti-Rabbit IgG (H L)-HRP Conjugate antibody, 1:3000, Bio-Rad, RRID:AB_11125142.

2.9 CD133 cell sorting

LM8 is cultured in T75 flasks for one week (21% O₂ and 1% O₂), harvested in Accutase (Sigma-Aldrich, St. Louis, USA) to preserve cell surface markers from degradation, and centrifuged at 100g for 5 minutes. The supernatant is discarded and cells are re-suspended in 1.5 ml of sterile PBS (Sigma Aldrich, United Kingdom) before incubating with CD133 antibody (abcam ab19898, 1:200 dilution). After 1 hour of antibody incubation on the rotator, cells are washed with PBS and incubated for 1 hour with 3 µl of Alexa Fluor 488 goat anti-rabbit IgG. Cells are then filtered with 5 ml Polystyrene Tube with Cell-Strainer Cap (Falcon 352235) and then sorted using a cell sorter (S3e Cell Sorter, Bio-Rad, Germany). After sorting, CD133+ cells are seeded in T75 flasks, kept for five days in the incubator to allow them to grow and then irradiated with 4 Gy X-rays. After irradiation, samples are harvested for Fluorescent Activated Cell Sorting (FACS) analysis, which is further described in paragraph 2.10. The Experimental Design 3 illustrates the cell sorting workflow.



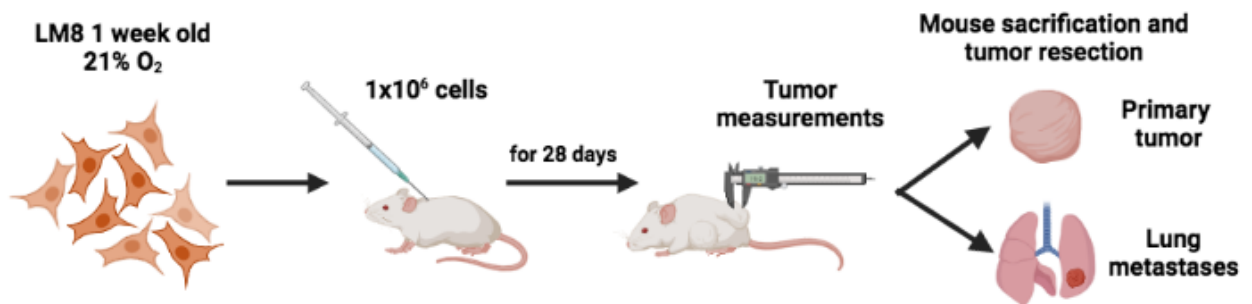
Experimental Design 3: CD133 cell sorting workflow (created with BioRender).

2.10 CD133+ FACS analysis

CD133+ sorted cells (for sorting protocol refer to paragraph 2.9) are harvested with Accutase (Sigma-Aldrich, St. Louis, USA), washed with PBS and incubated with TrK B antibody (1:50, Biorbyt, United Kingdom) for 30 minutes at room temperature, in the dark. Afterwards, cells are washed and re-suspended in 100 μ l of PBS and measured using a Flow Cytometer (CytoFLEX, Beckman Coulter, USA). Gating strategy for the analysis is performed using a Viability Dye (VivaFix 649/660, Biorad) to discriminate between living and dead cells and only viable cells are considered for the analysis. Data analysis is performed with the CytExpert v2.5 software.

2.11 LM8 injection in mice

LM8 cells were cultivated in 21% O₂ condition for 1 week and subsequently 1×10^6 cells were injected in the back of the neck (for histology of the lungs) or posterior limb (for blood extraction) of the animals. To monitor tumor growth, tumor size was measured with a caliper three times per week, for a maximum of 28 days. After 28 days, the animals were sacrificed and primary tumor and lungs were collected for further histological analysis and for counting the number of metastasis (Experimental Design 4).



Experimental Design 4: LM8 injection in mice workflow (created with BioRender).

2.12 CTC extraction from mice blood with magnetic beads

We based our analysis on the samples collected from an *in vivo* parasitic experiment (ethical permission number: DA17/2000). After animals were sacrificed, blood was collected over 5 distincted mice samples, to perform CTC isolation. Magnetic beads (Dynabeads FlowComp Flexi, Invitrogen, Germany) were used for the extraction. Dynabeads were re-suspended in the vial and added to a tube with 1 ml of Isolation Buffer. The washing step was performed by placing the tubes

with the beads in a Dynamag-2 magnet (Invitrogen, Germany), discarding the supernatant and washing the beads with the previous amount of buffer.

A biotinylated CD133 antibody (Abcam) was prepared and a volume of 25µl was added to the buffy coat of the sample. After 10 minutes of incubation at 4°C, 1 ml of Isolation Buffer was added and samples were centrifuged for 10 minutes at 350 x g. After removing the buffer, 75 µl of beads were added and samples were incubated on a rotating rotor for 15 minutes followed by adding 1 ml of Isolation Buffer, and the tube was then placed in the magnet. Supernatant was discarded and the procedure was performed again for washing. Afterwards, samples were re-suspended in 1 ml of Release Buffer and incubated for 10 minutes in the rotating rotor. Tubes were placed in the magnet, and the supernatant bead-free was transferred to a new tube and used for analysis. A detailed table with the solutions used can be found below (Table 6).

Table 6: Solutions used for magnetic beads.

FlowComp Dynabeads, Invitrogen, Germany
FlowComp Release Buffer, Invitrogen, Germany
DSB-X Biotin Protein Labelling Kit, Invitrogen, Germany

2.13 Cryostat sample preparation

The primary tumor and lungs were collected from four animals, from an *in vivo* parasitic experiment (ethical permission number: DA17/2000), and stored overnight at four °C in 4% PFA. The organs are transferred into the step of 10%, 20% and 30% sucrose solution (Roth, Karlsruhe, Germany) until equilibriate. Afterward, organs are washed with PBS, and are embedded with OCT (Optimal Cutting Temperature) compound (Tissue-Tek, Sakura Finetek, Germany). Samples are cutted at the cryostat (Leica CM1860 UV, Leica Biosystems, Nussloch, Germany), with a 15 µm thickness, and a temperature of -20°C.

2.14 Immunohistochemistry (IHC) staining

Six slides per organs have been prepared for the analysis. After cutting, glass slides (SuperFrost Plus Adhesion Microscope Slides, EpreDia, Germany) have been washed with PBS to remove the excess of OCT around the samples carefully. Coverslips are then incubated for 5 minutes at 3% H₂O₂ in PBS, washed twice with PBS and then incubated for 20 minutes with Blocking Buffer solution.

Afterwards, CD133 and CD47 primary antibodies (Table 3) are added to the respective samples, and incubation is performed for 1h at RT. After one wash, biotinylated secondary antibody is added for 30 minutes at RT. Tissues are then incubated for 30 minutes with ABC solution and then incubated for a maximum of 3 minutes with the DAB staining (for sample visualization). Details of all the material can be found in Table 7. For the counterstaining, samples are treated with hematoxylin (Hematoxylin Solution, Gill No.3, Merck) for 15 seconds and then rinsed with water. Afterwards, samples are dehydrated respectively with 96% of ethanol, 100% of ethanol and two times xylol and then mounted with Eukitt. Photos are taken using fluorescent microscope Olympus BX61 (camera: Olympus EP50; ocular lenses: WH1010×; objective lenses: UPlan FL N 20×/0.50 Ph1 ∞/0.17/FN26.5).

Table 7. Solutions used for IHC staining.

Ultra-Sensitive ABC Peroxidase Rabbit igG Staining kit, Thermo Fisher Scientific, Germany.
DAB Substrate Kit, BD Pharminogen, RRID: AB_2868905.
Aquatex mounting agent, Merck, Germany.
Blocking Buffer: 3 drops of Normal Serum (ABC Kit) to 10 ml PBS.
Biotinylated secondary antibody: 3 drops of normal serum and 1 drop of Biotinylated secondary antibody to 10 ml PBS.
ABC reagent: 4 Drops of Reagent A + 4 drops of reagent B in 10 ml PBS.

2.15 Statistical analysis

Statistical analysis was performed using the student's t-test. Values of $p < 0.05$ were considered statistically significant. All analysis were performed using ImageJ 1.53t software (Java 1.8.0_345 64-bit version), LASX 1.4.4 software, QuPath software (0.3.0 version) and GraphPad Prism 9 software.

3. Results

3.1 Migration ability and sphere formation capacity: preliminary results using the U2OS cells.

CCSC are cancer stem cells that undergo EMT transition, characterized by the E-cadherin/N-cadherin switch, moving towards a more mesenchymal phenotype (Loh et al., 2019). They are characterized by an increased migration capacity and increased ability to form spheres (Cao et al., 2011). In this study we used human osteosarcoma cell line U2OS to investigate the migration ability of the cells when exposed to hypoxia (1% O₂). Three independent experiments were done. Our findings show a slight difference in the normoxic cells, where the average wound width changes from 3.18 cm ± 0.1 (SEM) at 0h to 2.7 cm ± 0.2 (SEM) after 24h.

No migration instead was observed in the hypoxic samples (average size of the scratch at 0h: 2.3 cm ± 0.1 (SEM); average size of the scratch at 24h: 2.22 cm ± 0.1 (SEM) (Figure 17).

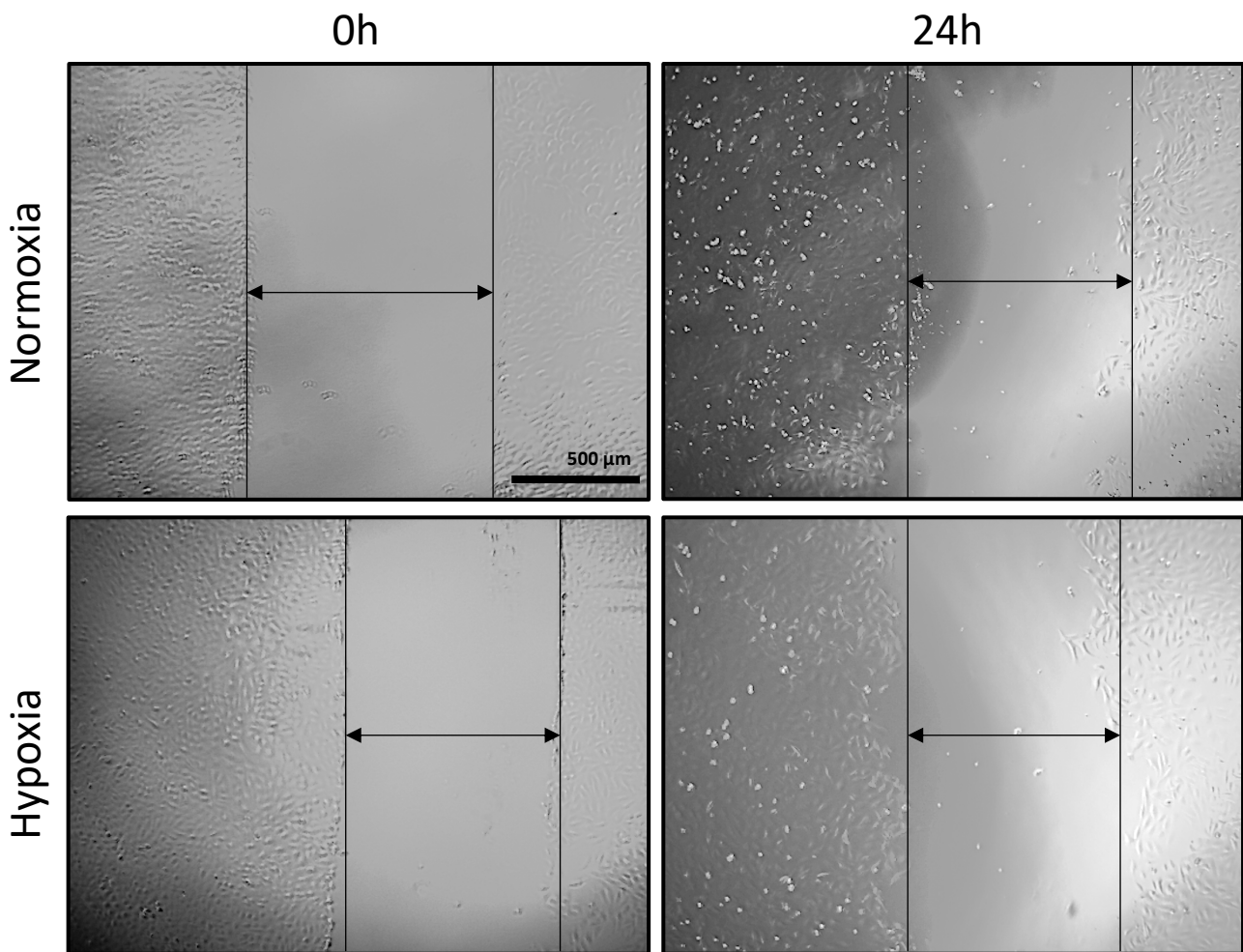


Figure 17. Migration assay of U2OS cells. Comparison done between normoxia and hypoxia cells, with 0h and 24h timepoints. 4× magnification, Motic AE31 microscope. Width of the scratch measured: Normoxia 0h (3.18 cm), normoxia 24h (2.7 cm); Hypoxia 0h (2.3 cm), hypoxia 24h (2.22 cm).

Furthermore, we conducted additional research to see whether these cells can undergo EMT transition after hypoxia and radiation (4 Gy X-rays). We analyzed E-cadherin and N-cadherin expression through western blot techniques (as seen in Fig.18A). Our findings revealed that U2OS cells express E-cadherin and N-cadherin under normal oxygen levels. However, its expression decreases when subjected to hypoxia alone or in combination with radiation (Fig.18A, B, and C), demonstrating the loss of the epithelial but not the increase of the mesenchymal feature.

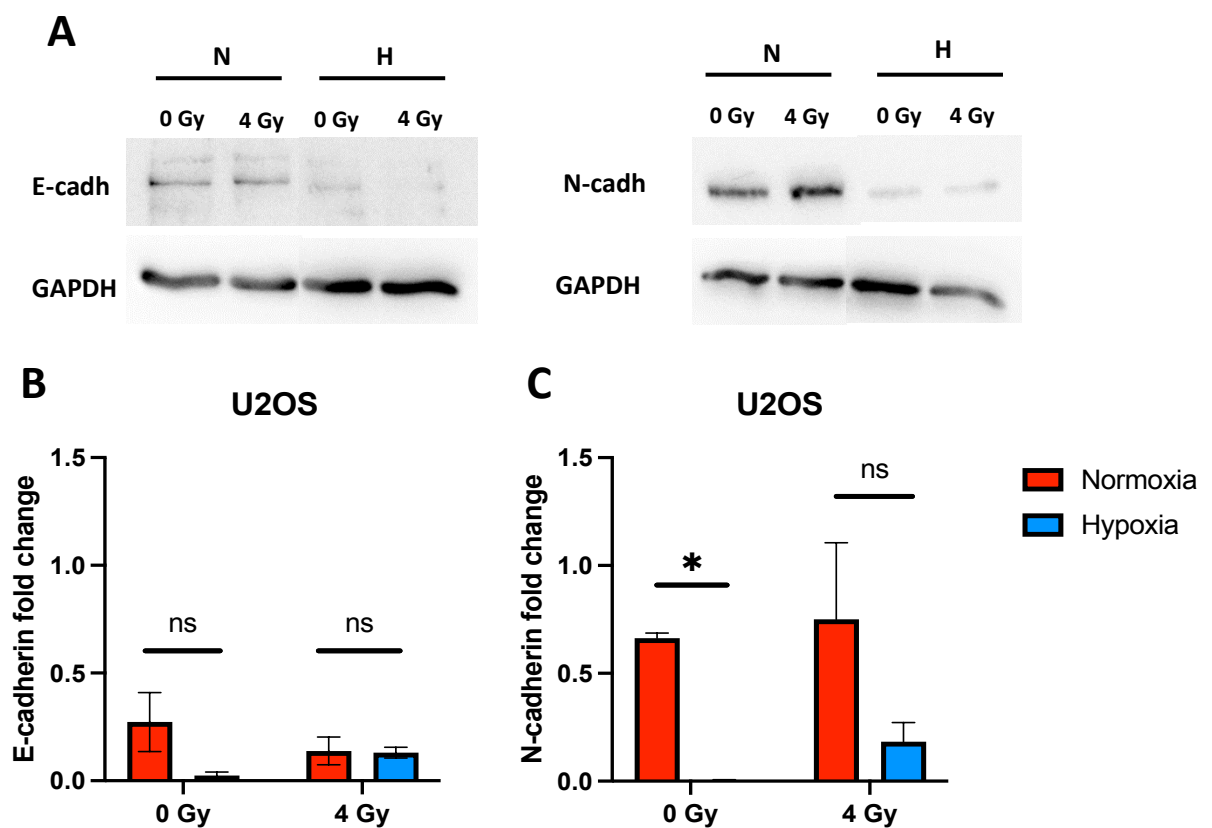


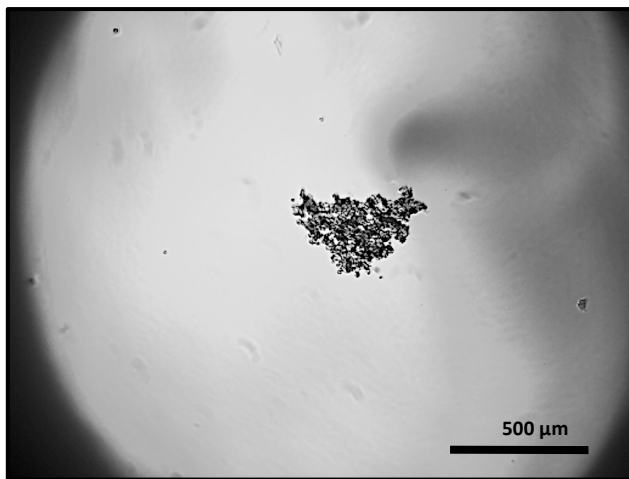
Figure 17. Figure 18. Western Blot analysis of E-cadherin and N-cadherin. (A) representative picture of Western Blot, (B) mean densitometry of E-cadherin relative to GAPDH expressed as arbitrary units. *Hypoxic cells vs normoxic control cells. \pm SEM, $P < 0.05$ and (C) mean densitometry of N-cadherin relative to GAPDH expressed as arbitrary units. *Hypoxic cells vs normoxic control cells. \pm SEM, $P < 0.05$

In the current experiment, a proper cadherin switch was not evident; we further investigated whether U2OS possess the capacity of forming spheres, by using the hanging drop technique. Results show that U2OS were not able to form proper spheres, with the tendency to generate aggregates of cells (Fig. 19A). No difference was observed comparing cells in normoxia and hypoxia without irradiation. The irradiated samples, instead, show a reduced tendency to aggregate, with no significant differences

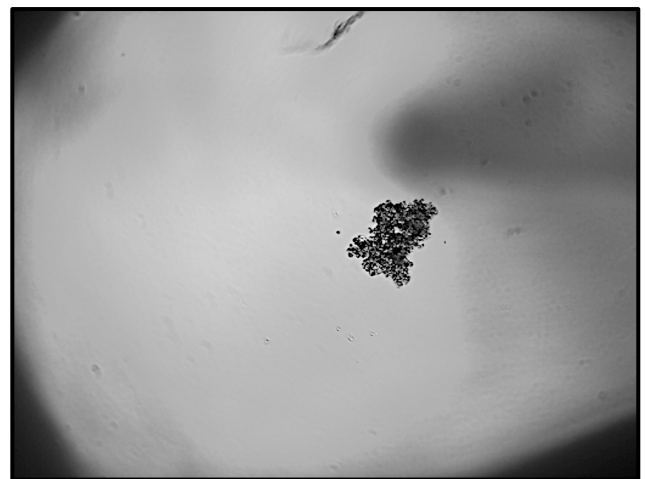
between normoxia and hypoxia. Moreover, we tried to assess the sphere formation capacity also with another technique, and we seeded the cells using ultra-low attachment well plates (Gao et al., 2018). We observed that U2OS were still not able to form proper spheres, but they displayed the tendency to aggregate. Less aggregates were found in hypoxia, compared to normoxia (Figure 19B). Therefore, we proceeded using another cell line, a murine osteosarcoma (LM8) cell line, that is not already differentiated like the U2OS and it is well known in literature for its stemness capacity and for being a highly metastatic cell line when injected subcutaneously in C3H mice (Tanaka et al., 2013; Tinganelli et al., 2022).

A

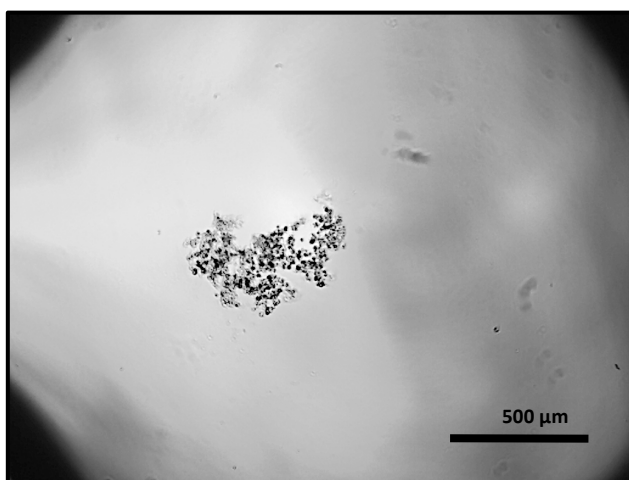
Normoxia 0 Gy



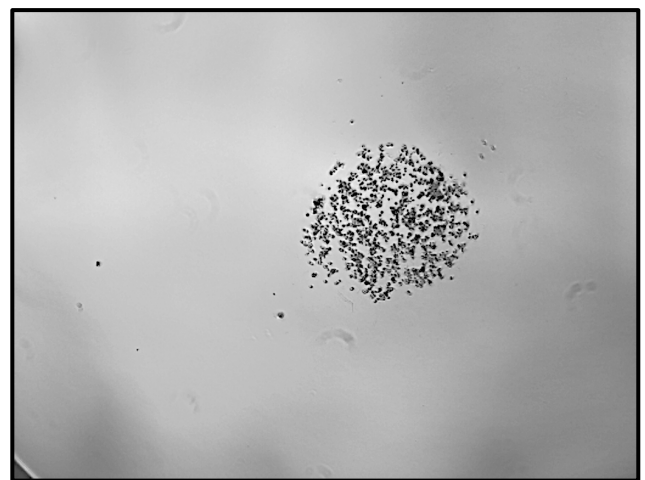
Hypoxia 0 Gy



Normoxia 4 Gy



Hypoxia 4 Gy



B

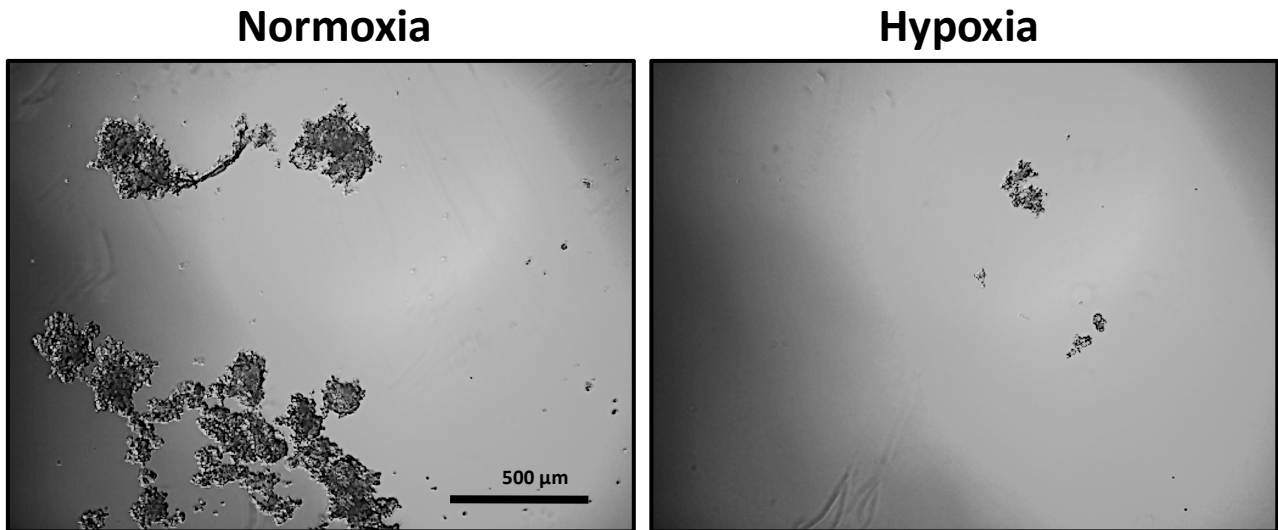


Figure 18. Sphere formation with U2OS. Comparison between normoxia and hypoxia. 4× magnification, Motic AE31 microscope. (A) Hanging drop technique (Normoxia vs Hypoxia, 0 Gy and 4 Gy) and (B) ultra-low attachment plate technique.

3.2 Clonogenic Survival Assay: a comparison between normoxia and acute hypoxia

The radiosensitivity of LM8 cell line in normoxia (21% O₂) and acute hypoxia (1% O₂, for 1 week) has been investigated by clonogenic survival assay (Figure 20). To perform the experiment, doses of 2, 4, 6 and 10 Gy have been delivered to the cells. Sham irradiated samples have also been prepared. Results show a slight increase in the survival of hypoxic cells, displaying an OER of 1.15 (Normoxia alpha value: 0.1386, beta value: 0.0480; Hypoxia alpha value: 0.1257, beta value: 0.0382). In literature is reported that Cancer Stem Cells and Circulating Tumor Cells are resistant to radiation (Schulz et al., 2019). To test their radioresistance and to select these cell subpopulation in the further experiments, we administered a 4 Gy dose of radiation.

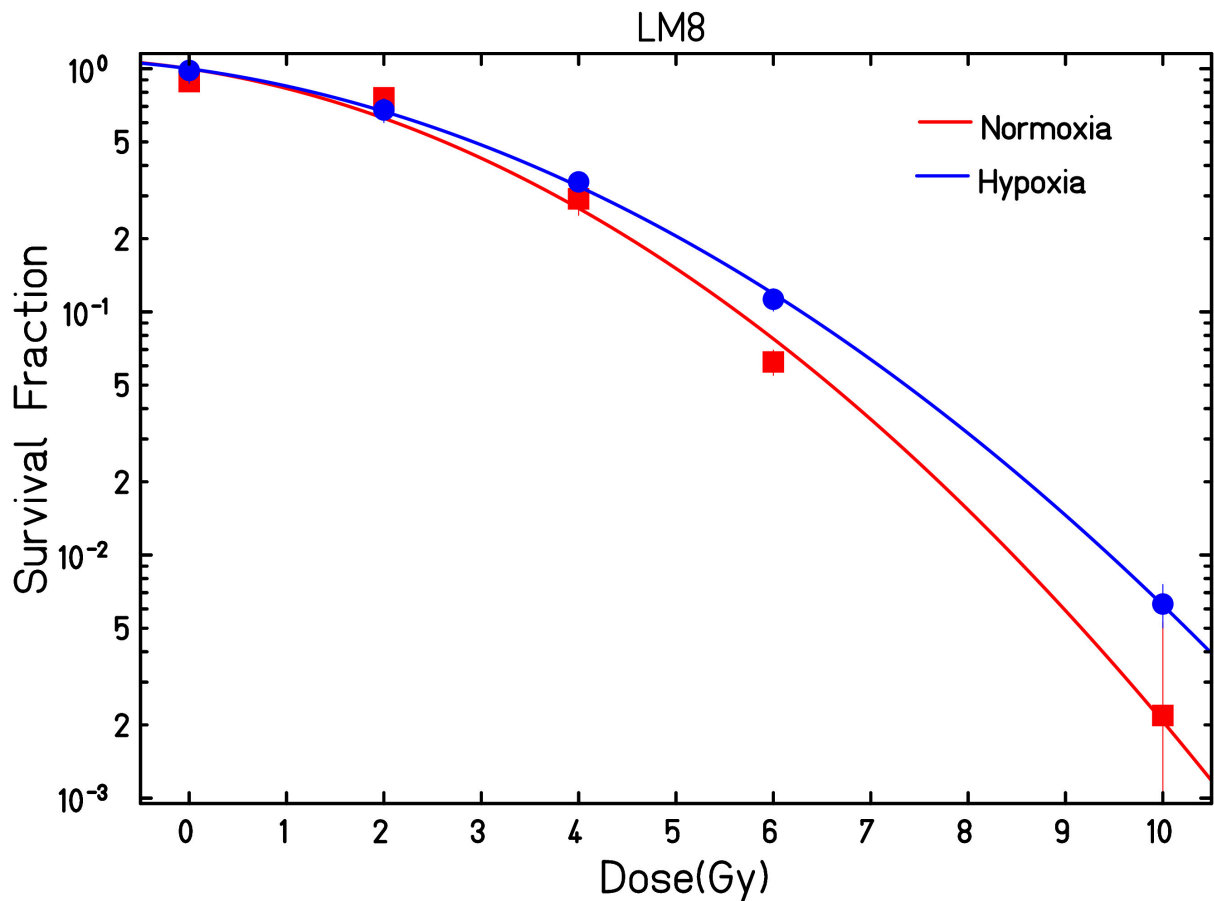


Figure 19. Clonogenic Survival Assay (CSA) of LM8 cell line: comparison between normoxia (21% O₂) and hypoxia (1% O₂).

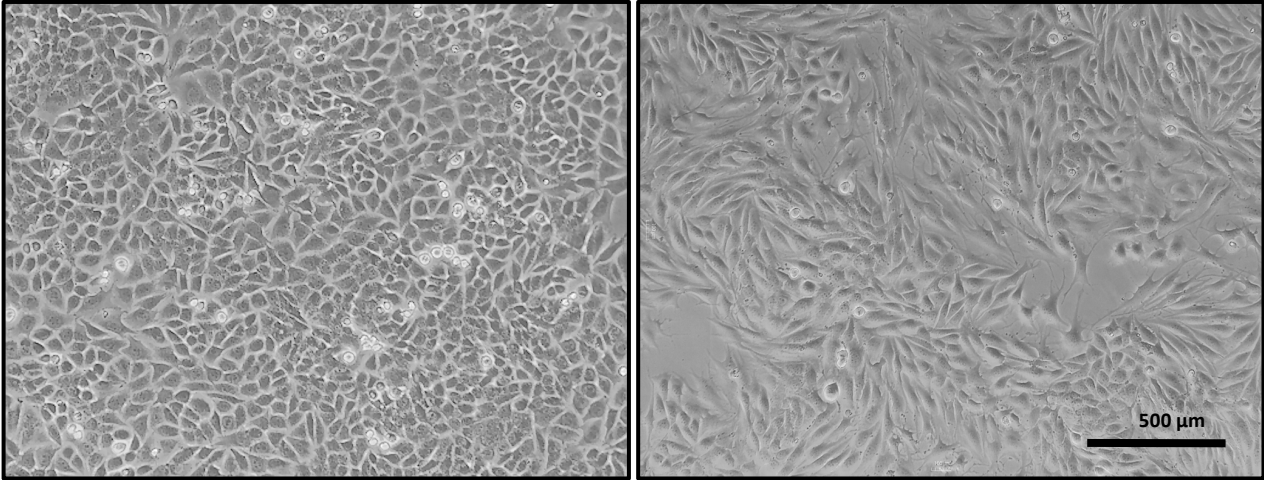
3.3 Hypoxia influences morphology of LM8 cells

To study the effect of hypoxia on the LM8 phenotype, cells were cultivated in normoxic and in 1% O₂ for 1 week. LM8 cells cultivated in normoxia display a round-shaped morphology and are fast growing, with a doubling time reported to be 13h (Asai et al., 1998). We observed that the hypoxic cells are characterized by a slower growth rate that is 24h, and appear to have more elongated shape, resembling the phenotype of more aggressive cancer cell type (Figure 21 A and B). These results are also evident in other studies by Northcott et al., 2018. Furthermore, the actin filament assembly also shows different architecture between normoxia and hypoxia, as shown in figure 21B.

A

Normoxia

Hypoxia



B

Normoxia

Hypoxia

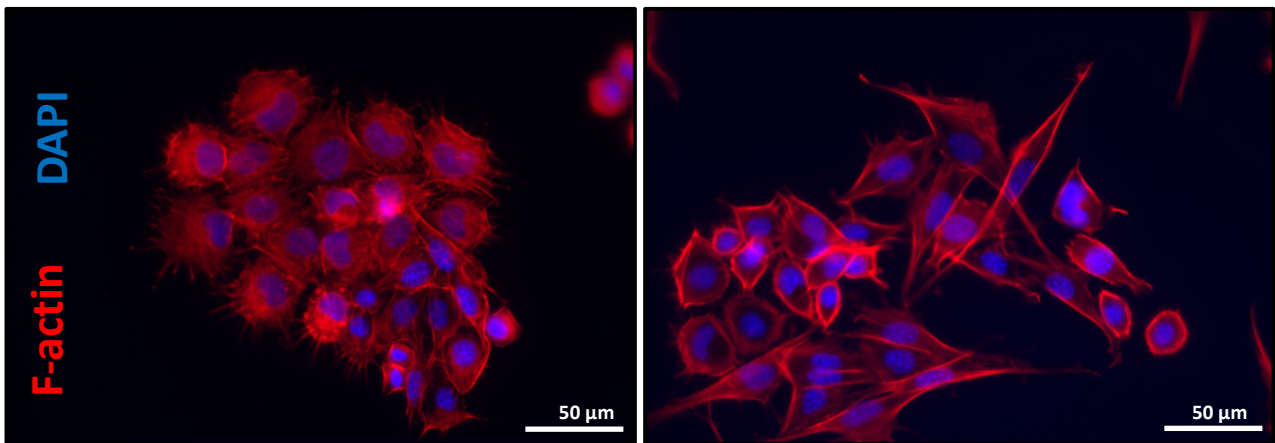


Figure 20. Morphological analysis of LM8 cells. (A) Normoxia (left) vs Hypoxia (right), 4X magnification, Motic AE31 microscope. (B) F-actin cytoskeleton analysis of LM8 comparing Normoxia and Hypoxia with a focus on the architecture of the actin filament assembly, 20X magnification, Confocal microscope, Leica microsystems.

We conducted a study to see if radiation affects the expression of E- and N-cadherins. Our western blot findings indicate no expression of these cadherines after radiation exposure, both under normoxia and hypoxia conditions (as shown in Figure 22).

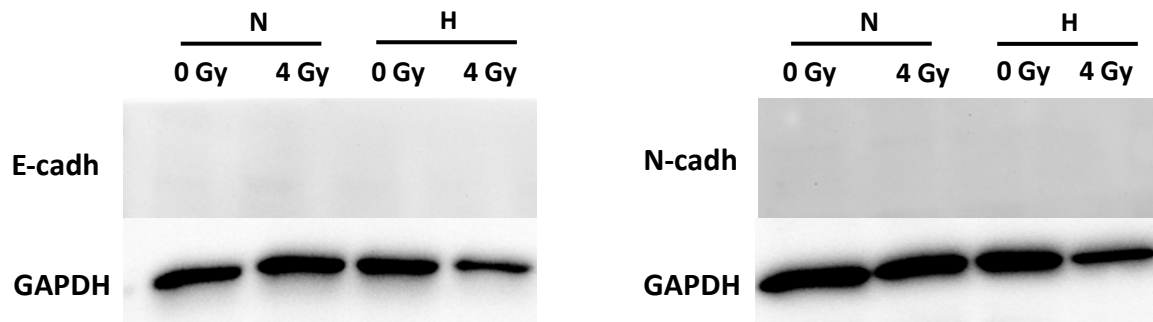
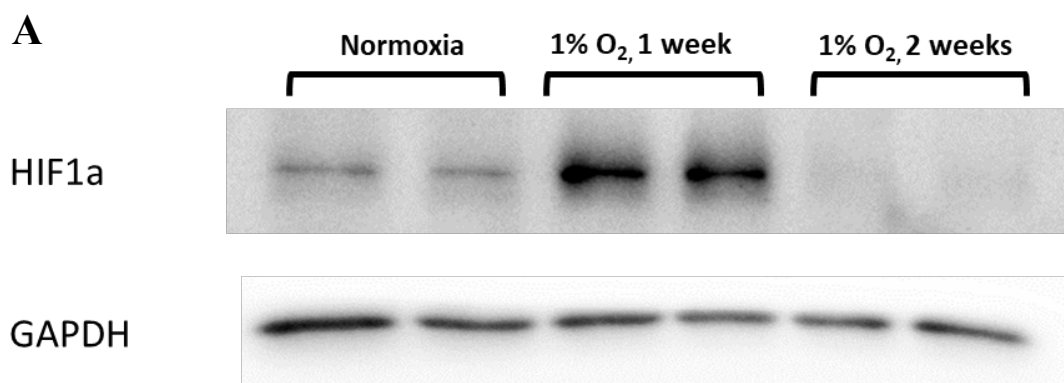


Figure 21. Western Blot analysis of E-cadherin (left) and N-cadherin (right) expression in LM8 murine osteosarcoma cell line.

3.4 Investigating the hypoxia inducible factor status of LM8 cells under hypoxia

Acute hypoxia is characterized by an overexpression of HIF1 α ; however, this marker decreases under chronic hypoxia, counterbalanced by an increase in HIF2 α expression (Roig et al., 2019; Saxena et al., 2019). Acute and chronic hypoxia trigger different sets of genes. According to Al Tameemi et al., 2019, the cells exposed to chronic hypoxia have a more aggressive phenotype.

We cultivated the LM8 cells in hypoxia (1% O₂) for one or two weeks. To determine whether the cells were in chronic or acute hypoxia we investigated the HIF1 α protein expression after 1 and 2 weeks of hypoxia. The cells exposed to 1 week of hypoxia showed an increase in HIF1 α expression, indicating that they were still in the acute hypoxic phase. On the other hand, the HIF1 α expression decreased after two weeks of hypoxia, suggesting the switch from acute to chronic hypoxia. Therefore, we refer to one week hypoxia as "acute hypoxia" and 2 weeks hypoxia as "chronic hypoxia" (see Figure 23).



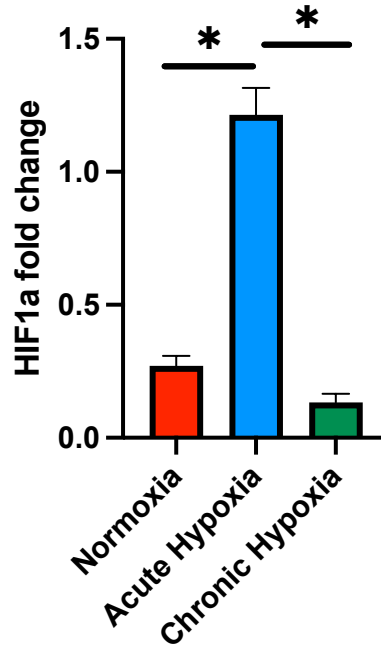
B**LM8**

Figure 22. HIF1 α expression levels in LM8 cells: (A) Western Blot analysis comparing normoxia, acute hypoxia (1 week) and Chronic hypoxia (2 weeks) and (B) mean densitometry of HIF1 α relative to GAPDH expressed as arbitrary units. *Hypoxic cells vs normoxic control cells. \pm SD, $P < 0.05$.

3.5 Hypoxia increases CD133 expression

To investigate the effects of hypoxia in increasing the CD133 expression on the LM8 cells, we measured the protein expression by western blot analysis. The LM8 cells express CD133 under normoxia, with approximately 0.5-fold change value compared to the housekeeping gene β -tubulin. Investigating whether hypoxia influences the expression of CD133, we observed that both acute and chronic hypoxia increase CD133, showing a fold change between 1.0 ± 0.19 (SEM) and 1.5 ± 0.07 (SEM) (Figure 24). However, there were no differences in the expression of CD133 between the control and irradiated groups.

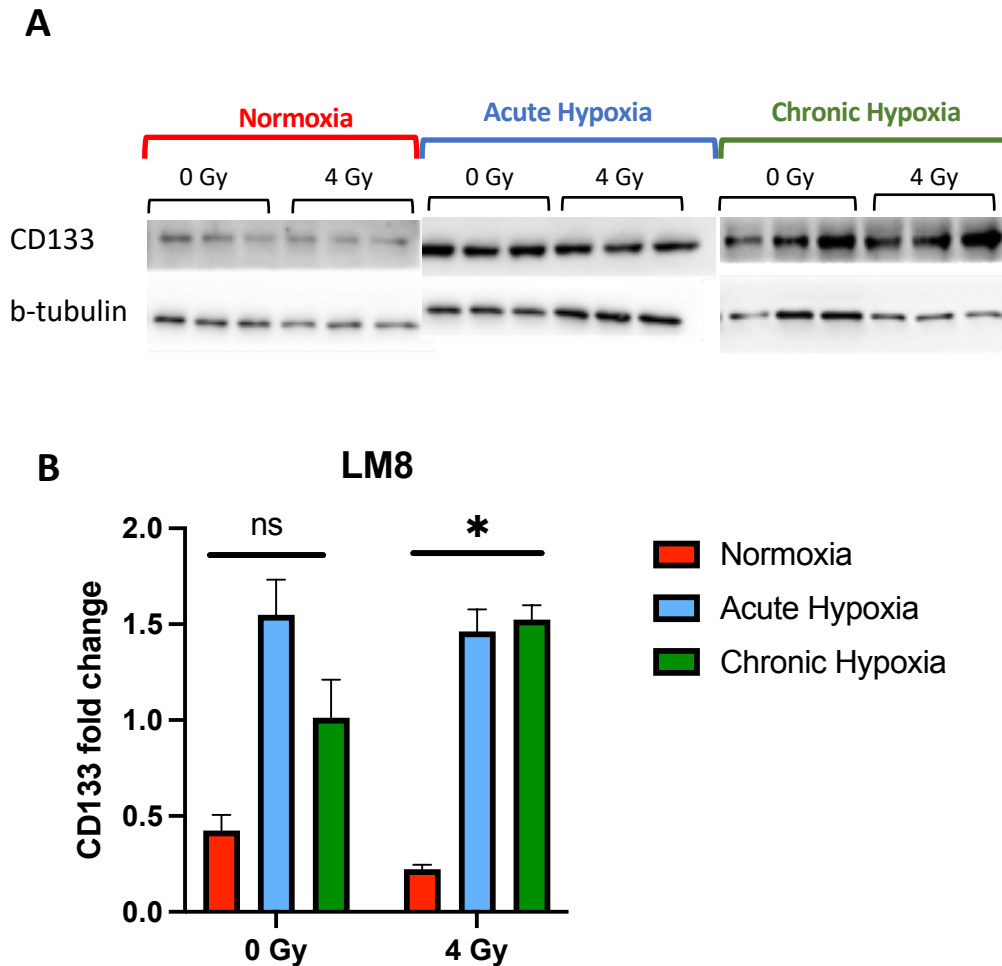


Figure 23. CD133 expression after hypoxia (acute and chronic) and radiation. (A) representative experiment of western blot and (B) mean densitometry of CD133 relative to β -tubulin expressed as arbitrary units. *Hypoxic cells vs normoxic control cells. \pm SEM, $P < 0.05$

3.6 Hypoxia increases the subpopulation of cells expressing TrK B

Circulating Tumor Cells express a tyrosine kinase receptor, TrK B, which allows them to resist the anoikis in blood circulation (Paoli et al., 2013). The FACS analysis show that the whole LM8 cell population displays a TrK B percentage of around 1%, while under hypoxic conditions, TrK B expression increases to 7% (Figure 25 A). We, furthermore, investigate the number of cells that express both the CD133 and TrK B markers. In the CD133 cell's subpopulation, TrK B expression significantly increases up to 40% under hypoxic conditions (Figure 25 B). No significant differences were found between the samples irradiated and the sham controls. Gating strategy for the analysis is performed to discriminate between living and dead cells and only viable cells are considered (Figure 25 C).

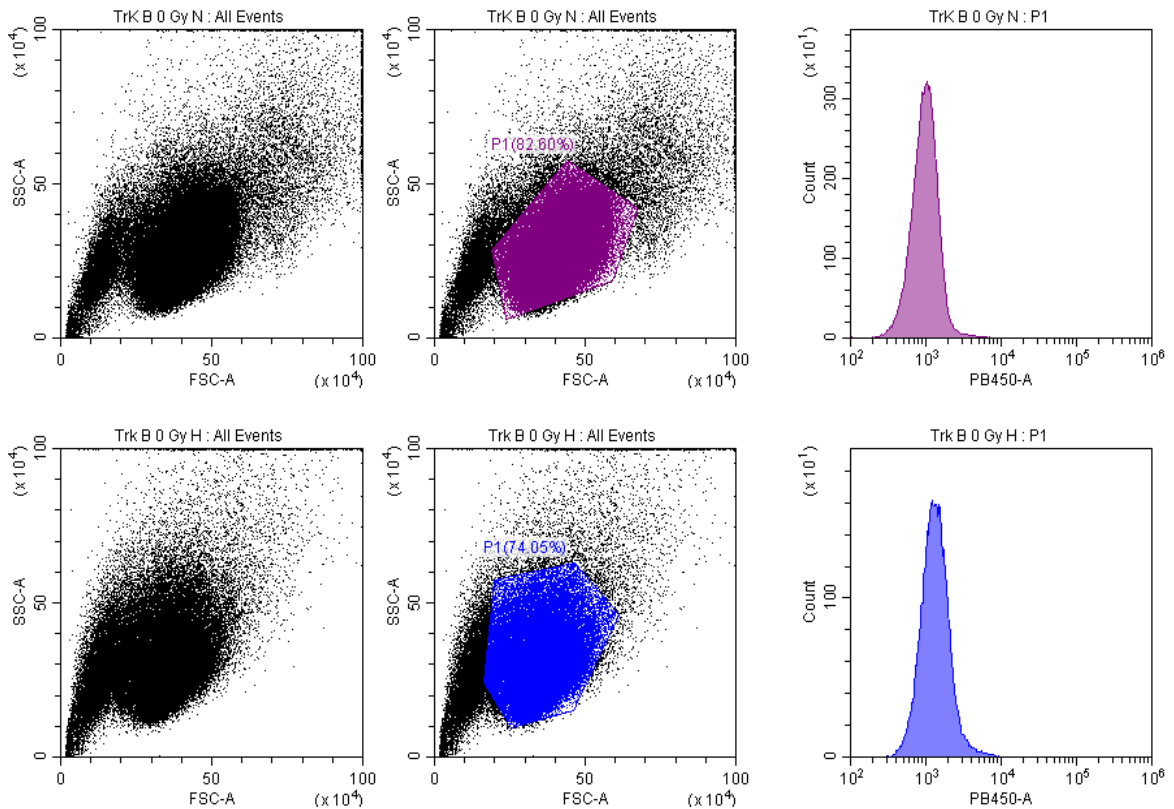
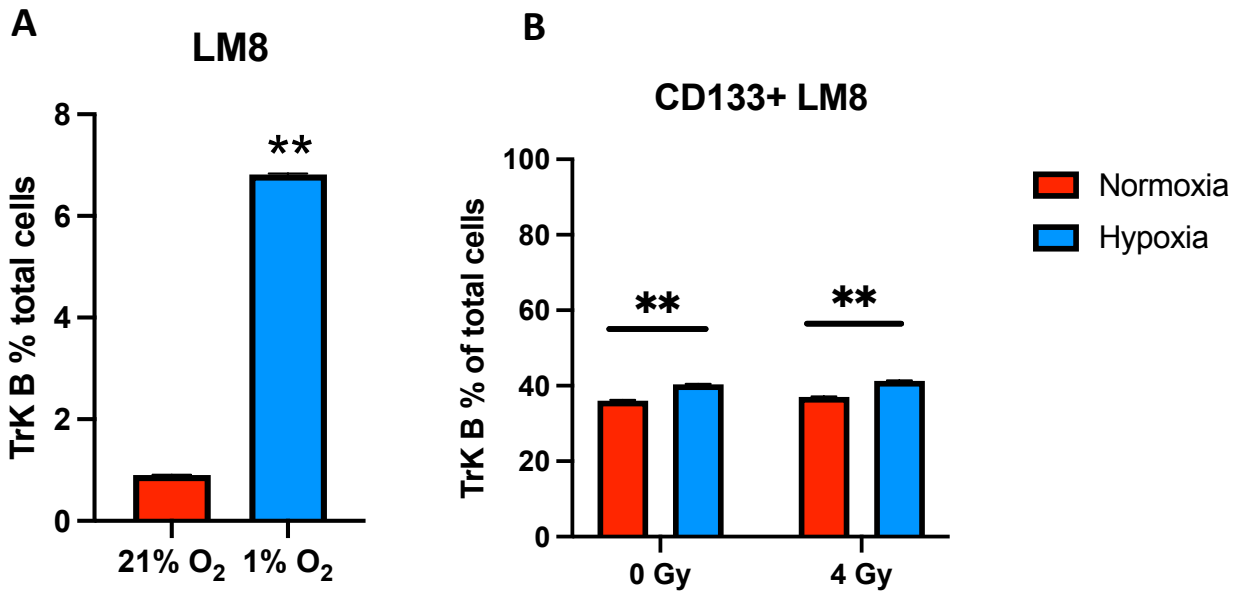
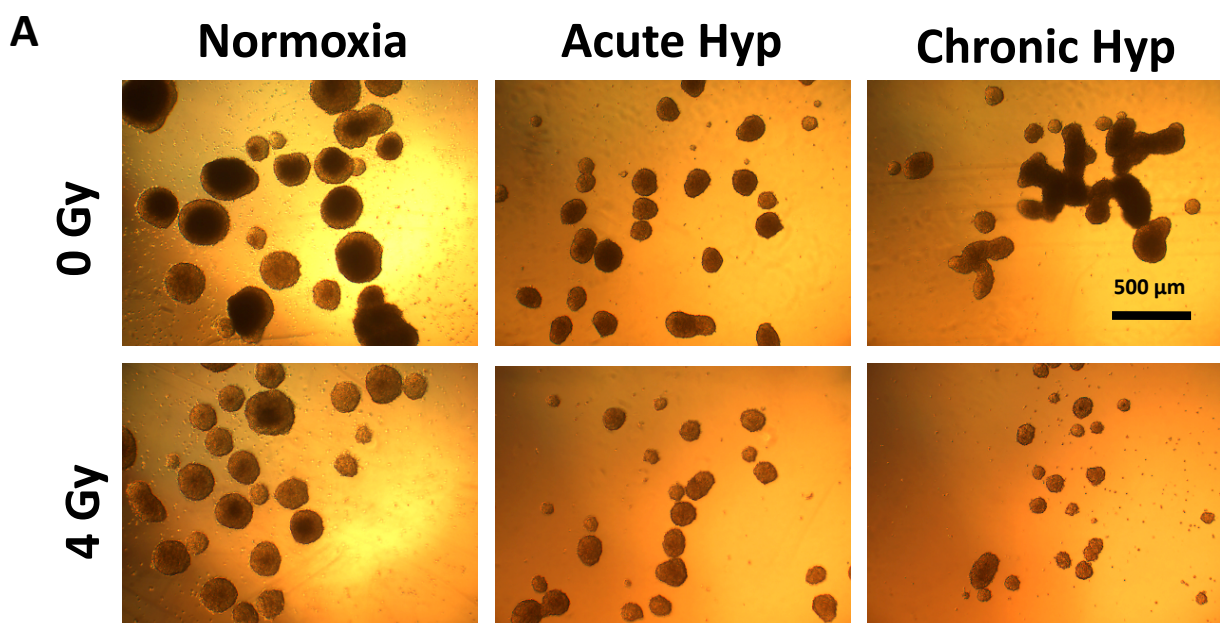


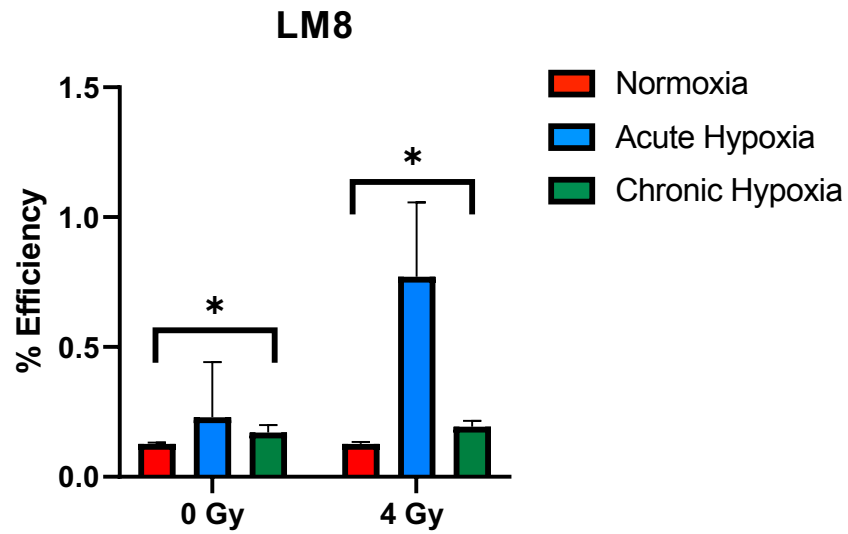
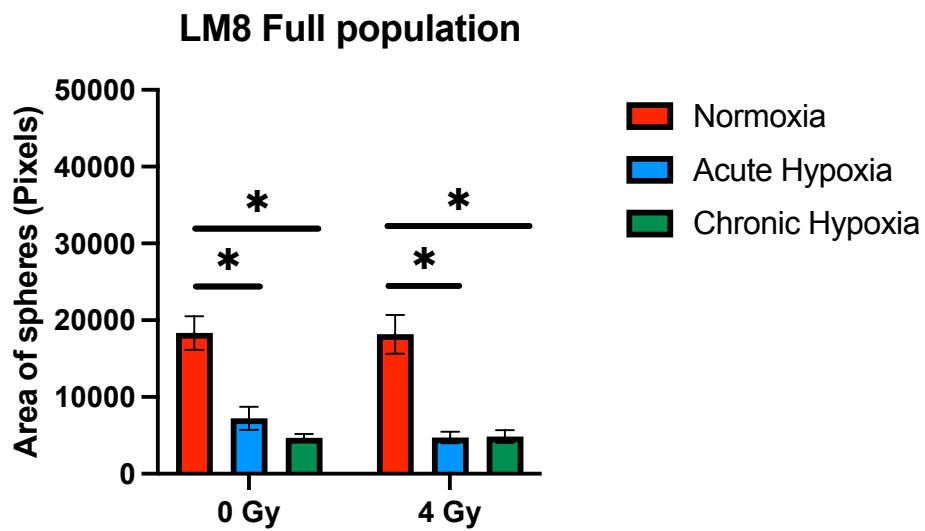
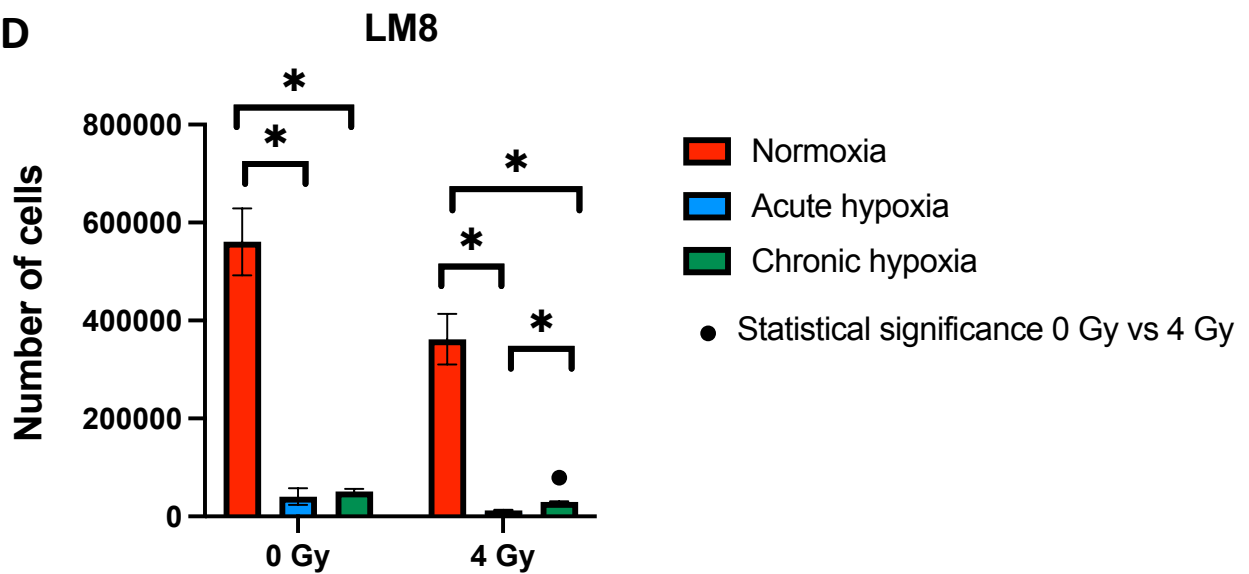
Figure 24. TrkB expression on LM8 cells. (A) TrkB expression in LM8 whole population, (B) TrkB expression in CD133+ cells and (C) gating strategy for sample analysis. * Hypoxic cells vs normoxic controls \pm SEM, $P < 0.01$.

3.7 Hypoxia and radiation influences sphere formation, size and cluster

It is known that hypoxia plays a central role in stimulating the stemness of cells, contributing to increasing the efficiency of forming spheres in osteosarcoma (Lin et al., 2021).

However, it is not yet known how acute and chronic hypoxia affect the stemness of cells. Therefore, we exposed the cells to varying durations of hypoxia and investigated their phenotype. Results show that time of exposure to hypoxia strongly affects the sphere formation ability and the sphere dimension in the whole LM8 cell population (Figure 26 A). Acute hypoxia increases the LM8 sphere formation efficiency, shifting the value from $0.12\% \pm 0.005$ of normoxic cells, to $0.22\% \pm 0.2$. Under chronic hypoxia instead, the cells' ability to form spheres decreases, $0.17\% \pm 0.03$. Radiation seems to play a role only in the acute hypoxic cells, increasing their efficiency from $0.11\% \pm 0.007$ of normoxia, to $0.77\% \pm 0.3$ (Figure 26 B). Concerning the sphere dimensions, the size decreases under hypoxia (both acute and chronic) together with the number of cells involved in sphere formation (Figure 26 C-D). Despite this, hypoxic cells show a higher tendency of cluster formation, with 4 to 7 spheres clumping together (Figure 26 E). Hypoxia and radiation combined significantly reduce the size of the spheres (p -value: 0.000105) and their capability of forming clusters (Figure 26 F).



B**C****D**

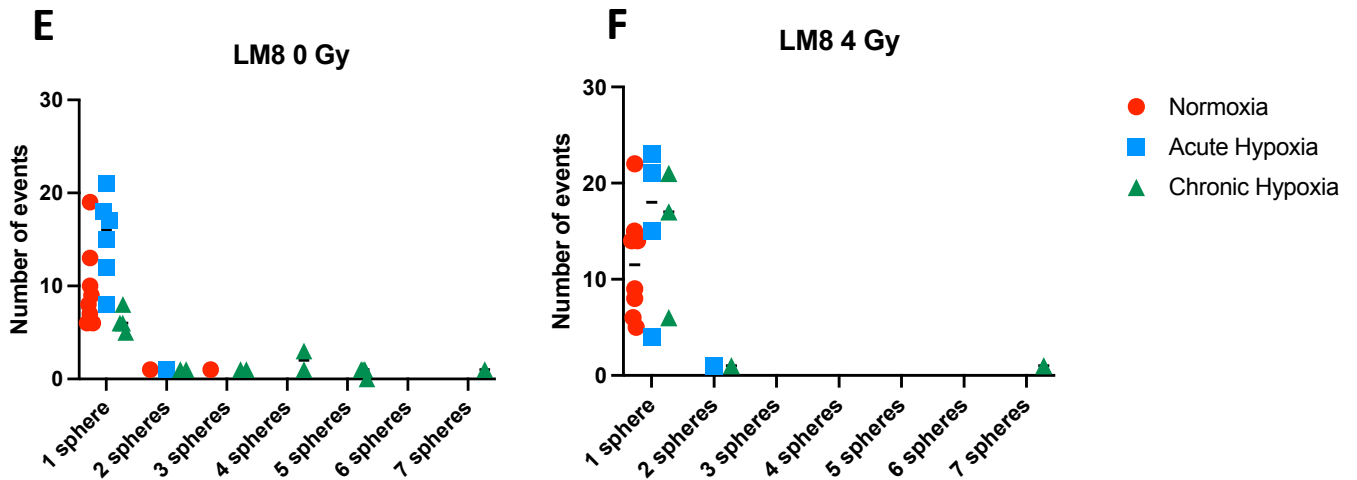


Figure 25. LM8 whole cell population: representative picture of the spheres (A), sphere formation efficiency (B), area of the spheres (C), number of cells forming spheres (D) and (E-F) number of spheres cluster. * Hypoxic cells vs normoxic controls \pm SEM, $P < 0.05$

3.8 CD133 influence on radioresistance, sphere and cluster formation

Results from the survival curve in normoxic condition show an increased radioresistance of the CD133+ sorted cells (S/PE 2 Gy: 1.4; S/PE 4 Gy: 0.71; S/PE 10 Gy: 0.018) compared to the LM8 whole population (S/PE 2 Gy: 0.84; S/PE 4 Gy: 0.38; S/PE 10 Gy: 0.007) (Figure 27).

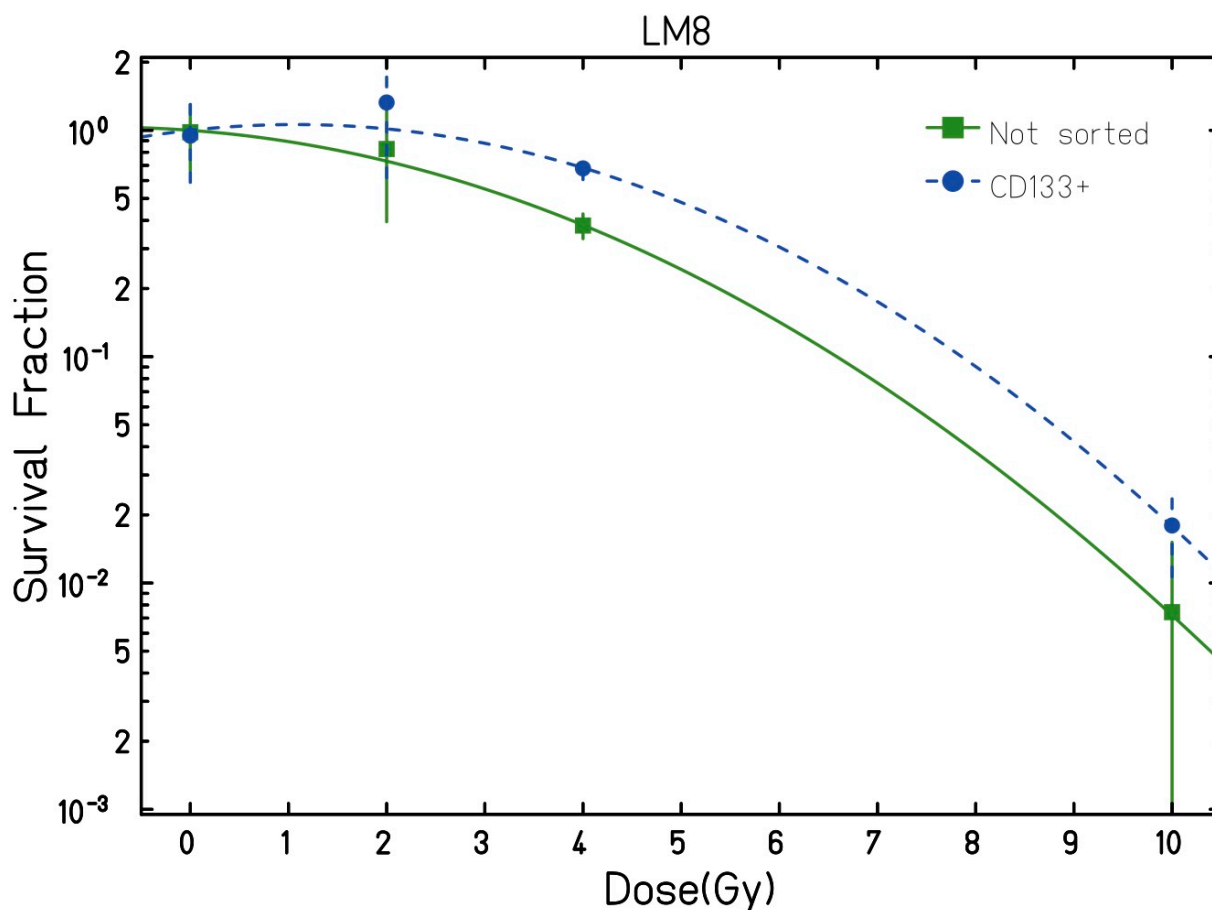
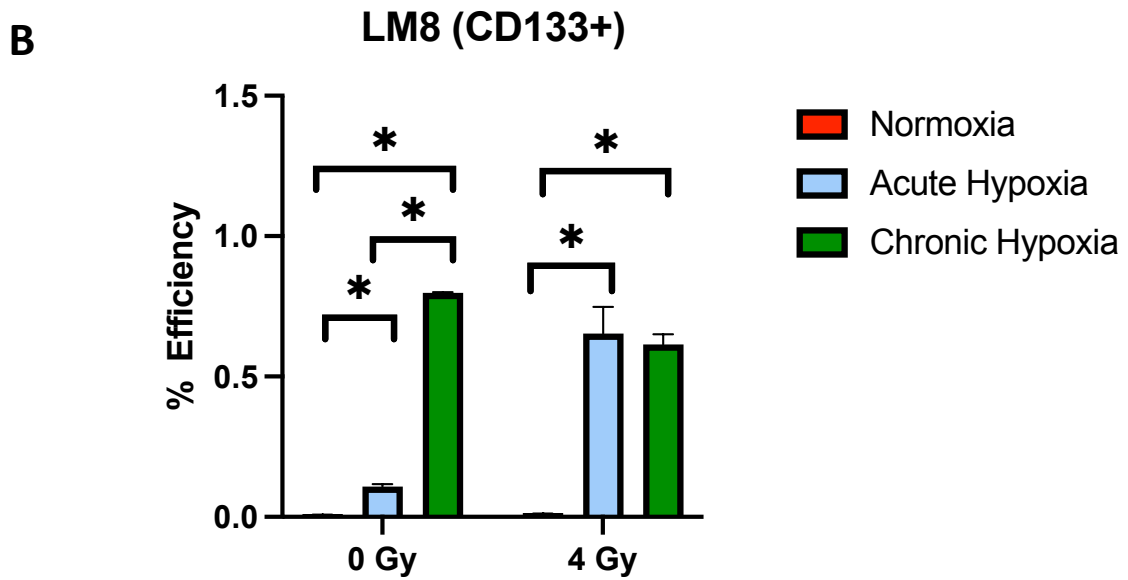
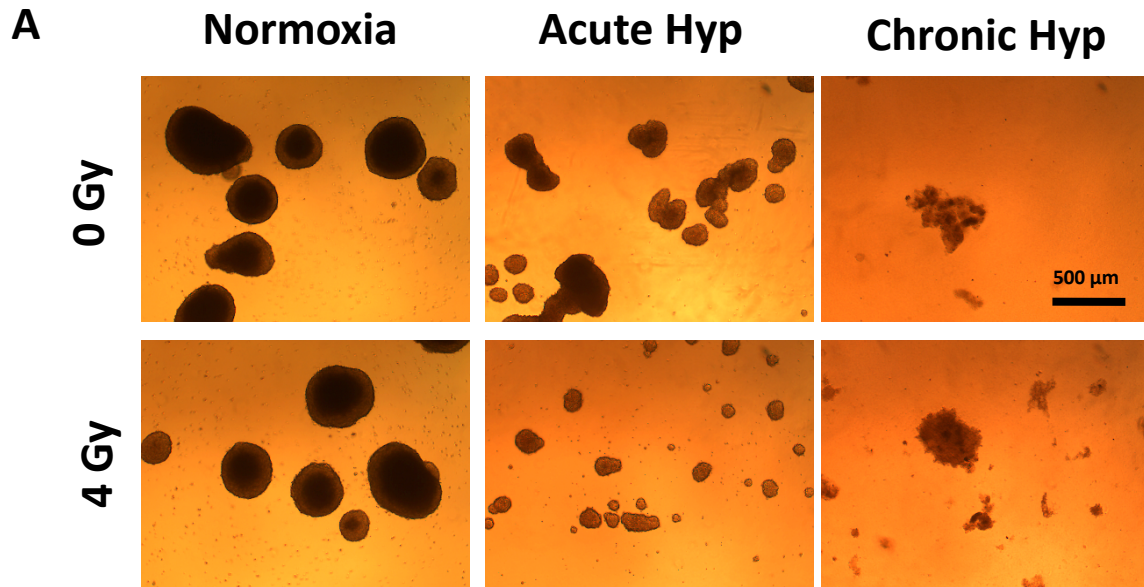


Figure 26. Clonogenic Survival Assay (CSA) of LM8 cell line: comparison between LM8 full population and CD133+ subpopulation.

Chronic hypoxia strongly increases the sphere formation capacity of the LM8 CD133+ cells, with almost 0.8% of efficiency alone and reaching 0.6% in combination with radiation (Figure 28 A-B). For the acute hypoxic cells, irradiation with 4 Gy X-rays is fundamental condition to increase sphere efficiency (~0.63%). However, sphere size of CD133+ cells and the number of cells forming spheres decreases while hypoxic exposition increases (Figure 28 C-D). The number of spheres clustering together increases under acute hypoxia, and even more in combination with radiation and chronic hypoxia (Figure 28 E-F).



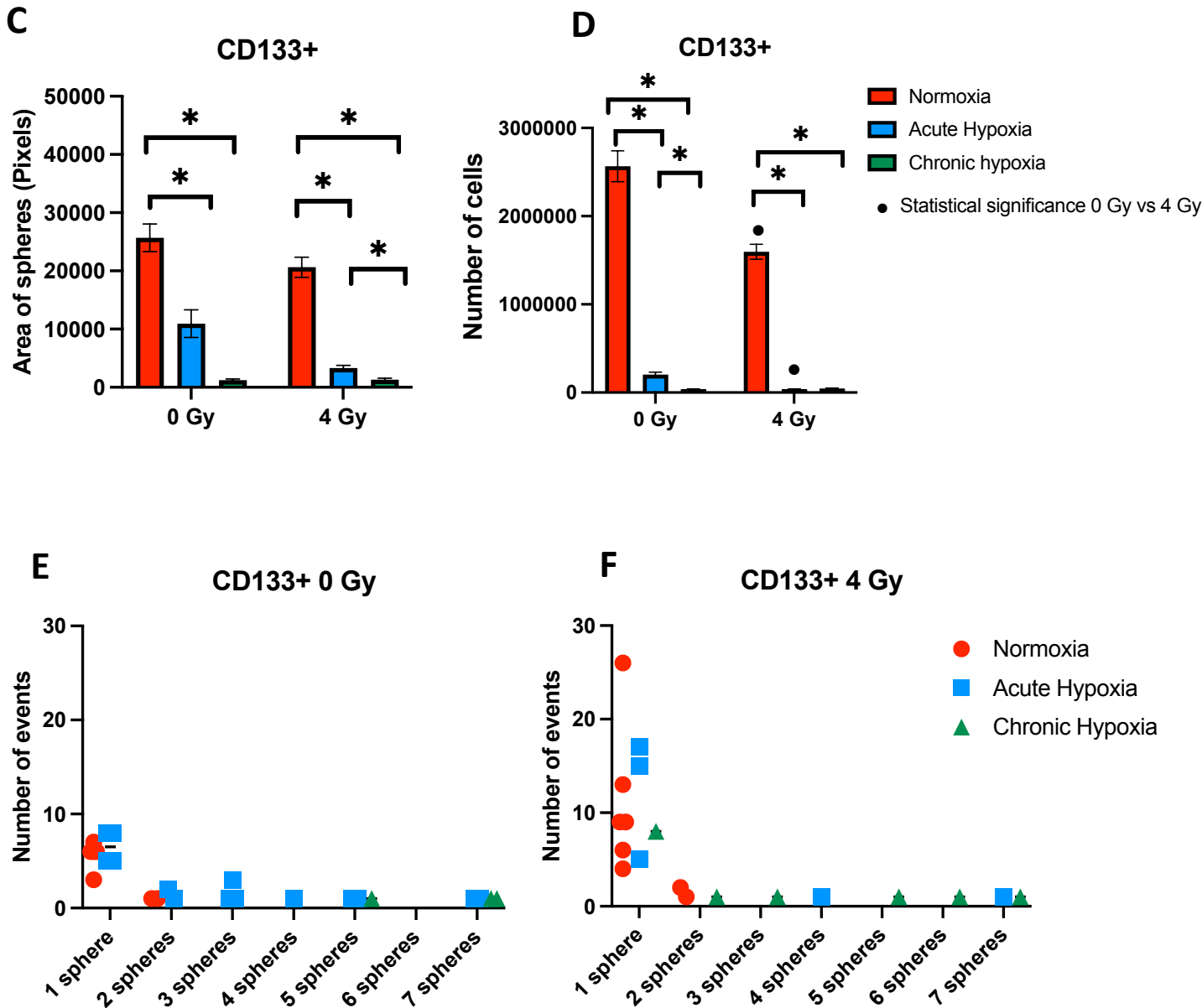
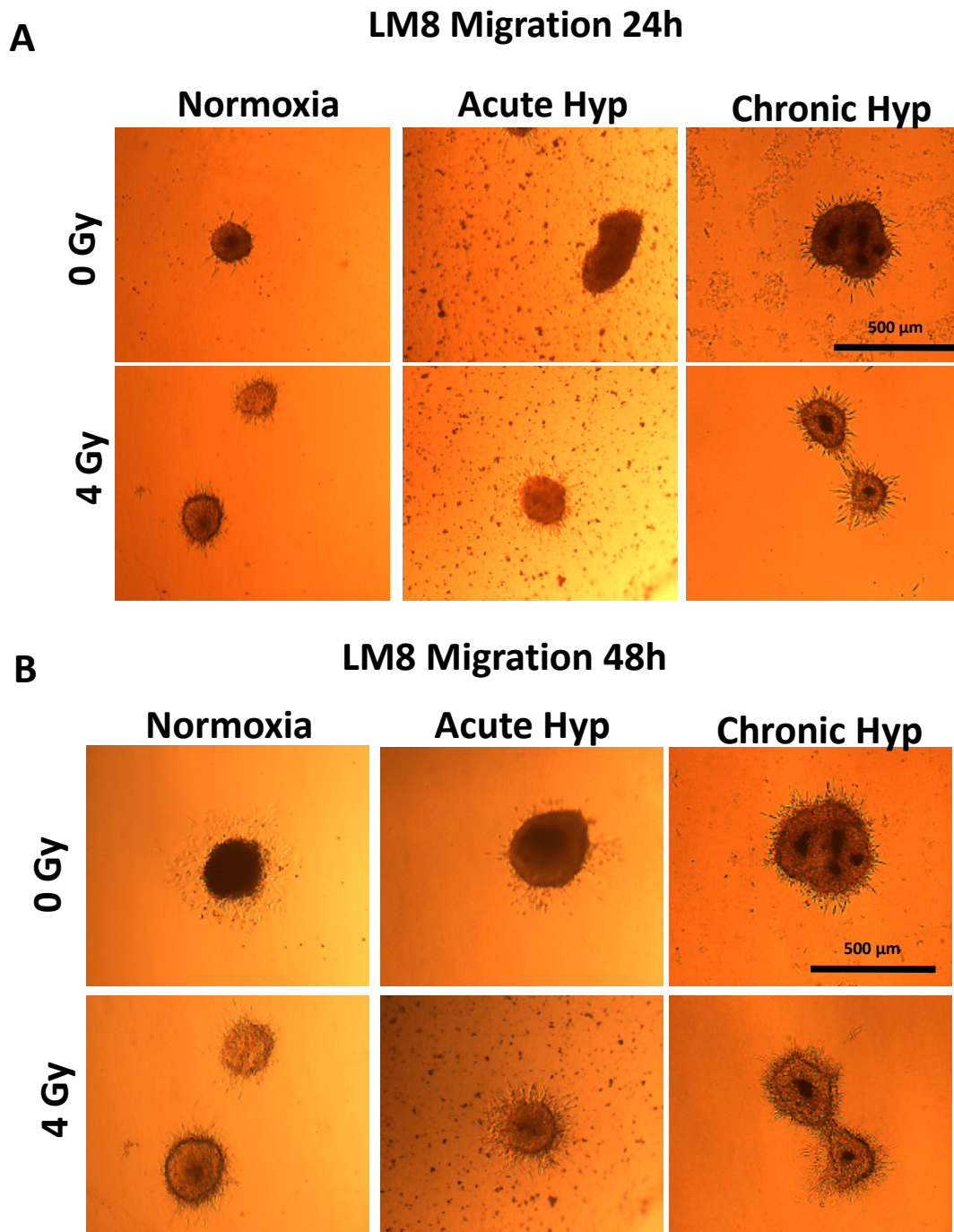


Figure 27. LM8 CD133+ cell population: representative picture of the spheres (A), sphere formation efficiency (B), area of the spheres (C), number of cells forming spheres (D) and (E-F) number of spheres cluster. * Hypoxic cells vs normoxic controls \pm SEM, $P < 0.05$. • Statistical significance comparing 0 Gy and 4 Gy.

3.9 Hypoxia influences the migration capacity of LM8 cells

In order to investigate the migration ability of the LM8 after hypoxia and radiation, we embedded the spheres in collagen and check the cells' migration after 24 h and 48 h. Results show that LM8 spheres strongly increase their migration ability when exposed to chronic hypoxia respect to normoxia and acute hypoxia, moving from 1600 pixels (normoxia) to 6000 pixels (chronic hypoxia) of area after 24h. The same trend is maintained also at 48h timepoint. Moreover, radiation increases the migration

ability only of the normoxic cells, while it does not affect the migration ability of the cells cultivated in acute or chronic hypoxia (Figure 29 A-B-C).



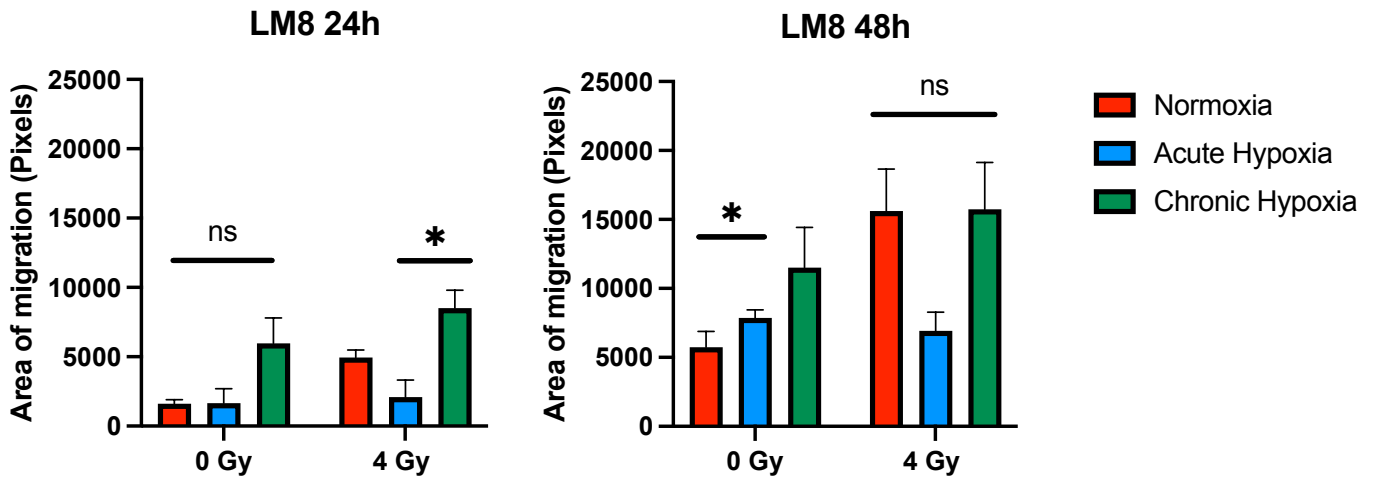
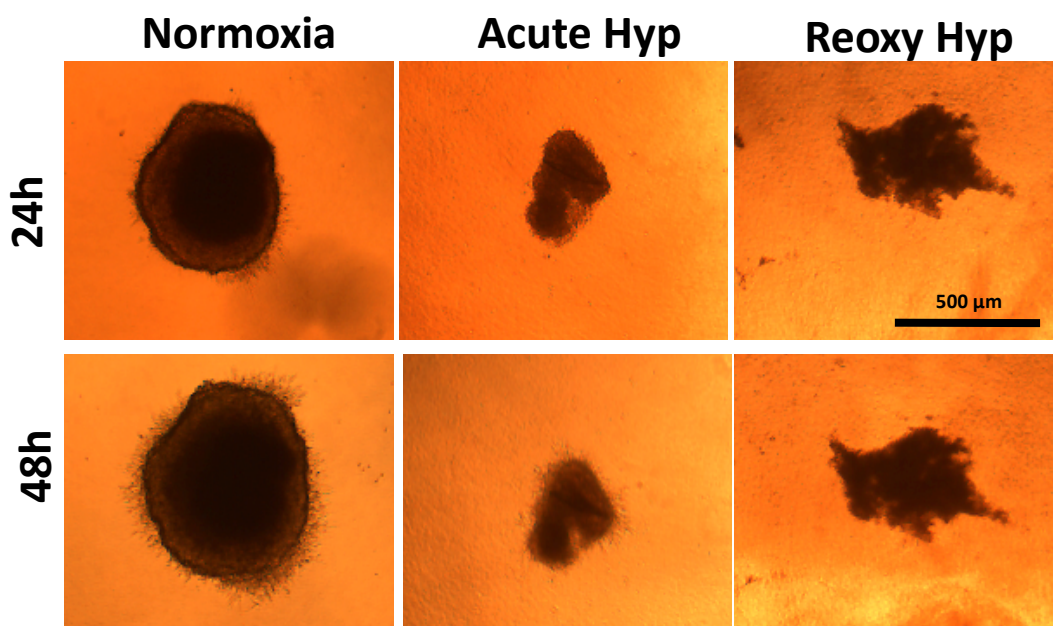
C

Figure 28. Sphere migration in collagen of LM8 whole population. (A) representative pictures of migration after 24h and (B) 48h. (C) area of migration of spheres after 24h and 48h. * Hypoxic cells vs normoxic controls \pm SEM, $P < 0.05$.

Regarding the migration study of the CD133+ cells, it is inevitable that the samples will undergo reoxygenation during the sorting procedure. For this reason, we do not have results of the CD133+ cells exposed to chronic hypoxia. After reoxygenation, the migration ability of the cells substantially decreases, with no differences between the controls and the irradiated samples (Figure 30 A-B-C). Sorted CD133+ cells cultivated in normoxia migrate more than those grown in hypoxia. The migrating behaviour is maintained the same between 24h and 48h timepoints.

A

CD133+ LM8 Migration 0 Gy



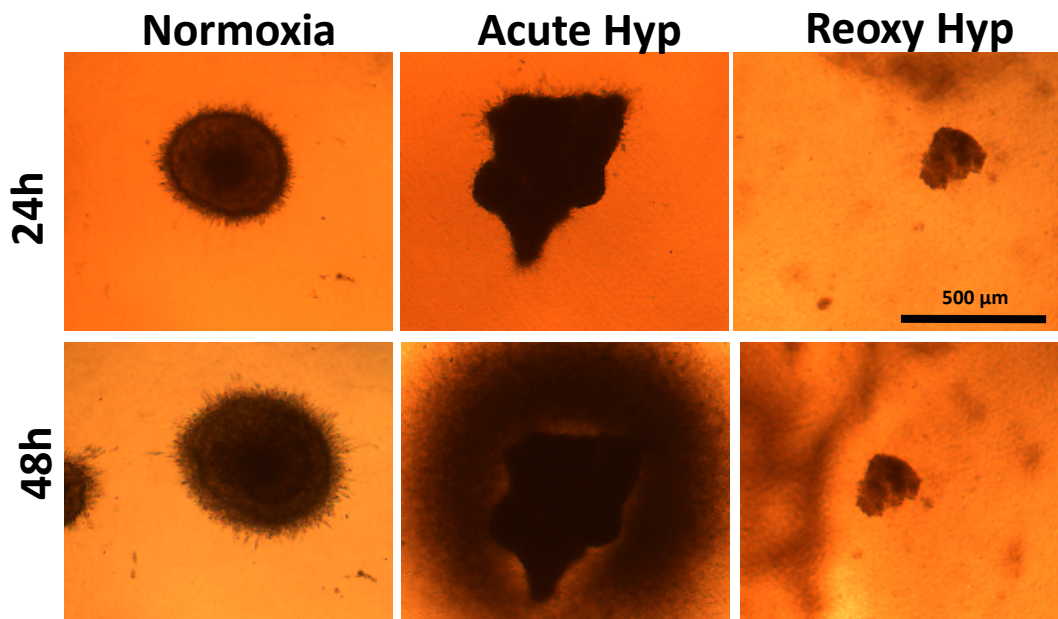
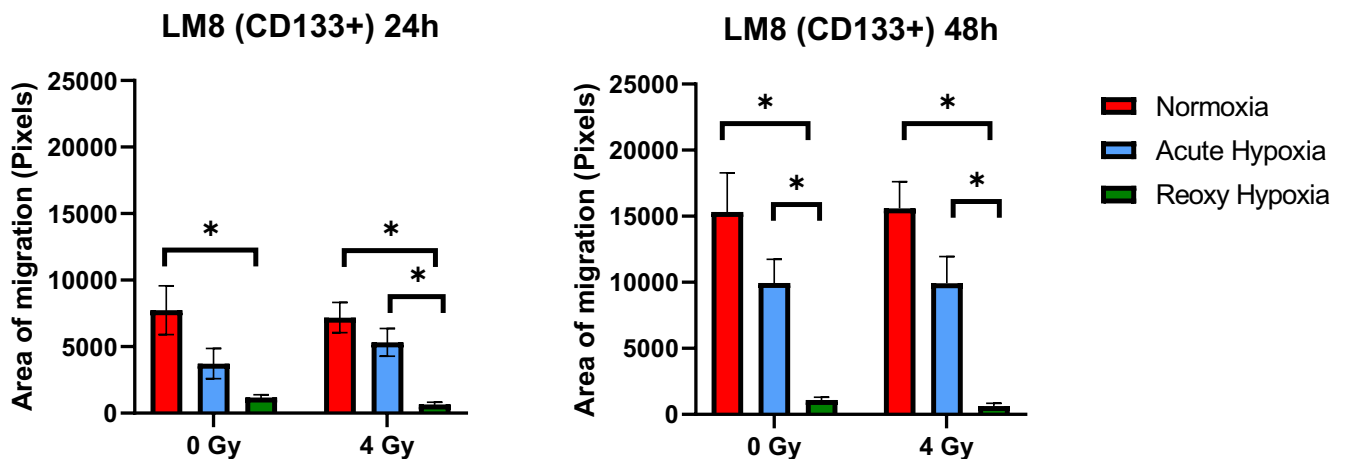
B**CD133+ LM8 Migration 4 Gy****C**

Figure 29. Sphere migration in collagen of CD133+ sorted LM8. (A-B) representative pictures of migration at 0 Gy and 4 Gy comparing 24h and 48h (C) area of migration of spheres after 24h and 48h. * Hypoxic cells vs normoxic controls \pm SEM, $P < 0.05$.

3.10 CD47 expression in CD133+ LM8 cells

We have found a particular subset of LM8 cells that exhibit an aggressive phenotype. These cells demonstrate elevated levels of stemness markers, increased ability to form spheres, the capacity to form clusters of spheres, and heightened migratory capabilities. As next step we further wanted to investigate whether these cells express the CD47 marker, the critical molecule used by the Circulating Cancer Stem Cells to evade the immune system (Yang et al., 2015). Chronic hypoxia significantly

increases the expression of CD47, particularly without irradiation (p -value: 0.0205). Normoxia and acute hypoxia instead do not influence CD47 expression (Figure 31 A-B).

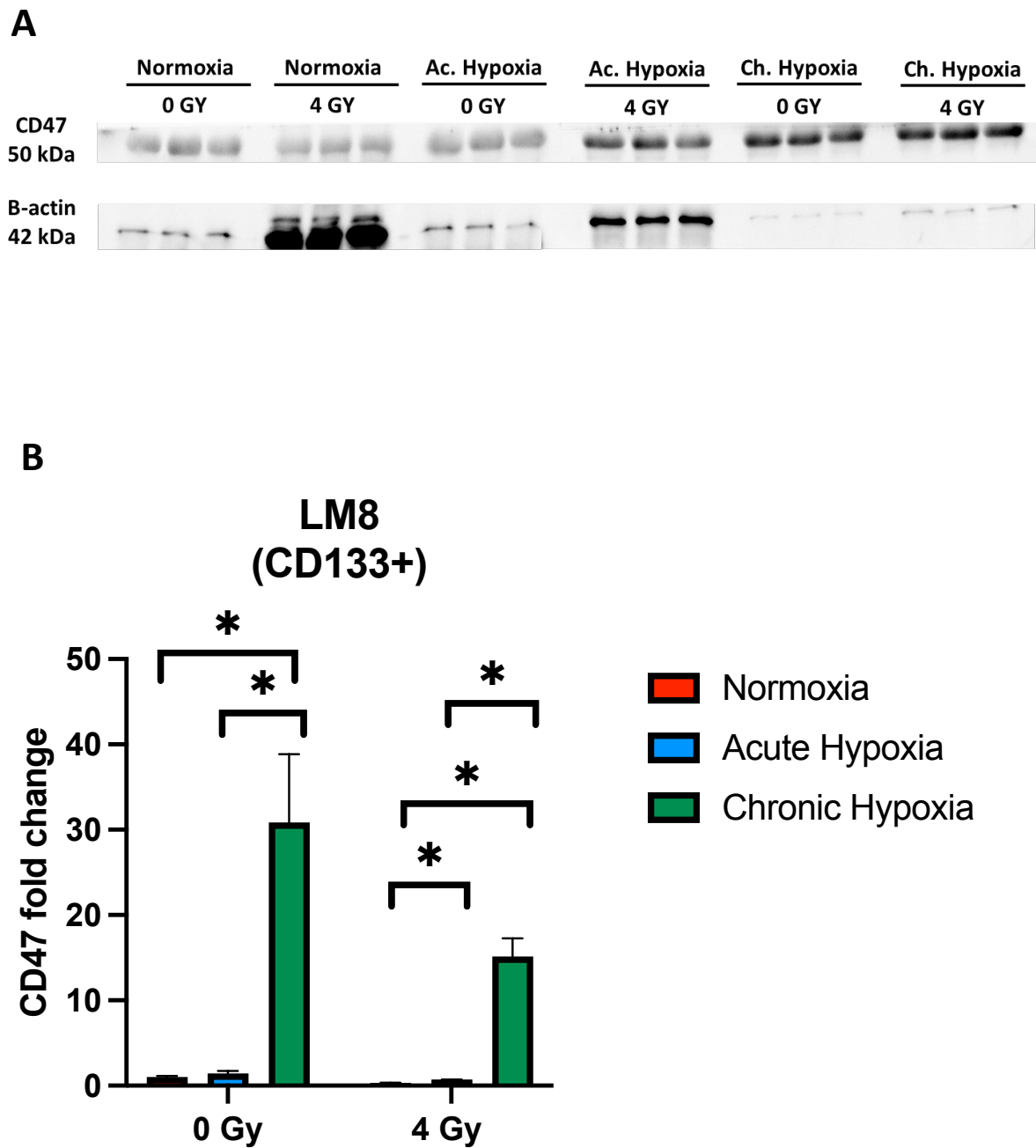


Figure 30. CD47 expression in CD133+ cells, comparing normoxia, acute hypoxia and chronic hypoxia. (A) representative experiment of western blot and (B) mean densitometry of CD47 relative to b-actin expressed as arbitrary units. *Hypoxic cells vs normoxic control cells. \pm SEM, $P < 0.05$.

3.11 CTC isolation *ex vivo*

After the characterization of cells with a CCSCs-like phenotype *in vitro*, we tried to isolate Circulating Cancer Stem Cells *ex vivo* from the mice blood after sacrificing them, from a parasitic experiment with the following ethical permission number: DA17/2000. For CTCs isolation we used the magnetic beads system, comparing sham controls to irradiated animals. CTCs are present in a few numbers in the blood; therefore, their identification and isolation is challenging (Bankò et al., 2019). We counted a high number of cells in the samples, with no observable differences between irradiated and sham controls (Fig.32). We observed cells with a biconcave disk shape, typical of red blood cells, meaning that the protocol we used was not efficient: the blood cells not being removed created an obstacle for CTCs identification. Therefore, we did not succeed in *ex vivo* CTCs isolation and a better protocol still needs to be established for this part of experiments.

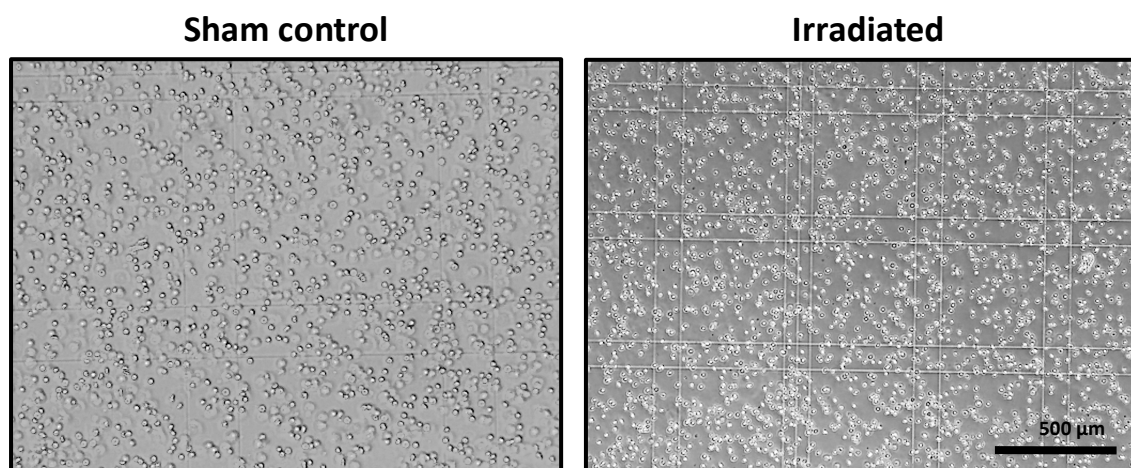


Figure 31. CTC isolation from blood of mice: comparison between sham control and irradiated samples. 10× magnification, Motic AE31 microscope.

We collected primary tumor and the metastases from the lungs of sacrificed animals and we proceeded to homogenize the samples in order to establish cell culture. We performed a western blot analysis to investigate the differential expression of CD133 between primary tumor and metastasis, comparing the irradiated samples to the sham controls. CD133 is overall expressed, showing a fold change around 0.6, with no difference between not irradiated and irradiated samples (Figure 33A-B). No differences in the expression were also observed between primary tumor and metastasis.

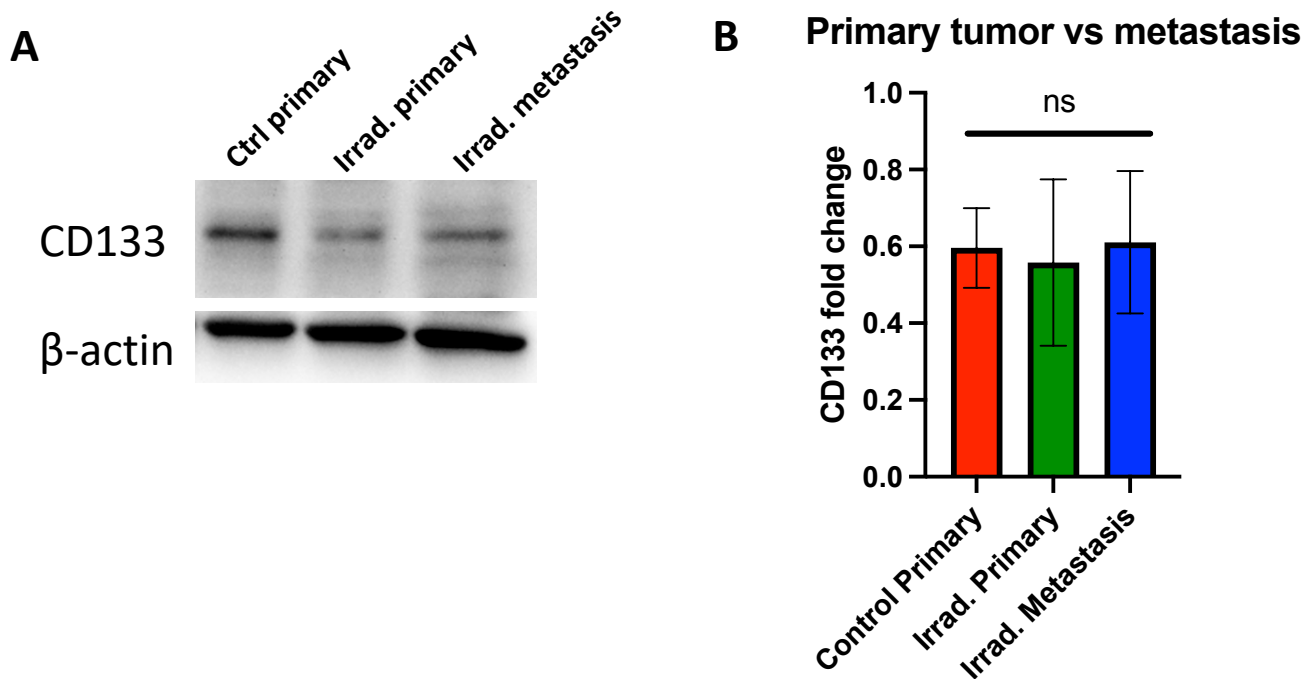
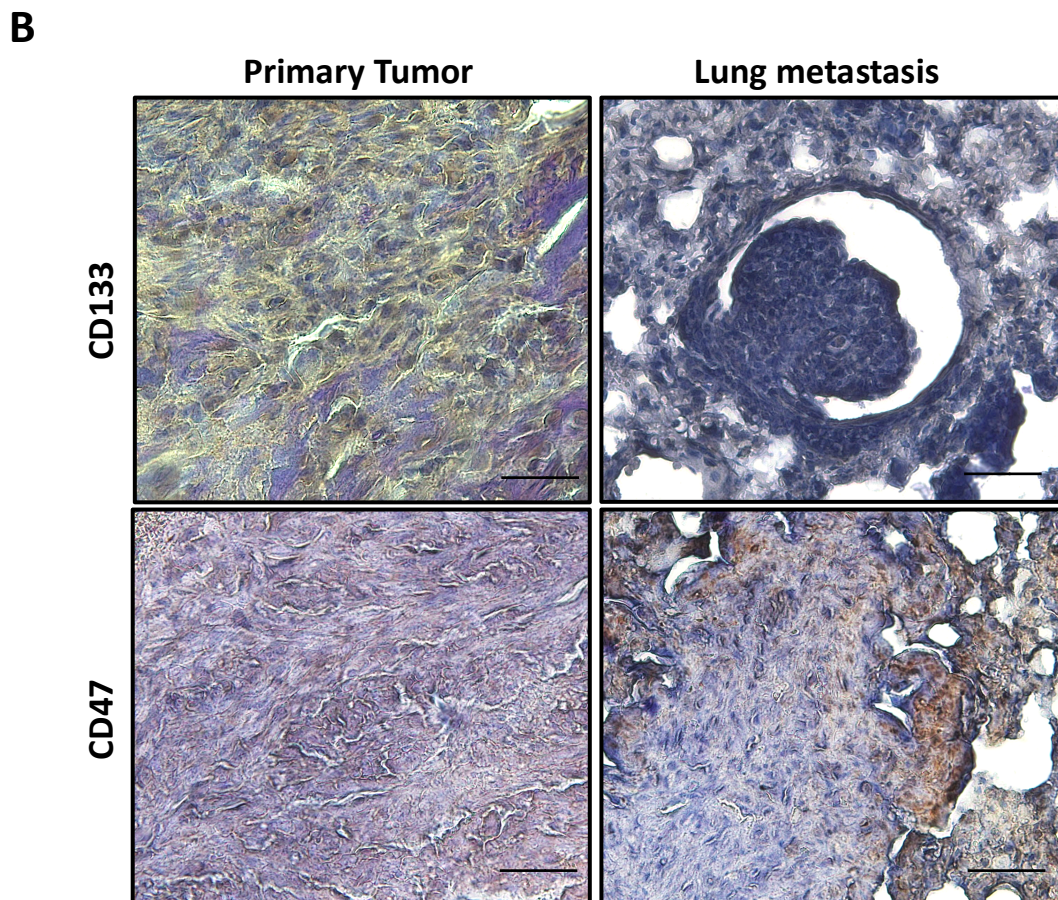
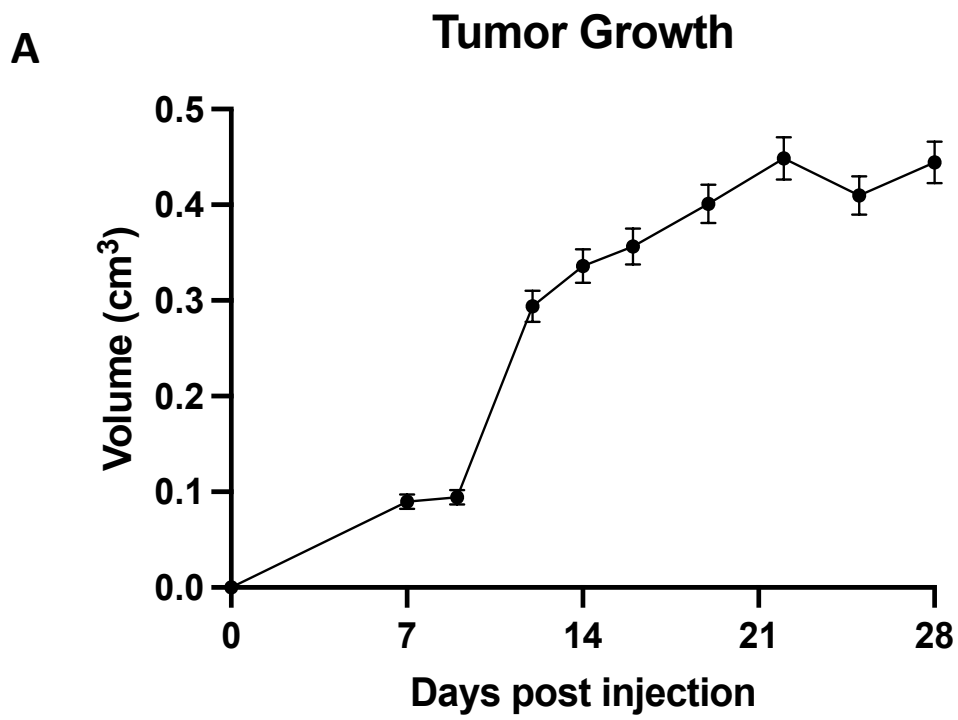


Figure 32. Western Blot analysis of primary tumor vs metastasis. (A) representative picture of WB experiment and (B) mean densitometry of CD133 relative to β -actin expressed as arbitrary units. Comparison done between control primary tumor, irradiated primary tumor and irradiated metastasis.

3.12 CD133 and CD47 expression in primary tumor and metastasis

We performed then a IHC analysis on primary tumor and metastases using samples that otherwise would have been wasted, from parasitic mice experiments approved under the ethical permission number DA17/2000. LM8 cells were subcutaneously injected in the posterior limb of C3H mice. Tumor growth was monitored (Figure 34A); afterwards the animals were sacrificed and primary tumor and lungs were collected for further IHC analysis (Figure 34B). Preliminary results from the *in vivo* experiment show not significant differences between the expression of CD133 signal in tumor tissues around 20%, and in the metastatic tissues around 30% (Fig. 34C). The expression of CD47 in the metastatic tissues instead is up to 80% with a relative increase, compared to the primary tumor tissues (Fig. 34 D).



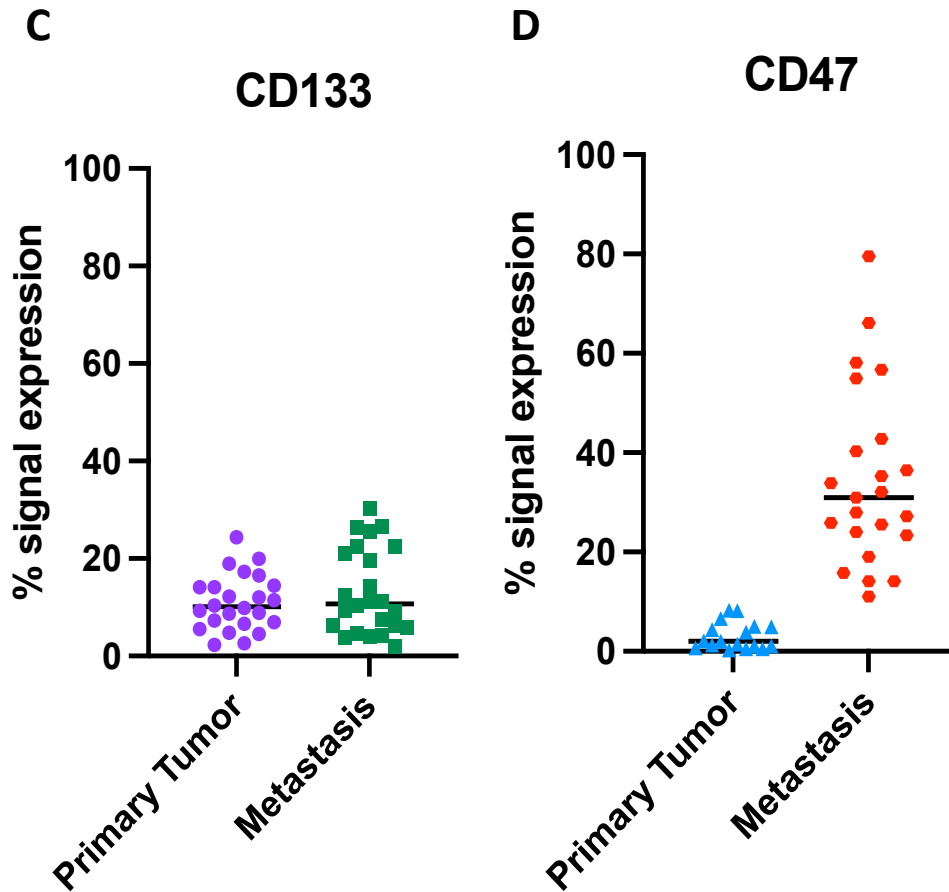


Figure 33. Tumor growth and immunohistochemical analysis of CD133 and CD47 expression between primary tumor and lung metastasis. (A) curve of tumor growth, (B) panel with representative pictures, 20 \times magnification with fluorescent microscope Olympus BX61: primary tumor vs metastasis, CD133 expression in primary tumor (DAB, brown signal) and CD47 expression in metastasis (DAB, brown signal), (C) dot plot of CD133 expression comparing primary tumor and metastasis and (D) dot plot of CD47 expression between primary tumor and metastasis. Each point represents the signal intensity measured for each picture of the sample taken. Scale bar corresponds to 50 μ m.

4. Discussion

CCSCs are characterized by specific and distinguishing surface markers that help in their identification and isolation (Tinganelli et al., 2020). One of the most important is CD133, involved in the remodelling of cytoskeleton, in cell migration, cell self-renewal and in the regulation of PI3K-Akt signalling in cancer stem cells; for this reason, it is also related to stemness capacity (Glumac et al., 2018). In literature is known that hypoxia triggers the expression of CD133 in osteosarcoma cells upregulating stemness genes Oct4 and Sox2 (Heddleston et al., 2010; Iida et al., 2012). CD133 binds to HIF1 α promoting its translocation and activation in the nucleus under hypoxia, while it interacts with HIF2 α promoting the pluripotency of the cells (Maeda et al., 2016; Heddleston et al., 2010). Besides, hypoxia influences the expression of TrK B, another relevant marker for the CCSCs, associated to resistance to *anoikis*. TrK B gene presents HIF1 α binding elements, therefore hypoxia by activation of HIF1 α enhances the Trk B production and signalling (Helan et al., 2014). When TrK B is overexpressed, it confers to the cells the ability to evade from a caspase-related programmed cell death, thus surviving in the blood circulation and allowing the cells to disseminate forming metastases at distant sites (Geiger et al., 2011; Douma et al., 2004). In addition, CCSCs are able to survive in the blood circulation and not only resist to programmed cell death but they are also able to escape from the immune system detection. This is possible because of another marker, CD47. Such marker works as a “do not eat me” signal, preventing the immune system to attack (Eladl et al., 2020; Helm et al., 2019). Hypoxia is also reported to regulate CD47 through HIF1 α signalling. HIF1 α directly activates the transcription of CD47; increased expression of it seems to enable cancer cells to escape phagocytosis, promoting a cancer stem cell phenotype (Zhang et al., 2015). Because the amount of these CCSCs in the blood circulation is very low, the possibility of selecting them *in vitro*, from the whole population of cancer cells, would certainly increase the knowledge that we have about the mechanisms involved in the metastasis formation.

4.1 Initial characterization of U2OS cell line

We used U2OS human osteosarcoma cell line to investigate the migration capacity, epithelial to mesenchymal transition (EMT) and ability of forming spheres, that is a characteristic of cancer stem cells. Our results presented in Figure 17 showed that U2OS cells display a slight migration capacity under normoxic condition, considering different timepoints, even though the difference is not statistically significant. Moreover, hypoxia seems not to influence cell migration of these cells either, since we did not observe any significant difference in comparison with the normoxic condition. Since cell migration is mediated by cadherin expression (Shih et al., 2012), we further investigated with

western blot analysis the expression of E-cadherin and N-cadherin in U2OS cells. Moreover, we wanted to observe whether U2OS display a cadherin switch, that is index of tumor aggressiveness (Huang et al., 2019). We noticed that cells cultured in hypoxia, compared to the ones maintained in normoxia, show a decrease in the expression of E-cadherin, as presented in figure 18; however, this decrease is not counterbalanced by an increment of N-cadherin, whose levels did not change significantly as well under hypoxic stress. Only normoxia and radiation seem to contribute to enhance its expression. Even though cadherin switch is one of the main characteristics of EMT transition and the loss of E-cadherin appears to be the initial step of EMT transition (Kalluri et al., 2009; Son et al., 2010; Yang et al., 2020), however it is not an exclusive feature of an aggressive behavior, because of tumor heterogeneity (Chu et al., 2013). The plasticity and reversibility of EMT transition, in fact, suggests that cancer cells can display feature of aggressiveness and invasion even if they retain an epithelial phenotype, without loss of E-cadherin (Ikushima et al., 2010). The absence of cadherin switch might be due to the fact that this cell line exploits other systems to synthesize proteins important for the EMT process, such as alternative mRNA translation mechanisms (cap-independent translation) (Bera et al., 2020), or that it is an already well differentiated line, thus not suitable for the purpose of our experiments. Moreover, N-cadherin also regulates cell migration and invasion (Shih et al., 2012). As a result, the low expression of this protein in U2OS cells might explain their lack of migration capacity both under normoxic and hypoxic conditions.

Although we did not observe a proper EMT transition and migration, we further tried to assess the stemness capacity of U2OS by investigating their ability to form spheres, using two different techniques: the hanging drop technique and the ultra-low attachment plates. Despite U2OS being a well differentiated cell line, we hypothesized the presence of a small subpopulation of stem cells or a phenotypical switch after hypoxia and radiation. Our results presented in Figure 19 show that U2OS were not able to form proper spheres but they were rather originating aggregates of cells, with no differences in the morphology between normoxia and hypoxia. No differences were observed as well in the irradiated samples, with an overall reduced ability to aggregate compared to the sham controls. This might be because from our experiments we observed that radiation decreases the E-cadherin expression, thus resulting in a reduced aggregation and adhesion ability of the cells. In order to form spheres and to maintain the stemness capacity, cancer cells require the expression of important genes such as the stem cell factors Oct4, Sox2 and Nanog, together with Twist, SNAILs and the cadherines (Gheytañchi et al., 2021). The U2OS inability to generate proper spheres in culture could be underlined by the fact that they are already differentiated cells, thus they do not possess a stemness capacity and do not express CSC transcription factors Oct4, Sox2 and Nanog, important for the stemness of cancer cells (Jubelin et al., 2022). Moreover, E-cadherin expression but not N-cadherin

could also explain their capacity to originate aggregates of cells but not spheres: U2OS express adhesion molecules that allows the cells to hold together but they do not express the stemness-related marker N-cadherin that would confer them a more aggressive phenotype and the capacity of sphere formation.

4.2 Initial characterization of LM8 cell line

In our further experiments we wanted to use a cell line characterized by a stemness capacity and that displays an aggressive phenotype. For this reason, we used the murine osteosarcoma cell line, LM8, a cell line that displays the abovementioned features and that is able to generate many metastases when injected in animal models (Tanaka et al., 2013; Tinganelli et al., 2022). Firstly we investigated the radioresistance of LM8 under acute hypoxia, and from the survival curve obtained we extrapolate a dose of radiation to use for the subsequent experiments. The selected dose strikes a balance between preserving most cells for molecular and phenotypical analysis and inducing a subpopulation of radioresistant cells (Figure 20). We chose the 4Gy as the dose from the survival curve to perform the following experiments.

Many authors report that hypoxia influences the ECM composition of cells: it can stimulate cell contractility leading to the disruption of epithelial barriers, modifying the actin composition of the cells' cytoskeleton (Zieseniss., 2014; Dekker et al., 2022; Gilkes et al., 2014). Cytoskeleton structure is also modified by EMT transition; during this process, apical-basal polarity of the epithelial cells' changes, cytoskeleton is reorganized thus leading to changes in cell shape (Datta et al., 2021). Our morphological analysis shows that hypoxia influences the shape of LM8 modifying the cytoskeleton and conferring a more elongated shape to the cell's structure as shown in figure 21. At this stage, LM8 by displaying a flattened shape, appear to acquire EMT-like phenotype, despite their inability to express cadherines, as it is reported in literature (Kashima et al., 2003). Our experiments support these data, since with a western blot analysis we were not able to detect E-cadherin and N-cadherin expression in LM8, as observable in Figure 22. This might be explained by the fact that this metastatic cell line exploits other signaling pathways to perform EMT transition, such as the β -catenin translocation from the cytoplasm to the nucleus of the cells (Basu et al, 2018). Considering this pathway, further studies need to be performed to investigate whether hypoxia and radiation are involved in the β -catenin translocation.

4.3 Prolonged hypoxia influence on LM8 cells

After we assessed the influence of hypoxia in the cell shape and structure, we investigated the effects that prolonged hypoxic exposition has in influencing the cell's phenotype. To do so, we cultivated the LM8 in different duration of hypoxia. Different authors refer to acute hypoxia as a short period of time that usually lasts until 24h, in which the cells are subjected to low level of oxygen concentration (Saxena et al., 2019; Liu et al., 2022). Chronic hypoxia, instead, is used to refer to a prolonged low oxygen exposition, that is usually comprised between 24h and 72h (Liu et al., 2022). Chronic hypoxia is also reported to be responsible for a more aggressive phenotype in cancer cells (Emami Nejad et al., 2021). The passage from acute to chronic hypoxia is documented by the switch from HIF1 α (in acute hypoxia) to HIF2 α (in chronic hypoxia). In these experiments we exposed the cells to a prolonged hypoxia of 1 week and 2 weeks to mimic the hypoxic conditions in the tumor microenvironment. Even though we were expecting that HIF1 α signal would have faded before 1 week of hypoxic exposition, being expressed during a short-term hypoxia, we performed western blot analyses noticing that HIF1 α was highly expressed at 1 week of hypoxia and was decreasing only after 2 weeks (Figure 23). Thus, we refer to the 1-week hypoxia as the "acute" hypoxia, and to the 2-week one as the "chronic" hypoxia. Knowing already from literature that hypoxia overall influences the CD133 expression in cells, we proved that LM8 express CD133, and that acute hypoxia increments CD133 expression in the whole population. This increment is not influenced or affected by photon irradiation, that contributes to the augment of CD133 expression only when combined to chronic hypoxia (Figure 24).

Once we assessed that hypoxia increases the cancer stem cell traits of our cells, we further investigated the possibility of selecting a subtype of cells that not only possess stemness characteristics but that also the ability of resisting to anoikis. For this purpose, we checked the percentage of cells expressing TrK B within the full LM8 population noticing that acute hypoxia increased the percentage of cells expressing it from 1% under normoxia to 7% (Figure 25A). Furthermore, we investigated whether there was a correlation between CD133 and TrK B. For this purpose, we sorted the cells for CD133: our results report a TrK B expression in 40%-50% of CD133+ cells, expression that was triggered in particular by acute hypoxia (Figure 25B). No influence of radiation was noticed overall. These results prove that CD133 and TrK B are associated, and that acute hypoxia as stressor is the first step to increase the sub-population of cells that have the phenotype of cancer stem cells and that are able to resist to programmed cell death.

4.4 Influence of hypoxia and radiation in sphere formation, size and cluster

Despite the anoikis resistance, other essential features of Circulating Cancer Stem Cells are their stemness capacity, that *in vitro* is exemplified by the sphere formation ability, and their capability to migrate (Ishiguro et al., 2017). We observed that acute hypoxia increases the sphere formation capacity of the cells, especially in combination with radiation (0.77%), while similar sphere forming ability was noticed between normoxia (0.12%) and chronic hypoxia (0.17%) with and without irradiation (Figure 26A). This difference in sphere formation might be explained by the fact that acute hypoxia displays an increased expression of HIF1 α . This marker, in fact, is also related to tumor spheres formation and it promotes tumor initiating cell activity, so it is involved in the first stages of tumor invasion (Schwab et al., 2012). Our results showed that HIF1 α was decreasing under chronic hypoxia compared to acute hypoxia, explaining the reduced cell capability to form spheres. Moreover, CTCs possess a specific phenotype that enables them to form small clusters, able to infiltrate in the blood vessels and disseminate in sites that are distant from primary tumor (Douma et al., 2004; Lin et al., 2021; Chen et al., 2022). In our research, we observed that prolonged exposure to hypoxia decreases the proliferation rate of the cells: we observed smaller spheres in size, but with the tendency to form more clusters, suggesting that hypoxia has an influence on the clustering ability of the cells and on the dimension of the spheres and contributes to the selection of cells with a CTCs-like phenotype (Figure 26 C-F). Our studies also showed that radiation influences the clumping capacity of the spheres, resulting in a lower number of clusters. Moreover, we investigated, by sorting the cells, whether CD133 cells were more radioresistant compared to the whole population one and if this marker influences the sphere formation and dimension (Figure 27-28). Our results showed an increased radioresistance of the CD133+ cells compared to the whole LM8 population. The survival of the whole population of cells is 0.38 ± 0.02 compared to 0.71 ± 0.05 for the sorted subpopulation when exposed to 4 Gy of radiation. The full survival values are reported in the paragraph 3.8 of the result section. This subpopulation was also able to form spheres in particular when cultivated under prolonged hypoxic exposition. Also in this case, photon irradiation is essential for increasing the sphere formation efficiency, but only when combined to acute hypoxia. Moreover, in the CD133+ spheres, even though the area of the spheres decreases with an increased exposition to hypoxia, we observed an incremented capacity to form clusters under chronic hypoxia and radiation. This might indicate that irradiation and prolonged exposure to hypoxia select aggressive cells with CTC-like phenotype. CD133 is as well relevant for the selection of cells with such characteristics. It influences the sphere forming capability of LM8, when combined to hypoxia that is already known for increasing CD133 expression. Additionally, this cancer stemness marker seems to influence the cluster capacity, increasing the number of sphere clusters already under acute hypoxia exposition.

Overall, the size of sphere and the ability to form clusters is a hallmark of cell aggressiveness (Zhao et al., 2023), and from our experiments hypoxia seems to select a very aggressive phenotype, with spheres that are smaller in size and that display an increased cluster capacity.

4.5 LM8 migration capacity

After assessing the LM8 stemness capacity by forming spheres, we further studied the aggressiveness of the cells by observing their migration ability (Rossi et al., 2018), embedding the spheres in collagen to mimic the Extracellular Matrix environment. Interestingly, we documented an increase in cell migration, associated to a more aggressive condition, under chronic hypoxia; such increase was already evident after 24h, and was still maintained with a similar trend at 48h timepoint (Figure 29). Radiation does not affect migration under acute and chronic hypoxia, but it increases the capability only in normoxic cells. This increased migration only in normoxia could be due to the fact that, as it is described in literature, photon irradiation increases the expression of genes involved in EMT transition, thus increasing the invasive/migratory capability of the cells *in vitro* (Lamouille et al., 2014). Moreover, it was observed an increase of matrix metalloproteinases (MMPs) by photon irradiation in normoxic condition, that contributes to degradation of connective tissue of the Extracellular matrix, allowing the cells to migrate more. Such degradation was decreased under hypoxia following irradiation (Wozny et al., 2021). These results support and could motivate the ones obtained from our experiments.

Additionally, we compared the migration of the cells composing the spheres from the whole population to the CD133+ sorted ones (Figure 30). We noticed an inverted trend in which normoxic cells were migrating more compared to hypoxic ones, and no differences were observed comparing the controls with the irradiated samples. However, since after the sorting the reoxygenation of the samples was not avoidable, the overall migration results take into consideration the reoxygenation factor and cannot be compared to the one of the full populations.

4.6 Hypoxia-induced expression of CD47

After we observed an increased migration ability in chronic hypoxia LM8 cells, we wanted to investigate whether this subpopulation of aggressive and high migratory cells express CD47, the “do not eat me” signal that would confer them the ability to escape from the immune system detection, once they move in blood circulation (Chen et al., 2022). Our experiment show that CD47 is significantly increased under chronic hypoxia, while normoxia and acute hypoxia have no influence on the expression of CD47 (Figure 31). Moreover, we observed that prolonged exposition to hypoxia

influences the expression of the loading controls. To perform our Western Blot experiments we always loaded the same amount of proteins (25µg) for all the conditions so that the housekeeping gene would not vary. Even though we tried with different housekeepings (e.g: β -actin) we always observed instability between the different conditions, with a decreased expression particularly under chronic hypoxia. We found that hypoxia changes the expression of these housekeeping genes, and we found confirmation in literature. Indeed, other authors report that hypoxia influences β -actin, GAPDH and Histone H3 expression (Foldager et al., 2009; Turkoglu et al., 2012). Housekeeping genes such as β -2 microglobulin (B2M) are reported to be more stable under hypoxia (Caradec et al., 2010), but also in this case we observed a variation in the expression in different conditions. Overall, from our *in vitro* experiments we can argue that the duration of hypoxia influences the behaviour of the cells in stemness capacity, migration ability and clustering: our findings show that chronic hypoxia not only increases cell mobility, ability to form clusters and decreases sphere area, but also increases the expression of CD47. Such marker is fundamental for CTC-like formation (Lian et al., 2019).

4.7 CTC isolation from mice blood

After we set up a protocol for characterizing CCSC-like cells *in vitro*, we wanted to investigate whether we were able to find the same features in Circulating Tumor Cells isolated from the blood of animals. CTCs are very useful tool to assess the aggressiveness of tumors and the subsequent advancement of it in distant organs (Tanaka et al., 2013). Isolating living CTCs is a very complicated procedure. In patients with advanced stage solid cancer, scientists reported the ability to isolate ~ 1 CTC per ten million white blood cells in a 7.5 ml blood sample (Alix-Panabieres et al., 2014). Complexity of their isolation is also due to the fact that CTCs are the result of a subpopulation of cells that derive from the primary tumor and that survive in the blood circulation being able to resist to anoikis, thus rendering very low the capacity to detect them (Van der Toom et al., 2016). Authors have successfully reported the ability to detect CTCs from the blood of mice already 1 week after murine LM8 osteosarcoma cell injection (Tanaka et al., 2013). Therefore, we injected the LM8 cells in C3H mouse models and we waited 28 days in order to allow the tumor and metastasis to form; afterwards we performed CTC isolation from the blood, considering CD133 as the reference marker used for the isolation, since we wanted to compare these results with the ones that we obtained *in vitro*.

Photon irradiation is reported to increment the number of CTCs in blood, because of the damage that radiation does to the blood vessels, thus releasing viable CTCs in circle (Tinganelli et al., 2020). For this purpose, we compared animals not irradiated (sham controls) to the irradiated ones, to investigate

further differences in the number of isolated CTCs (Figure 32). We assumed to notice a difference in the number of cells between the sham controls and the irradiated ones, although we expected to detect a low number of them overall, being CTCs present in a very low amount already in human blood samples, that have a higher volume compared to the blood collected from mice. We noticed a high amount of red blood cells in the samples, meaning that the protocol for blood cells removal was not successful. Moreover, not being able to properly remove the blood cells from the samples, the CTC identification was compromised. In conclusion, the CTC protocol that we tried to perform *ex vivo* was not successful, and further trials need to be performed in order to optimize it.

4.8 IHC analysis of CD133 and CD47 expression in primary tumor and metastasis

After mice were sacrificed, primary tumor and metastasis from the lungs were excised, collected and maintained in culture. Having in mind that CD133 should be highly expressed in the primary tumor, and that irradiation should stimulate the stemness in cancer cells, we wanted to investigate the difference in the expression of CD133 comparing the controls, to the irradiated primary tumor and metastasis, through a western blot analysis. Our results show that CD133 is expressed both in control and in the irradiated samples of primary tumor and metastasis (Figure 33). The expression of this marker does not vary among the different samples' types: it seems to slightly decrease in irradiated primary tumor (0.55-fold change) and slightly increase in the metastases (0.61-fold change) compared to the control (0.59-fold change), even though the data are not statistically significant. Even if there was no observable difference among the samples, its expression is relevant, because CD133 is the initiator of tumor dissemination, as reported in literature (Liou., 2019). This marker expressed by cancer stem cells is significant during the initial phases of metastatic cascade, when the cells that bear stemness capacity detach from the primary tumor undergoing EMT transition and starting intravasation (Irollo et al., 2013). Moreover, *in vivo* experiments performed on different tumor cell lines were able to identify through immunohistochemical analysis, an expression of CD133 on the primary tumor surface (Zhao et al., 2016). Once the cancer cells are able to invade the blood vessels, intravasating and entering in the circulation, they acquire resistance to programmed cell death, and they are able to evade from the immune system. Such ability is due to the expression of CD47, that works as a “do not eat me” signal for the cells (Lian et al., 2019). At this stage, such cells are defined as disseminating cells, that after extravasating from the blood vessels are able to disseminate to distant organs in the body, thus generating metastases (Kang et al., 2013). In order to localize the signal of these markers and to investigate the difference in their expression between primary tumor and metastases, we performed an immunohistochemical analysis after collecting the organs from the mice

(Figure 34). We expected to observe an increase of CD47 expression in the metastases, since this marker starts to be expressed at a later stage of the metastatic cascade, while CD133 should be expressed more in the primary tumor. Our results showed that CD133 reaches 20% of intensity in the primary tumor, with a slight increase up to 30% in the metastasis, but overall showing no significant differences between primary tumor and metastasis (Figure 34C). CD47 instead is less expressed in the primary tumor compared to CD133, while in the metastasis is highly expressed and reaches up to 80% in signal intensity (Figure 34D). As expected, CD133 is more expressed in the primary tumor, as it is the marker of cancer stem cells relevant in the first stages of the metastatic cascade. At this stage, CD47 is not yet expressed because it appears later on during the cascade. Indeed, this “do not eat me” signalling marker is highly expressed in the metastases, because metastases are originated by cells that survive in the blood circulation also by escaping from the immune system detection and disseminate to distal organs.

4.9 Conclusions

The primary objective of our study was to establish an *in vitro* protocol for identifying CCSCs-like cells. With our initial experiments, we aimed to demonstrate an influence of hypoxia and radiation in the selection of these subgroup of aggressive cells. We observed that U2OS cells were not able to migrate under hypoxia; moreover, such stressor together with photon irradiation was not showing any effect on the cadherin switch of these cells, suggesting that U2OS, being already differentiated cells, did not possess stemness capacity and the phenotype similar to CCSCs. Our studies on murine osteosarcoma LM8 cells, instead, showed that hypoxia and radiation both contribute to increase the stemness capacity of LM8, by allowing them to form more spheres and reducing them in size. Even though they both display a contribution, they play a role at different steps of the metastatic cascade. Photon irradiation is more involved in the first steps of the cascade and it plays a significant role when combined to acute hypoxia: by increasing the cell ability to form spheres, it stimulates the stemness capacity of the cells, thus conferring them an aggressive phenotype. Equally important, we investigate the impact of hypoxia and radiation on CD47 expression, as highlighted by a study demonstrating its contribution to augmented CD47 expression *in vivo* (Candas-Green et al., 2020). This specific expression pattern becomes vital for tumor cells, allowing them to evade the anti-tumor immune response, thereby fostering an environment that results in cancer progression (Rostami et al., 2022). From our results, we observed that chronic hypoxia becomes relevant in later steps of the metastatic process, increasing the migration of the cells and CD47 expression. Hypoxia also influences, together with CD133, the number of cells expressing TrK B, meaning that there is a

correlation between these two markers. In this study we identify, *in vitro*, a subpopulation of cells that are positive for CD133, more radioresistant, are able to resist to anoikis (Trk B) and have the capacity to evade the immune system control (CD47). These results suggest that hypoxia has a relevant role in conferring to murine osteosarcoma cells, LM8, a Circulating Cancer Stem Cell-like phenotype, with the two different conditions influencing different steps of the CCSCs formation. In the second part of the experiments, we tried to correlate the results of the *in vitro* part with IHC analysis from mice tumor samples *in vivo*. The results obtained can be considered as a confirmation that we were able to characterize cells with CCSC-like phenotype and that display an expression of CD133 that is relevant in the beginning of the process and needed in order to start the isolation of the subpopulation of cells responsible for metastases. Moreover, cells that already possess stemness capacity by expressing CD133, also showed to express CD47 under stressors, going towards the real selection of a subgroup of cells that display the same characteristics of Circulating Tumor Cells. Indeed, we were able to find an increased expression of CD47 in the metastasis, which is the link between the experiments performed *in vitro* and the IHC analysis *in vivo*.

In conclusion, our multifaceted study endeavors to shed light on the complex interactions between radiation, hypoxia, and cellular responses, providing critical insights into the challenges and opportunities in cancer treatment. This deeper understanding has the potential to pave the way for innovative therapeutic strategies aimed at improving patient outcomes and enhancing the efficacy of cancer therapies.

4.10 Future perspectives

From our current experiments it is clear the involvement of hypoxia in the selection of CCSCs-like cells. Moreover, further experiments need to be performed considering different cell lines, to observe whether they behave similarly to the LM8 under such stressor conditions. In our experiments we always used 1% O₂ for the hypoxic condition exposing the cells to it for one week and two weeks; for future experiments could be useful to test new oxygen concentrations and exposure times. Additionally, studies with particle radiation (e.g: carbon-ion) could be performed, based on publications that confirm a relevant role of such radiation in reducing the amount of CCSCs in the circulation (Tinganelli et al., 2020). Furthermore, since we were not able to isolate CTCs from blood of mice, more experiments need to be performed to set up an efficient protocol for extraction. Once able to isolate this subpopulation of cells, Next Generation Sequencing (NGS) studies could be performed to study the panel of genes that are expressed in our cells of interest. Afterwards, an

upregulation or downregulation of these genes can be done with siRNA vectors, to perform *in vivo* metastases formation studies.

APPENDIX

A List of abbreviations

BDNF	Brain Derived Neurotrophic Factor
CCSCs	Circulating Cancer Stem Cells
CSCs	Cancer Stem Cells
CTCs	Circulating Tumor Cells
DTCs	Disseminated Tumor Cells
EC	Extracellular Domain
ECM	Extracellular Matrix
EMT	Epithelial-to-Mesenchymal transition
HIF	Hypoxia Inducible Factors
IC	Intracellular Domain
ICC	Immunocytochemistry
IHC	Immunohistochemistry
MET	Mesenchymal-to-Epithelial transition
MMPs	Matrix Metalloproteinases
MSCs	Mesenchymal Stem Cells
OER	Oxygen enhancement ratio
OS	Osteosarcoma
PHD	Prolyl-hydroxylase domain
TM	Transmembrane Domain
TrK B	Receptor Tyrosine Kinase B

B List of materials

B.1 Chemicals

Accutase (Sigma Aldrich)
BSA solution (PanReac Applichem)
Collagen type I (Enzo Life Sciences)
DAPI solution (Sigma Life Science)
Deoxycholic acid (Sigma Aldrich)
DMEM (Gibco)
Eosin solution (Roth)
FBS superior (Sigma)
Halt Protease Inhibitor (Thermo Scientific)
Hematoxylin solution (Merck)
Isolation Buffer (Invitrogen)
Methylenblue Solution (Merck)
Mytomicin-C (Sigma Aldrich)
Na-Fluorid (Sigma Aldrich)
Na-Orthovanadat (Alfa Aesar)
NaCl (Sigma Aldrich)
OCT compound (Sakura Finetek)
PBS Dulbecco (Sigma Aldrich)
Penicillin-Streptomycin (Pan Biotech)
PermaFluor mounting medium (Thermo Scientific)
PFA Solution (Roth)
Release Buffer (Invitrogen)
SDS (Applichem)
Sucrose solution (Roth)
Tris pH 8,0 (Roth)
Triton X-100 (Roth)
Trypsin-EDTA (Pan Biotech)

B.2 Solutions, buffer and gels

3% BSA solution

1,5 g BSA

50 ml PBS

DAPI solution

1 µg/ml in PBS

3,7% PFA solution

1 ml 37% PFA stock solution

10 ml PBS

1X RIPA buffer (for 2 ml)

200 µl 10x RIPA

20 µl 100x Halt Protease Inhibitor

10 µl Na-Orthovanadat (200 mM)

8 µl Na-Fluorid (500 mM)

1762 µl ddH₂O

Running Buffer (10x)

30,3 g Tris

144g Glycin

10g SDS

1 L ddH₂O

10x TBS

87,7 g NaCl

12,1 g Tris

Adjust with 5M HCl for pH 7,5

1 L ddH₂O

Transfer Buffer

Solution A (upper part):

0.3 M Tris

5% Metanol

Solution B (for the membrane):

25mM tris

5% Metanol

Solution C (bottom part):

40mM 6-aminocapron acid

25mM tris

5% Metanol

Western Blot Running Gel (10%)

4,7 ml ddH₂O

5,4 ml Acrylamid 30%

6 ml Tris/HCL pH 8,8

0,162 ml 10% SDS

0,054 ml 20% APS

0,012 ml TEMED

Western Blot Stacking Gel

3,52 ml ddH₂O

0,836 ml Acrylamid 30%

0,626 ml 1M Tris/HCl pH 6,8

0,05 ml 10% SDS

0,04 ml 20% APS

0,005 ml TEMED

B.3 Cell culture media

Complete medium

500 ml DMEM

50 ml FBS superior

5,5 ml Penicillin and Streptomycin

Cryo medium

19 ml DMEM

1 ml DMSO

B.4 Consumables

15 ml/50 ml tubes (Falcon)

5 ml polystyrene tube (Falcon)

Dynamag-2 magnet (Invitrogen)

Glass slides (Epredia)

Petri dishes 60 mm (TPP)

T25/T75 tissue culture flasks (Falcon)

Ultra low attachment 6-well plates (Greiner Bio-one)

B.5 Antibodies

Anti b-actin antibody (Sigma-Aldrich)

Anti GAPDH antibody (Sigma-Aldrich)

CD133 Prominin I (Abcam)

CD47 Polyclonal Ab (Invitrogen)

E-cadherin monoclonal antibody (Invitrogen)

Goat anti-mouse antibody (BioRad)

Goat anti-rabbit antibody (BioRad)

HIF1a Polyclonal Ab (Bethyl laboratories)

N-cadherin monoclonal antibody (cell signaling)

Rhodamine Phalloidin (F-actin) antibody (Invitrogen)

TrK B antibody (Biorbyt)

B.6 Kit systems

DAB Substrate kit (Pharminogen)

DC protein Assay Kit (BioRad)

DSB-X Biotin Protein labelling kit (Invitrogen)

Ultra-Sensitive ABC Peroxidase Rabbit igG staining kit (Thermo Fisher Scientific)

B.7 Devices

Beckman Coulter cell counter

CondoCell box (Baker Ruskinn)

Cryostat Leica CM1860 UV

CytoFLEX Flow Cytometer (Beckman Coulter)

Hypoxia working station InVivO₂ 400 (Baker Ruskinn)

Leica DMI 4000B Confocal microscope

Motic AE31 microscope

S3e Cell Sorter (BioRad)

X-ray tube

B.8 Softwares

GraphPad Prism 9

ImageJ 1.53t software (Java 1.8.0_345 64-bit version)

LASX 1.4.4

QuPath (0.3.0 version)

BIBLIOGRAPHY

1. Adeshakin, F. O., Adeshakin, A. O., Afolabi, L. O., Yan, D., Zhang, G., and Wan, X. (2021). Mechanisms for Modulating Anoikis Resistance in Cancer and the Relevance of Metabolic Reprogramming. *Front Oncol* 11. doi: 10.3389/fonc.2021.626577.
2. Aguirre-Ghiso JA (2007). Models, mechanisms and clinical evidence for cancer dormancy. *Nat Rev Cancer*. 2007 Nov;7(11):834-46. doi: 10.1038/nrc2256.
3. Akpe, V., Kim, T. H., Brown, C. L., and Cock, I. E. (2020). Circulating tumour cells: a broad perspective. *J R Soc Interface* 17. doi: 10.1098/rsif.2020.0065.
4. Al Tameemi, W., Dale, T. P., Al-Jumaily, R. M. K., and Forsyth, N. R. (2019). Hypoxia-Modified Cancer Cell Metabolism. *Front Cell Dev Biol* 7. doi: 10.3389/fcell.2019.00004.
5. Albin, A., Bruno, A., Gallo, C., Pajardi, G., Noonan, D. M., and Dallaglio, K. (2015). Cancer stem cells and the tumor microenvironment: Interplay in tumor heterogeneity. *Connect Tissue Res* 56, 414–425.
6. Alix-Panabières, C., and Pantel, K. (2014). Challenges in circulating tumour cell research. *Nat Rev Cancer* 14, 623–631. doi: 10.1038/nrc3820.
7. Amintas, S., Bedel, A., Moreau-Gaudry, F., Boutin, J., Buscail, L., Merlio, J. P., et al. (2020). Circulating tumor cell clusters: United we stand divided we fall. *Int J Mol Sci* 21. doi: 10.3390/ijms21072653.
8. Arnold, C. R., Mangesius, J., Skvortsova, I. I., and Ganswindt, U. (2020). The Role of Cancer Stem Cells in Radiation Resistance. *Front Oncol* 10. doi: 10.3389/fonc.2020.00164.
9. Asai, T., Ueda, T., Itoh, K., Yoshioka, K., Aoki, Y., Mori, S., et al. (1998). Establishment and characterization of a murine osteosarcoma cell line (LM8) with high metastatic potential to the lung. *Int J Cancer* 76, 418–422. doi: 10.1002/(SICI)1097-0215(19980504)76:3<418::AID-IJC21>3.0.CO;2-5.

10. Ayob, A. Z., and Ramasamy, T. S. (2018). Cancer stem cells as key drivers of tumour progression. *J Biomed Sci* 25. doi: 10.1186/s12929-018-0426-4.
11. Bahmad, H. F., Cheaito, K., Chalhoub, R. M., Hadadeh, O., Monzer, A., Ballout, F., et al. (2018). Sphere-Formation Assay: Three-dimensional in vitro culturing of prostate cancer stem/Progenitor sphere-forming cells. *Front Oncol* 8. doi: 10.3389/fonc.2018.00347.
12. Bankó, P., Lee, S. Y., Nagygyörgy, V., Zrínyi, M., Chae, C. H., Cho, D. H., et al. (2019). Technologies for circulating tumor cell separation from whole blood. *J Hematol Oncol* 12. doi: 10.1186/s13045-019-0735-4.
13. Banyard, J., and Bielenberg, D. R. (2015). The role of EMT and MET in cancer dissemination. *Connect Tissue Res* 56, 403–413. doi: 10.3109/03008207.2015.1060970.
14. Bao, B., Azmi, A. S., Ali, S., Ahmad, A., Li, Y., Banerjee, S., et al. (2012). The biological kinship of hypoxia with CSC and EMT and their relationship with deregulated expression of miRNAs and tumor aggressiveness. *Biochim Biophys Acta Rev Cancer* 1826, 272–296. doi: 10.1016/j.bbcan.2012.04.008.
15. Bar, E. E. (2011). Glioblastoma, cancer stem cells and hypoxia. *Brain Pathology* 21, 119–129. doi: 10.1111/j.1750-3639.2010.00460.x.
16. Barnett, G. C., West, C. M. L., Dunning, A. M., Elliott, R. M., Coles, C. E., Pharoah, P. D. P., et al. (2009). Normal tissue reactions to radiotherapy: Towards tailoring treatment dose by genotype. *Nat Rev Cancer* 9, 134–142. doi: 10.1038/nrc2587.
17. Baskar, R., Lee, K. A., Yeo, R., and Yeoh, K. W. (2012). Cancer and radiation therapy: Current advances and future directions. *Int J Med Sci* 9, 193–199. doi: 10.7150/ijms.3635.
18. Basu, S., Cheriyaundath, S., and Ben-Ze'ev, A. (2018). Cell–cell adhesion: Linking wnt/ β -catenin signaling with partial emt and stemness traits in tumorigenesis [version 1; peer review: 4 approved]. *F1000Res* 7. doi: 10.12688/F1000RESEARCH.15782.1.

19. Behrooz, A. B., and Syahir, A. (2021). Could We Address the Interplay Between CD133, Wnt/ β -Catenin, and TERT Signaling Pathways as a Potential Target for Glioblastoma Therapy? *Front Oncol* 11. doi: 10.3389/fonc.2021.642719.
20. Bera A, Lewis SM. (2020). Regulation of Epithelial-to-Mesenchymal Transition by Alternative Translation Initiation Mechanisms and Its Implications for Cancer Metastasis. *Int J Mol Sci*. 2020 Jun 7;21(11):4075. doi: 10.3390/ijms21114075. PMID: 32517298; PMCID: PMC7312463.
21. Berens, E. B., Holy, J. M., Riegel, A. T., and Wellstein, A. (2015). A cancer cell spheroid assay to assess invasion in a 3D setting. *Journal of Visualized Experiments* 2015. doi: 10.3791/53409.
22. Boria, A. J., and Perez-Torres, C. J. (2019). Minimal difference between fractionated and single-fraction exposure in a murine model of radiation necrosis. *Radiation Oncology* 14. doi: 10.1186/s13014-019-1356-3.
23. Boulefour, W., Rowinski, E., Louati, S., Sotton, S., Wozny, A. S., Moreno-Acosta, P., et al. (2021). A review of the role of hypoxia in radioresistance in cancer therapy. *Medical Science Monitor* 27. doi: 10.12659/MSM.934116.
24. Brochu-gaudreau, K., Charbonneau, M., Harper, K., and Dubois, C. M. (2022). Hypoxia Selectively Increases a SMAD3 Signaling Axis to Promote Cancer Cell Invasion. *Cancers (Basel)* 14. doi: 10.3390/cancers14112751.
25. Butturini, E., de Prati, A. C., Boriero, D., and Mariotto, S. (2019). Tumor dormancy and interplay with hypoxic tumor microenvironment. *Int J Mol Sci* 20. doi: 10.3390/ijms20174305.
26. Candas-Green D, Xie B, Huang J, Fan M, Wang A, Mena C, Zhang Y, Zhang L, Jing D, Azghadi S, Zhou W, Liu L, Jiang N, Li T, Gao T, Sweeney C, Shen R, Lin TY, Pan CX, Ozpiskin OM, Woloschak G, Grdina DJ, Vaughan AT, Wang JM, Xia S, Monjazebe AM, Murphy WJ, Sun LQ, Chen HW, Lam KS, Weichselbaum RR, Li JJ (2020). Dual blockade of CD47 and HER2 eliminates radioresistant breast cancer cells. *Nat Commun*. 2020 Sep 14;11(1):4591. doi: 10.1038/s41467-020-18245-7. PMID: 32929084; PMCID: PMC7490264.

27. Cao, L., Zhou, Y., Zhai, B., Liao, J., Xu, W., Zhang, R., et al. (2011). Sphere-forming cell subpopulations with cancer stem cell properties in human hepatoma cell lines. *BMC Gastroenterol* 11. doi: 10.1186/1471-230X-11-71.
28. Caradec J, Sirab N, Keumeugni C, Moutereau S, Chimingqi M, Matar C, Revaud D, Bah M, Manivet P, Conti M, Loric S. (2010). 'Desperate house genes': the dramatic example of hypoxia. *Br J Cancer*. 2010 Mar 16;102(6):1037-43. doi: 10.1038/sj.bjc.6605573. Epub 2010 Feb 23. PMID: 20179706; PMCID: PMC2844028.
29. Carlos-Reyes A, Muñiz-Lino MA, Romero-Garcia S, López-Camarillo C, Hernández-de la Cruz ON. (2021). Biological Adaptations of Tumor Cells to Radiation Therapy. *Front Oncol*. 2021 Nov 24;11:718636. doi: 10.3389/fonc.2021.718636. PMID: 34900673; PMCID: PMC8652287.
30. Carnero, A., and Lleonaart, M. (2016). The hypoxic microenvironment: A determinant of cancer stem cell evolution. *BioEssays* 38, S65–S74. doi: 10.1002/bies.201670911.
31. Cavallaro, Ugo & Christofori, Gerhard. (2004). Adhesion and signaling by cadherins and Ig-CAMs in cancer. *Nat Rev Cancer* 4: 118-132. Nature reviews. Cancer. 4. 118-32. 10.1038/nrc1276.
32. Celià-Terrassa, T., and Jolly, M. K. (2020). Cancer stem cells and epithelial-to-mesenchymal transition in cancer metastasis. *Cold Spring Harb Perspect Med* 10, 1–17. doi: 10.1101/cshperspect.a036905.
33. Chao, M. P., Weissman, I. L., and Majeti, R. (2012). The CD47-SIRPα pathway in cancer immune evasion and potential therapeutic implications. *Curr Opin Immunol* 24, 225–232. doi: 10.1016/j.coi.2012.01.010.
34. Chen, A., Beetham, H., Black, M. A., Priya, R., Telford, B. J., Guest, J., et al. (2014). E-cadherin loss alters cytoskeletal organization and adhesion in non-malignant breast cells but is insufficient to induce an epithelial-mesenchymal transition. *BMC Cancer* 14. doi: 10.1186/1471-2407-14-552.

35. Chen, Q., Zou, J., He, Y., Pan, Y., Yang, G., Zhao, H., et al. (2022). A narrative review of circulating tumor cells clusters: A key morphology of cancer cells in circulation promote hematogenous metastasis. *Front Oncol* 12. doi: 10.3389/fonc.2022.944487.
36. Chiang, S. P., Cabrera, R. M., and Segall, J. E. (2016). Tumor cell intravasation. *Am J Physiol Cell Physiol* 311, 1–14. doi: 10.1152/ajpcell.00238.2015.-The.
37. Choong, P. F. M., Broadhead, M. L., Clark, J. C. M., Myers, D. E., and Dass, C. R. (2011). The molecular pathogenesis of osteosarcoma: A review. *Sarcoma* 2011. doi: 10.1155/2011/959248.
38. Chu, K., Boley, K. M., Moraes, R., Barsky, S. H., and Robertson, F. M. (2013). The Paradox of E-Cadherin: Role in response to hypoxia in the tumor microenvironment and regulation of energy metabolism. Available at: www.impactjournals.com/oncotarget.
39. Corre, I., Verrecchia, F., Crenn, V., Redini, F., and Trichet, V. (2020). The osteosarcoma microenvironment: A complex but targetable ecosystem. *Cells* 9. doi: 10.3390/cells9040976.
40. Cortini, M., Avnet, S., and Baldini, N. (2017). Mesenchymal stroma: Role in osteosarcoma progression. *Cancer Lett* 405, 90–99. doi: 10.1016/j.canlet.2017.07.024.
41. Damen, M. P. F., van Rheenen, J., and Scheele, C. L. G. J. (2021). Targeting dormant tumor cells to prevent cancer recurrence. *FEBS Journal* 288, 6286–6303. doi: 10.1111/febs.15626.
42. Dasgupta, A., Lim, A. R., and Ghajar, C. M. (2017). Circulating and disseminated tumor cells: harbingers or initiators of metastasis? *Mol Oncol* 11, 40–61. doi: 10.1002/1878-0261.12022.
43. Datta, A., Deng, S., Gopal, V., Yap, K. C. H., Halim, C. E., Lye, M. L., et al. (2021). Cytoskeletal dynamics in epithelial-mesenchymal transition: Insights into therapeutic targets for cancer metastasis. *Cancers (Basel)* 13. doi: 10.3390/cancers13081882.
44. de Azevedo, J. W. V., de Medeiros Fernandes, T. A. A., Fernandes, J. V., de Azevedo, J. C. V., Lanza, D. C. F., Bezerra, C. M., et al. (2020). Biology and pathogenesis of human osteosarcoma (Review). *Oncol Lett* 19, 1099–1116. doi: 10.3892/ol.2019.11229.

45. De Luca, A., Raimondi, L., Salamanna, F., Carina, V., Costa, V., Bellavia, D., et al. (2018). Relevance of 3d culture systems to study osteosarcoma environment. *Journal of Experimental and Clinical Cancer Research* 37. doi: 10.1186/s13046-017-0663-5.
46. Debela, D. T., Muzazu, S. G. Y., Heraro, K. D., Ndalama, M. T., Mesele, B. W., Haile, D. C., et al. (2021). New approaches and procedures for cancer treatment: Current perspectives. *SAGE Open Med* 9. doi: 10.1177/20503121211034366.
47. Dekker Y, Le Dévédec SE, Danen EHJ, Liu Q. (2022). Crosstalk between Hypoxia and Extracellular Matrix in the Tumor Microenvironment in Breast Cancer. *Genes (Basel)*. 2022 Sep 3;13(9):1585. doi: 10.3390/genes13091585. PMID: 36140753; PMCID: PMC9498429.
48. Delaney, G., Jacob, S., Featherstone, C., and Barton, M. (2005). The role of radiotherapy in cancer treatment: Estimating optimal utilization from a review of evidence-based clinical guidelines. *Cancer* 104, 1129–1137. doi: 10.1002/cncr.21324.
49. Deng, Z., Wu, S., Wang, Y., and Shi, D. (2022). Circulating tumor cell isolation for cancer diagnosis and prognosis-NC-ND license (<http://creativecommons.org/licenses/by-nc-nd/4.0/>). *EBioMedicine* 83, 104237. doi: 10.1016/j.
50. Desouky, O., Ding, N., and Zhou, G. (2015). Targeted and non-targeted effects of ionizing radiation. *J Radiat Res Appl Sci* 8, 247–254. doi: 10.1016/j.jrras.2015.03.003.
51. Donato, C., Kunz, L., Castro-Giner, F., Paasinen-Sohns, A., Strittmatter, K., Szczerba, B. M., et al. (2020). Hypoxia Triggers the Intravasation of Clustered Circulating Tumor Cells. *Cell Rep* 32. doi: 10.1016/j.celrep.2020.108105.
52. Douma, S., Van Laar, T., Zevenhoven, J., Meuwissen, R., Van Garderen, E., and Peeper, D. S. (2004). Suppression of anoikis and induction of metastasis by the neurotrophic receptor TrkB. *Nature* 430, 1034–1040. doi: 10.1038/nature02765.
53. Dujon, A. M., Capp, J. P., Brown, J. S., Pujol, P., Gatenby, R. A., Ujvari, B., et al. (2021). Is there one key step in the metastatic cascade? *Cancers (Basel)* 13. doi: 10.3390/cancers13153693.

54. Eladl, E., Tremblay-Lemay, R., Rastgoo, N., Musani, R., Chen, W., Liu, A., et al. (2020). Role of CD47 in Hematological Malignancies. *J Hematol Oncol* 13. doi: 10.1186/s13045-020-00930-1.
55. Emami Nejad, A., Najafgholian, S., Rostami, A., Sistani, A., Shojaeifar, S., Esparvarinha, M., et al. (2021). The role of hypoxia in the tumor microenvironment and development of cancer stem cell: a novel approach to developing treatment. *Cancer Cell Int* 21. doi: 10.1186/s12935-020-01719-5.
56. Eskiizmir, G. (2015). Tumor Microenvironment in Head and Neck Squamous Cell Carcinomas. *Turk Otolarengoloji Arsivi/Turkish Archives of Otolaryngology* 53, 120–127. doi: 10.5152/tao.2015.1065.
57. Ferrandina, G., Petrillo, M., Bonanno, G., and Scambia, G. (2009). Targeting CD133 antigen in cancer. *Expert Opin Ther Targets* 13, 823–837. doi: 10.1517/14728220903005616.
58. Flaherty JD, Barr M, Fennell D, Richard D, Reynolds J, O'Leary J, O'Byrne K. (2012). The cancer stem-cell hypothesis: its emerging role in lung cancer biology and its relevance for future therapy. *J Thorac Oncol*. 2012 Dec;7(12):1880-1890. doi: 10.1097/JTO.0b013e31826bfb6.
59. Foldager CB, Munir S, Ulrik-Vinther M, Søballe K, Bünger C, Lind M. (2009). Validation of suitable house keeping genes for hypoxia-cultured human chondrocytes. *BMC Mol Biol*. 2009 Oct 9;10:94. doi: 10.1186/1471-2199-10-94. PMID: 19818117; PMCID: PMC2764705.
60. Follain G, Herrmann D, Harlepp S, Hyenne V, Osmani N, Warren SC, Timpson P, Goetz JG. (2020). Fluids and their mechanics in tumour transit: shaping metastasis. *Nat Rev Cancer*. 2020 Feb;20(2):107-124. doi: 10.1038/s41568-019-0221-x. Epub 2019 Nov 28. PMID: 31780785.
61. Franken, B., de Groot, M. R., Mastboom, W. J. B., Vermes, I., van der Palen, J., Tibbe, A. G. J. (2012). Circulating tumor cells, disease recurrence and survival in newly diagnosed breast cancer. *Breast Cancer Research* 14. doi: 10.1186/bcr3333.
62. Fukui R, Saga R, Matsuya Y, Tomita K, Kuwahara Y, Ohuchi K, Sato T, Okumura K, Date H, Fukumoto M, Hosokawa Y. (2022). Tumor radioresistance caused by radiation-induced changes of stem-like cell content and sub-lethal damage repair capability. *Sci Rep*. 2022 Jan 20;12(1):1056. doi: 10.1038/s41598-022-05172-4. PMID: 35058559; PMCID: PMC8776741.

63. Gao, X. L., Zhang, M., Tang, Y. L., and Liang, X. H. (2017). Cancer cell dormancy: Mechanisms and implications of cancer recurrence and metastasis. *Onco Targets Ther* 10, 5219–5228. doi: 10.2147/OTT.S140854.
64. Geiger, T. R., and Peeper, D. S. (2005). The neurotrophic receptor TrkB in anoikis resistance and metastasis: A perspective. *Cancer Res* 65, 7033–7036. doi: 10.1158/0008-5472.CAN-05-0709.
65. Geiger, T. R., Song, J. Y., Rosado, A., and Peeper, D. S. (2011). Functional characterization of human cancer-derived TRKB mutations. *PLoS One* 6. doi: 10.1371/journal.pone.0016871.
66. Gheytaichi, E., Naseri, M., Karimi-Busheri, F., Atyabi, F., Mirsharif, E. S., Bozorgmehr, M., Ghods R., Madjd Z. (2021). Morphological and molecular characteristics of spheroid formation in HT-29 and Caco-2 colorectal cancer cell lines. *Cancer Cell Int* 21. doi: 10.1186/s12935-021-01898-9.
67. Giancotti, F. G. (2013). Mechanisms governing metastatic dormancy and reactivation. *Cell* 155, 750. doi: 10.1016/j.cell.2013.10.029.
68. Giannoni, E., Buricchi, F., Grimaldi, G., Parri, M., Cialdai, F., Taddei, M. L., Raugei G., Ramponi G., Chiarugi P. (2008). Redox regulation of anoikis: Reactive oxygen species as essential mediators of cell survival. *Cell Death Differ* 15, 867–878. doi: 10.1038/cdd.2008.3.
69. Gilkes DM, Semenza GL, Wirtz D. (2014). Hypoxia and the extracellular matrix: drivers of tumour metastasis. *Nat Rev Cancer*. 2014 Jun;14(6):430-9. doi: 10.1038/nrc3726. Epub 2014 May 15. PMID: 24827502; PMCID: PMC4283800.
70. Glumac, P. M., and LeBeau, A. M. (2018). The role of CD133 in cancer: a concise review. *Clin Transl Med* 7. doi: 10.1186/s40169-018-0198-1.
71. Gomis, R. R., and Gawrzak, S. (2017). Tumor cell dormancy. *Mol Oncol* 11, 62–78. doi: 10.1016/j.molonc.2016.09.009.
72. González-González R, Ortiz-Sarabia G, Molina-Frechero N, Salas-Pacheco JM, Salas-Pacheco SM, Lavallo-Carrasco J, López-Verdín S, Tremillo-Maldonado O, Bologna-Molina R.

- (2021). Epithelial-Mesenchymal Transition Associated with Head and Neck Squamous Cell Carcinomas: A Review. *Cancers (Basel)*. 2021 Jun 17;13(12):3027. doi: 10.3390/cancers13123027. PMID: 34204259; PMCID: PMC8234594.
73. Grada, A., Otero-Vinas, M., Prieto-Castrillo, F., Obagi, Z., and Falanga, V. (2017). Research Techniques Made Simple: Analysis of Collective Cell Migration Using the Wound Healing Assay. *Journal of Investigative Dermatology* 137, e11–e16. doi: 10.1016/j.jid.2016.11.020.
74. Guarino, M., Rubino, B., and Ballabio, G. (2007). The role of epithelial-mesenchymal transition in cancer pathology. *Pathology* 39, 305–318. doi: 10.1080/00313020701329914.
75. Gustafsson, M. V., Zheng, X., Pereira, T., Gradin, K., Jin, S., Lundkvist, J., Ruas JL., Poellinger L., Lendahl U., Bondesson M. (2005). Hypoxia requires Notch signaling to maintain the undifferentiated cell state. *Dev Cell* 9, 617–628. doi: 10.1016/j.devcel.2005.09.010.
76. Hao, Y., Baker, D., and Dijke, P. Ten (2019). TGF- β -mediated epithelial-mesenchymal transition and cancer metastasis. *Int J Mol Sci* 20. doi: 10.3390/ijms20112767.
77. Hardin, H., Zhang, R., Helein, H. (2017). The evolving concept of cancer stem-like cells in thyroid cancer and other solid tumors. *Lab Invest* 97, 1142–1151 <https://doi.org/10.1038/labinvest.2017.41>
78. Harris, M. A., and Hawkins, C. J. (2022). Recent and Ongoing Research into Metastatic Osteosarcoma Treatments. *Int J Mol Sci* 23. doi: 10.3390/ijms23073817.
79. Heddleston, J. M., Li, Z., Lathia, J. D., Bao, S., Hjelmeland, A. B., and Rich, J. N. (2010). Hypoxia inducible factors in cancer stem cells. *Br J Cancer* 102, 789–795. doi: 10.1038/sj.bjc.6605551.
80. Helan, M., Aravamudan, B., Hartman, W. R., Thompson, M. A., Johnson, B. D., Pabelick, C. M., Prakash YS. (2014). BDNF secretion by human pulmonary artery endothelial cells in response to hypoxia. *J Mol Cell Cardiol* 68, 89–97. doi: 10.1016/j.yjmcc.2014.01.006.

81. Helm, A., Ebner, D. K., Tinganelli, W., Simoniello, P., Bisio, A., Marchesano, V., Durante M., Yamada S., Shimokawa T. (2019). Combining heavy-ion therapy with immunotherapy: An update on recent developments. *Int J Part Ther* 5, 84–93. doi: 10.14338/IJPT-18-00024.1.
82. Hemmings, B. A., and Restuccia, D. F. (2012). PI3K-PKB/Akt pathway. *Cold Spring Harb Perspect Biol* 4. doi: 10.1101/cshperspect.a011189.
83. Huang, H., Wright, S., Zhang, J., and Brekken, R. A. (2019). Getting a grip on adhesion: Cadherin switching and collagen signaling. *Biochim Biophys Acta Mol Cell Res* 1866. doi: 10.1016/j.bbamcr.2019.04.002.
84. Huang X, Zhao J, Bai J, Shen H, Zhang B, Deng L, Sun C, Liu Y, Zhang J, Zheng J. (2019). Risk and clinicopathological features of osteosarcoma metastasis to the lung: A population-based study. *J Bone Oncol*. 2019 Mar 7;16:100230. doi: 10.1016/j.jbo.2019.100230. PMID: 30923668; PMCID: PMC6423404.
85. Hur, W., and Yoon, S. K. (2017). Molecular pathogenesis of radiation-induced cell toxicity in stem cells. *Int J Mol Sci* 18. doi: 10.3390/ijms18122749.
86. Hurtado, P., Martínez-Pena, I., Yepes-Rodríguez, S., Bascoy-Otero, M., Abuín, C., Fernández-Santiago, C., Sanchez L., Lopez-Lopez R., Pineiro R. (2023). Modelling metastasis in zebrafish unveils regulatory interactions of cancer-associated fibroblasts with circulating tumour cells. *Front Cell Dev Biol* 11. doi: 10.3389/fcell.2023.1076432.
87. Iida, H., Suzuki, M., Goitsuka, R., and Ueno, H. (2012). Hypoxia induces CD133 expression in human lung cancer cells by up-regulation of OCT3/4 and SOX2. *Int J Oncol* 40, 71–79. doi: 10.3892/ijo.2011.1207.
88. Ikushima, H., and Miyazono, K. (2010). Cellular context-dependent “colors” of transforming growth factor- β signaling. *Cancer Sci* 101, 306–312. doi: 10.1111/j.1349-7006.2009.01441.x.
89. Irollo E, Pirozzi G. (2013). CD133: to be or not to be, is this the real question? *Am J Transl Res*. 2013 Sep 25;5(6):563-81. PMID: 24093054

90. Isakoff, M. S., Bielack, S. S., Meltzer, P., and Gorlick, R. (2015). Osteosarcoma: Current treatment and a collaborative pathway to success. *Journal of Clinical Oncology* 33, 3029–3035. doi: 10.1200/JCO.2014.59.4895.
91. Ishiguro, T., Ohata, H., Sato, A., Yamawaki, K., Enomoto, T., and Okamoto, K. (2017). Tumor-derived spheroids: Relevance to cancer stem cells and clinical applications. *Cancer Sci* 108, 283–289. doi: 10.1111/cas.13155.
92. Jang, J. W., Song, Y., Kim, S. H., Kim, J., and Seo, H. R. (2017). Potential mechanisms of CD133 in cancer stem cells. *Life Sci* 184, 25–29. doi: 10.1016/j.lfs.2017.07.008.
93. Jaśkiewicz M, Moszyńska A, Króliczewski J, Cabaj A, Bartoszewska S, Charzyńska A, Gebert M, Dąbrowski M, Collawn JF, Bartoszewski R. (2022). The transition from HIF-1 to HIF-2 during prolonged hypoxia results from reactivation of PHDs and HIF1A mRNA instability. *Cell Mol Biol Lett*. 2022 Dec 8;27(1):109. doi: 10.1186/s11658-022-00408-7. PMID: 36482296; PMCID: PMC9730601.
94. Jiang, J., Tang, Y. L., and Liang, X. H. (2011). EMT: A new vision of hypoxia promoting cancer progression. *Cancer Biol Ther* 11, 714–723. doi: 10.4161/cbt.11.8.15274.
95. Ju, F., Atyah, M. M., Horstmann, N., Gul, S., Vago, R., Bruns, C. J. (2022). Characteristics of the cancer stem cell niche and therapeutic strategies. *Stem Cell Res Ther* 13. doi: 10.1186/s13287-022-02904-1.
96. Jubelin, C., Muñoz-García, J., Cochonneau, D., Moranton, E., Heymann, M. F., and Heymann, D. (2022). Biological evidence of cancer stem-like cells and recurrent disease in osteosarcoma. *Cancer Drug Resistance* 5, 184–198. doi: 10.20517/cdr.2021.130.
97. Kalluri, R., and Weinberg, R. A. (2009). The basics of epithelial-mesenchymal transition. *Journal of Clinical Investigation* 119, 1420–1428. doi: 10.1172/JCI39104.
98. Kang, Y., and Pantel, K. (2013). Tumor Cell Dissemination: Emerging Biological Insights from Animal Models and Cancer Patients. *Cancer Cell* 23, 573–581. doi: 10.1016/j.ccr.2013.04.017.

99. Kansara, M., Teng, M. W., Smyth, M. J., and Thomas, D. M. (2014). Translational biology of osteosarcoma. *Nat Rev Cancer* 14, 722–735. doi: 10.1038/nrc3838.
100. Kashima T, Nakamura K, Kawaguchi J, Takanashi M, Ishida T, Aburatani H, Kudo A, Fukayama M, Grigoriadis AE. (2003). Overexpression of cadherins suppresses pulmonary metastasis of osteosarcoma in vivo. *Int J Cancer*. 2003 Mar 20;104(2):147-54. doi: 10.1002/ijc.10931. PMID: 12569568.
101. Kawamoto, A., Tanaka, K., Saigusa, S., Toiyama, Y., Morimoto, Y., Fujikawa, H. (2012). Clinical significance of radiation-induced CD133 expression in residual rectal cancer cells after chemoradiotherapy. *Exp Ther Med* 3, 403–409. doi: 10.3892/etm.2011.438.
102. Kepka, L., and Socha, J. (2021). Dose and fractionation schedules in radiotherapy for non-small cell lung cancer. *Transl Lung Cancer Res* 10, 1969–1982. doi: 10.21037/tlcr-20-253.
103. Khanna, C., Wan, X., Bose, S., Cassaday, R., Olomu, O., Mendoza, A. (2004). The membrane-cytoskeleton linker ezrin is necessary for osteosarcoma metastasis. *Nat Med* 10, 182–186. doi: 10.1038/nm982.
104. Kim, M. S., Bolia, I. K., Iglesias, B., Sharf, T., Roberts, S. I., Kang, H. (2022). Timing of treatment in osteosarcoma: challenges and perspectives – a scoping review. *BMC Cancer* 22. doi: 10.1186/s12885-022-10061-0.
105. Kim, R.-K., Kaushik, N., Suh, Y., Yoo, K.-C., Cui, Y.-H., Kim, M.-J. (2016). Radiation driven epithelial-mesenchymal transition is mediated by Notch signaling in breast cancer. Available at: www.impactjournals.com/oncotarget.
106. Kim, Y. H., Yoo, K. C., Cui, Y. H., Uddin, N., Lim, E. J., Kim, M. J. (2014). Radiation promotes malignant progression of glioma cells through HIF-1alpha stabilization. *Cancer Lett* 354, 132–141. doi: 10.1016/j.canlet.2014.07.048.
107. Klopp, A. H., Spaeth, E. L., Dembinski, J. L., Woodward, W. A., Munshi, A., Meyn, R. E. (2007). Tumor irradiation increases the recruitment of circulating mesenchymal stem cells into the tumor microenvironment. *Cancer Res* 67, 11687–11695. doi: 10.1158/0008-5472.CAN-07-1406.

108. Koh, M. Y., and Powis, G. (2012). Passing the baton: The HIF switch. *Trends Biochem Sci* 37, 364–372. doi: 10.1016/j.tibs.2012.06.004.
109. Koonce, N. A., Juratli, M. A., Cai, C., Sarimollaoglu, M., Menyae, Y. A., Dent, J. (2017). Real-time monitoring of circulating tumor cell (CTC) release after nanodrug or tumor radiotherapy using in vivo flow cytometry. *Biochem Biophys Res Commun* 492, 507–512. doi: 10.1016/j.bbrc.2017.08.053.
110. Lamouille S, Xu J, Derynck R. (2014). Molecular mechanisms of epithelial-mesenchymal transition. *Nat Rev Mol Cell Biol*. 2014 Mar;15(3):178-96. doi: 10.1038/nrm3758. PMID: 24556840; PMCID: PMC4240281.
111. Lee, S. Y., Jeong, E. K., Ju, M. K., Jeon, H. M., Kim, M. Y., Kim, C. H. (2017). Induction of metastasis, cancer stem cell phenotype, and oncogenic metabolism in cancer cells by ionizing radiation. *Mol Cancer* 16. doi: 10.1186/s12943-016-0577-4.
112. Li, J., Wu, D. M., Han, R., Deng, Y. Y. S. H., Liu, T., Zhang, T. (2020). Low-dose radiation promotes invasion and migration of A549 cells by activating the CXCL1/ NF- κ B signaling pathway. *Oncotargets Ther* 13, 3619–3629. doi: 10.2147/OTT.S243914.
113. Li, Y., Zhao, L., and Li, X. F. (2021). Hypoxia and the Tumor Microenvironment. *Technol Cancer Res Treat* 20. doi: 10.1177/15330338211036304.
114. Lian S, Xie R, Ye Y, Lu Y, Cheng Y, Xie X, Li S, Jia L. (2019). Dual blockage of both PD-L1 and CD47 enhances immunotherapy against circulating tumor cells. *Sci Rep*. 2019 Mar 14;9(1):4532. doi: 10.1038/s41598-019-40241-1. PMID: 30872703; PMCID: PMC6418176.
115. Lian, S., Xie, X., Lu, Y., and Jia, L. (2019). Checkpoint CD47 function on tumor metastasis and immune therapy. *Oncotargets Ther* 12, 9105–9114. doi: 10.2147/OTT.S220196.
116. Lim, J. R., Mouawad, J., Gorton, O. K., Bubb, W. A., and Kwan, A. H. (2021). Cancer stem cell characteristics and their potential as therapeutic targets. *Medical Oncology* 38. doi: 10.1007/s12032-021-01524-8.

117. Lin, D., Shen, L., Luo, M., Zhang, K., Li, J., Yang, Q. (2021). Circulating tumor cells: biology and clinical significance. *Signal Transduct Target Ther* 6. doi: 10.1038/s41392-021-00817-8.
118. Lin, Q., Cong, X., and Yun, Z. (2011). Differential hypoxic regulation of hypoxia-inducible factors 1 α and 2 α . *Molecular Cancer Research* 9, 757–765. doi: 10.1158/1541-7786.MCR-11-0053.
119. Lin, Y. H., Jewell, B. E., Gingold, J., Lu, L., Zhao, R., Wang, L. L. (2017). Osteosarcoma: Molecular Pathogenesis and iPSC Modeling. *Trends Mol Med* 23, 737–755. doi: 10.1016/j.molmed.2017.06.004.
120. Liou, G. Y. (2019). CD133 as a regulator of cancer metastasis through the cancer stem cells. *International Journal of Biochemistry and Cell Biology* 106, 1–7. doi: 10.1016/j.biocel.2018.10.013.
121. Liu, J., Lian, J., Chen, Y., Zhao, X., Du, C. Z., Xu, Y. (2021). Circulating Tumor Cells (CTCs): A Unique Model of Cancer Metastases and Non-invasive Biomarkers of Therapeutic Response. *Front Genet* 12. doi: 10.3389/fgene.2021.734595.
122. Liu, J., Xiao, Q., Xiao, J., Niu, C., Li, Y., Zhang, X. (2022). Wnt/ β -catenin signalling: function, biological mechanisms, and therapeutic opportunities. *Signal Transduct Target Ther* 7. doi: 10.1038/s41392-021-00762-6.
123. Liu, Q., Palmgren, V. A. C., Danen, E. H., and Le Dévédec, S. E. (2022). Acute vs. chronic vs. intermittent hypoxia in breast Cancer: a review on its application in in vitro research. *Mol Biol Rep* 49, 10961–10973. doi: 10.1007/s11033-022-07802-6.
124. Liu, Y., Yang, M., Luo, J., and Zhou, H. (2020). Radiotherapy targeting cancer stem cells “awakens” them to induce tumour relapse and metastasis in oral cancer. *Int J Oral Sci* 12. doi: 10.1038/s41368-020-00087-0.
125. Loh, C. Y., Chai, J. Y., Tang, T. F., Wong, W. F., Sethi, G., Shanmugam, M. K. (2019). The e-cadherin and n-cadherin switch in epithelial-to-mesenchymal transition: Signaling, therapeutic implications, and challenges. *Cells* 8. doi: 10.3390/cells8101118.

126. Loh, C. Y., Chai, J. Y., Tang, T. F., Wong, W. F., Sethi, G., Shanmugam, M. K. (2019). The e-cadherin and n-cadherin switch in epithelial-to-mesenchymal transition: Signaling, therapeutic implications, and challenges. *Cells* 8. doi: 10.3390/cells8101118.
127. Lorenz, S., Barøy, T., Sun, J., Nome, T., Vodák, D., Bryne, J.-C. (2015). Unscrambling the genomic chaos of osteosarcoma reveals extensive transcript fusion, recurrent rearrangements and frequent novel TP53 aberrations. Available at: www.impactjournals.com/oncotarget.
128. Luo BH, Carman CV, Springer TA. (2007). Structural basis of integrin regulation and signaling. *Annu Rev Immunol.* 2007;25:619-47. doi: 10.1146/annurev.immunol.25.022106.141618. PMID: 17201681; PMCID: PMC1952532.
129. Maeda, K., Ding, Q., Yoshimitsu, M., Kuwahata, T., Miyazaki, Y., Tsukasa, K. (2016). CD133 modulate HIF-1 α expression under hypoxia in EMT phenotype pancreatic cancer stem-like cells. *Int J Mol Sci* 17. doi: 10.3390/ijms17071025.
130. Marxsen JH, Stengel P, Doege K, Heikkinen P, Jokilehto T, Wagner T, Jelkmann W, Jaakkola P, Metzen E. (2004). Hypoxia-inducible factor-1 (HIF-1) promotes its degradation by induction of HIF-alpha-prolyl-4-hydroxylases. *Biochem J.* 2004 Aug 1;381(Pt 3):761-7. doi: 10.1042/BJ20040620. PMID: 15104534; PMCID: PMC1133886.
131. McKeown, S. R. (2014). Defining normoxia, physoxia and hypoxia in tumours - Implications for treatment response. *British Journal of Radiology* 87. doi: 10.1259/bjr.20130676.
132. Micalizzi DS, Maheswaran S, Haber DA.(2017). A conduit to metastasis: circulating tumor cell biology. *Genes Dev.* 2017 Sep 15;31(18):1827-1840. doi: 10.1101/gad.305805.117. PMID: 29051388; PMCID: PMC5695084.
133. Mingyuan, X., Shengquan, X., Chenyi, Y., Rui, L., Yichen, S., and Jinghong, X. (2018). Hypoxia-inducible factor-1 α activates transforming growth factor- β 1/Smad signaling and increases collagen deposition in dermal fibroblasts. Available at: www.impactjournals.com/oncotarget.
134. Miyoshi, E., Moriwaki, K., and Nakagawa, T. (2008). Biological function of fucosylation in cancer biology. *J Biochem* 143, 725–729. doi: 10.1093/jb/mvn011.

135. Moncharmont, C., Levy, A., Guy, J. B., Falk, A. T., Guilbert, M., Trone, J. C. (2014). Radiation-enhanced cell migration/invasion process: A review. *Crit Rev Oncol Hematol* 92, 133–142. doi: 10.1016/j.critrevonc.2014.05.006.
136. Morrison, B. J., Steel, J. C., and Morris, J. C. (2012). Sphere Culture of Murine Lung Cancer Cell Lines Are Enriched with Cancer Initiating Cells. *PLoS One* 7. doi: 10.1371/journal.pone.0049752.
137. Mrozik, K. M., Blaschuk, O. W., Cheong, C. M., Zannettino, A. C. W., and Vandyke, K. (2018). N-cadherin in cancer metastasis, its emerging role in haematological malignancies and potential as a therapeutic target in cancer. *BMC Cancer* 18. doi: 10.1186/s12885-018-4845-0.
138. Mutsaers, A. J., and Walkley, C. R. (2014). Cells of origin in osteosarcoma: Mesenchymal stem cells or osteoblast committed cells? *Bone* 62, 56–63. doi: 10.1016/j.bone.2014.02.003.
139. Mutschelknaus, L., Azimzadeh, O., Heider, T., Winkler, K., Vetter, M., Kell, R. (2017). Radiation alters the cargo of exosomes released from squamous head and neck cancer cells to promote migration of recipient cells. *Sci Rep* 7. doi: 10.1038/s41598-017-12403-6.
140. Muz, B., de la Puente, P., Azab, F., and Azab, A. K. (2015). The role of hypoxia in cancer progression, angiogenesis, metastasis, and resistance to therapy. *Hypoxia*, 83. doi: 10.2147/hp.s93413.
141. Mylavarapu, S., Kumar, H., Kumari, S., Sravanthi, L. S., Jain, M., Basu, A. (2019). Activation of Epithelial-Mesenchymal Transition and Altered β -Catenin Signaling in a Novel Indian Colorectal Carcinoma Cell Line. *Front Oncol* 9. doi: 10.3389/fonc.2019.00054.
142. Northcott, J. M., Dean, I. S., Mouw, J. K., and Weaver, V. M. (2018). Feeling stress: The mechanics of cancer progression and aggression. *Front Cell Dev Biol* 6. doi: 10.3389/fcell.2018.00017.
143. Odri, G. A., Tchicaya-Bouanga, J., Yoon, D. J. Y., and Modrowski, D. (2022). Metastatic Progression of Osteosarcomas: A Review of Current Knowledge of Environmental versus Oncogenic Drivers. *Cancers (Basel)* 14. doi: 10.3390/cancers14020360.

144. Oh J, Takahashi R, Kondo S, Mizoguchi A, Adachi E, Sasahara RM, Nishimura S, Imamura Y, Kitayama H, Alexander DB, Ide C, Horan TP, Arakawa T, Yoshida H, Nishikawa S, Itoh Y, Seiki M, Itohara S, Takahashi C, Noda M. (2001). The membrane-anchored MMP inhibitor RECK is a key regulator of extracellular matrix integrity and angiogenesis. *Cell*. 2001 Dec 14;107(6):789-800. doi: 10.1016/s0092-8674(01)00597-9.
145. Ohnishi S, Maehara O, Nakagawa K, Kameya A, Otaki K, Fujita H, Higashi R, Takagi K, Asaka M, Sakamoto N, Kobayashi M, Takeda H. (2013). Hypoxia-Inducible Factors Activate CD133 Promoter through ETS Family Transcription Factors. *PLoS One* 8. doi: 10.1371/journal.pone.0066255.
146. Oskarsson, T., Batlle, E., and Massagué, J. (2014). Metastatic stem cells: Sources, niches, and vital pathways. *Cell Stem Cell* 14, 306–321. doi: 10.1016/j.stem.2014.02.002.
147. Panzetta V, Verde G, Pugliese M, Artiola V, Arrichiello C, Muto P, Commara M, Netti PA, Fusco S. (2020). Adhesion and Migration Response to Radiation Therapy of Mammary Epithelial and Adenocarcinoma Cells Interacting with Different Stiffness Substrates. *Cancers (Basel)*. 2020 May 6;12(5):1170. doi: 10.3390/cancers12051170. PMID: 32384675; PMCID: PMC7281676.
148. Paoli, P., Giannoni, E., and Chiarugi, P. (2013). Anoikis molecular pathways and its role in cancer progression. *Biochim Biophys Acta Mol Cell Res* 1833, 3481–3498. doi: 10.1016/j.bbamcr.2013.06.026.
149. Papaccio, F. (2020). Circulating cancer stem cells: an interesting niche to explore. *Explor Target Antitumor Ther* 1, 253–258. doi: 10.37349/etat.2020.00016.
150. Park, S. Y., and Nam, J. S. (2020). The force awakens: metastatic dormant cancer cells. *Exp Mol Med* 52, 569–581. doi: 10.1038/s12276-020-0423-z.
151. Parker, A. L., Benguigui, M., Fornetti, J., Goddard, E., Lucotti, S., Insua-Rodríguez, J., Wiegmans AP. (2022). Current challenges in metastasis research and future innovation for clinical translation. *Clin Exp Metastasis* 39, 263–277. doi: 10.1007/s10585-021-10144-5.

152. Patel, P., and Chen, E. I. (2012). Cancer stem cells, tumor dormancy, and metastasis. *Front Endocrinol (Lausanne)* 3. doi: 10.3389/fendo.2012.00125.
153. Pei, D., Shu, X., Gassama-Diagne, A., and Thiery, J. P. (2019). Mesenchymal–epithelial transition in development and reprogramming. *Nat Cell Biol* 21, 44–53. doi: 10.1038/s41556-018-0195-z.
154. Pistollato, F., Rampazzo, E., Persano, L., Abbadi, S., Frasson, C., Denaro, L., D’Avella D., Panchision DM., Della Puppa A., Scienza R., Basso G. (2010). Interaction of hypoxia-inducible factor-1 α and Notch signaling regulates medulloblastoma precursor proliferation and fate. *Stem Cells* 28, 1918–1929. doi: 10.1002/stem.518.
155. Plaks, V., Kong, N., and Werb, Z. (2015). The cancer stem cell niche: How essential is the niche in regulating stemness of tumor cells? *Cell Stem Cell* 16, 225–238. doi: 10.1016/j.stem.2015.02.015.
156. Potdar, P., and Lotey, N. (2015). Role of circulating tumor cells in future diagnosis and therapy of cancer. *J Cancer Metastasis Treat* 1, 44. doi: 10.4103/2394-4722.158803.
157. Pradhan, S., Sperduto, J. L., Farino, C. J., and Slater, J. H. (2018). Engineered in Vitro Models of Tumor Dormancy and Reactivation. *J Biol Eng* 12. doi: 10.1186/s13036-018-0120-9.
158. Reiterer, M., Colaço, R., Emrouznejad, P., Jensen, A., Rundqvist, H., Johnson, R. S., Branco C.. (2019). Acute and chronic hypoxia differentially predispose lungs for metastases. *Sci Rep* 9. doi: 10.1038/s41598-019-46763-y.
159. Riggio, A. I., Varley, K. E., and Welm, A. L. (2021). The lingering mysteries of metastatic recurrence in breast cancer. *Br J Cancer* 124, 13–26. doi: 10.1038/s41416-020-01161-4.
160. Roig, E. M., Groot, A. J., Yaromina, A., Hendrickx, T. C., Barbeau, L. M. O., Giuranno, L., Dams G., Ient J., Olivo Pimentel V., van Gisbegen MW., Dubois LJ., Vooijs MA. (2019). HIF-1 α and HIF-2 α ; differently regulate the radiation sensitivity of NSCLC cells. *Cells* 8. doi: 10.3390/cells8010045.

161. Rossi, S., Cordella, M., Tabolacci, C., Nassa G., D’Arcangelo D., Pagnotto C., Magliozzi R., Salvati A., Weisz A., Facchiano A., Facchiano F. (2018). TNF-alpha and metalloproteases as key players in melanoma cells aggressiveness. *J Exp Clin Cancer Res* **37**, 326. <https://doi.org/10.1186/s13046-018-0982-1>
162. Rostami E, Bakhshandeh M, Ghaffari-Nazari H, Alinezhad M, Alimohammadi M, Alimohammadi R, Mahmoodi Chalbatani G, Hejazi E, Webster TJ, Tavakkol-Afshari J, Jalali SA. (2022). Combining ablative radiotherapy and anti CD47 monoclonal antibody improves infiltration of immune cells in tumor microenvironments. *PLoS One*. 2022 Aug 26;17(8):e0273547. doi: 10.1371/journal.pone.0273547. PMID: 36018888; PMCID: PMC9417014.
163. Rothzerg, E., Pfaff, A. L., and Koks, S. (2022). Innovative approaches for treatment of osteosarcoma. *Exp Biol Med* **247**, 310–316. doi: 10.1177/15353702211067718.
164. Saxena, K., and Jolly, M. K. (2019). Acute vs. Chronic vs. cyclic hypoxia: Their differential dynamics, molecular mechanisms, and effects on tumor progression. *Biomolecules* **9**. doi: 10.3390/biom9080339.
165. Schiavone, K., Garnier, D., Heymann, M. F., and Heymann, D. (2019). “The heterogeneity of osteosarcoma: The role played by cancer stem cells,” in *Advances in Experimental Medicine and Biology* (Springer New York LLC), 187–200. doi: 10.1007/978-3-030-14366-4_11.
166. Schulz, A., Meyer, F., Dubrovskaya, A., and Borgmann, K. (2019). Cancer stem cells and radioresistance: DNA repair and beyond. *Cancers (Basel)* **11**. doi: 10.3390/cancers11060862.
167. Schwab LP, Peacock DL, Majumdar D, Ingels JF, Jensen LC, Smith KD, Cushing RC, Seagroves TN. (2012). Hypoxia-inducible factor 1 α promotes primary tumor growth and tumor-initiating cell activity in breast cancer. *Breast Cancer Res*. 2012 Jan 7;14(1):R6. doi: 10.1186/bcr3087. PMID: 22225988; PMCID: PMC3496121.
168. Serafim Junior, V., Fernandes, G. M. de M., Oliveira-Cucolo, J. G. de, Pavarino, E. C., and Goloni-Bertollo, E. M. (2020). Role of Tropomyosin-related kinase B receptor and brain-derived neurotrophic factor in cancer. *Cytokine* **136**. doi: 10.1016/j.cyto.2020.155270.

169. Shao, H., Ge, M., Zhang, J., Zhao, T., and Zhang, S. (2022). Osteoclasts differential-related prognostic biomarker for osteosarcoma based on single cell, bulk cell and gene expression datasets. *BMC Cancer* 22. doi: 10.1186/s12885-022-09380-z.
170. Shen, M., and Kang, Y. (2020). Stresses in the metastatic cascade: Molecular mechanisms and therapeutic opportunities. *Genes Dev* 34, 1577–1598. doi: 10.1101/gad.343251.120.
171. Sheng, G., Gao, Y., Yang, Y., and Wu, H. (2021). Osteosarcoma and Metastasis. *Front Oncol* 11. doi: 10.3389/fonc.2021.780264.
172. Shih, W., and Yamada, S. (2012). N-cadherin as a key regulator of collective cell migration in a 3D environment. *Cell Adh Migr* 6, 513–517. doi: 10.4161/cam.21766.
173. Shiozawa, Y., Nie, B., Pienta, K. J., Morgan, T. M., and Taichman, R. S. (2013). Cancer stem cells and their role in metastasis. *Pharmacol Ther* 138, 285–293. doi: 10.1016/j.pharmthera.2013.01.014.
174. Siegel RL, Miller KD, Wagle NS, Jemal A (2023). Cancer statistics, 2023. *CA Cancer J Clin*. 2023 Jan;73(1):17-48. doi: 10.3322/caac.21763. PMID: 36633525.
175. Silva, J. A. M., Marchiori, E., de Macedo, F. C., da Silva, P. R. G., and Amorim, V. B. (2022). Pulmonary metastasis of osteosarcoma: multiple presentations in a single patient. *Jornal Brasileiro de Pneumologia* 48. doi: 10.36416/1806-3756/e20210478.
176. Simsek, T., Kocabas, F., Zheng, J., Deberardinis, R. J., Mahmoud, A. I., Olson, E. N., Schneider JW., Zhang CC., Sadek HA.. (2010). The distinct metabolic profile of hematopoietic stem cells reflects their location in a hypoxic niche. *Cell Stem Cell* 7, 380–390. doi: 10.1016/j.stem.2010.07.011.
177. Son H, Moon A. (2010). Epithelial-mesenchymal Transition and Cell Invasion. *Toxicol Res*. 2010 Dec;26(4):245-52. doi: 10.5487/TR.2010.26.4.245. PMID: 24278531; PMCID: PMC3834497.

178. Song, Y. J., Xu, Y., Zhu, X., Fu, J., Deng, C., Chen, H., Xu H., Song G., Lu J., Tang Q., Wang J. (2020). Immune Landscape of the Tumor Microenvironment Identifies Prognostic Gene Signature CD4/CD68/CSF1R in Osteosarcoma. *Front Oncol* 10. doi: 10.3389/fonc.2020.01198.
179. Sosa, M. S., Bragado, P., and Aguirre-Ghiso, J. A. (2014). Mechanisms of disseminated cancer cell dormancy: An awakening field. *Nat Rev Cancer* 14, 611–622. doi: 10.1038/nrc3793.
180. Taddei, M. L., Giannoni, E., Fiaschi, T., and Chiarugi, P. (2012). Anoikis: An emerging hallmark in health and diseases. *Journal of Pathology* 226, 380–393. doi: 10.1002/path.3000.
181. Takubo, K., Goda, N., Yamada, W., Iriuchishima, H., Ikeda, E., Kubota, Y. (2010). Regulation of the HIF-1 α level is essential for hematopoietic stem cells. *Cell Stem Cell* 7, 391–402. doi: 10.1016/j.stem.2010.06.020.
182. Tam, S. Y., Wu, V. W. C., and Law, H. K. W. (2020). Hypoxia-Induced Epithelial-Mesenchymal Transition in Cancers: HIF-1 α and Beyond. *Front Oncol* 10. doi: 10.3389/fonc.2020.00486.
183. Tanabe, S., Quader, S., Cabral, H., and Ono, R. (2020). Interplay of EMT and CSC in Cancer and the Potential Therapeutic Strategies. *Front Pharmacol* 11. doi: 10.3389/fphar.2020.00904.
184. Tanaka T, Yui Y, Naka N, Wakamatsu T, Yoshioka K, Araki N, Yoshikawa H, Itoh K. (2013). Dynamic analysis of lung metastasis by mouse osteosarcoma LM8: VEGF is a candidate for anti-metastasis therapy. *Clin Exp Metastasis*. 2013 Apr;30(4):369-79. doi: 10.1007/s10585-012-9543-8. Epub 2012 Oct 18. PMID: 23076771; PMCID: PMC3616224.
185. Tataria, M., Quarto, N., Longaker, M. T., and Sylvester, K. G. (2006). Absence of the p53 tumor suppressor gene promotes osteogenesis in mesenchymal stem cells. *J Pediatr Surg* 41, 624–632. doi: 10.1016/j.jpedsurg.2005.12.001.
186. Taylor, C. T., and Scholz, C. C. (2022). The effect of HIF on metabolism and immunity. *Nat Rev Nephrol* 18, 573–587. doi: 10.1038/s41581-022-00587-8.

187. Telarovic, I., Wenger, R. H., and Pruschy, M. (2021). Interfering with Tumor Hypoxia for Radiotherapy Optimization. *Journal of Experimental and Clinical Cancer Research* 40. doi: 10.1186/s13046-021-02000-x.
188. Thomas, S. N., Liao, Z., Clark, D., Chen, Y., Samadani, R., Mao, L., Ann DK., Baulch JE., Shapiro P., Yang AJ. (2013). Exosomal proteome profiling: A potential multi-marker cellular phenotyping tool to characterize hypoxia-induced radiation resistance in breast cancer. *Proteomes* 1, 87–108. doi: 10.3390/proteomes1020087.
189. Tinganelli, W., and Durante, M. (2020). Tumor hypoxia and circulating tumor cells. *Int J Mol Sci* 21, 1–15. doi: 10.3390/ijms21249592.
190. Tinganelli, W., Durante, M., Hirayama, R., Krämer, M., Maier, A., Kraft-Weyrather, W., Furusawa Y., Friedrich T., Scifoni E. (2015). Kill-painting of hypoxic tumours in charged particle therapy. *Sci Rep* 5. doi: 10.1038/srep17016.
191. Tinganelli W, Weber U, Puspitasari A, Simoniello P, Abdollahi A, Oppermann J, Schuy C, Horst F, Helm A, Fournier C, Durante M. (2022). FLASH with carbon ions: Tumor control, normal tissue sparing, and distal metastasis in a mouse osteosarcoma model. *Radiother Oncol*. 2022 Oct;175:185-190. doi: 10.1016/j.radonc.2022.05.003. Epub 2022 May 7. PMID: 35537606.
192. Todd, V. M., and Johnson, R. W. (2020). Hypoxia in bone metastasis and osteolysis. *Cancer Lett* 489, 144–154. doi: 10.1016/j.canlet.2020.06.004.
193. Torgovnick, A., and Schumacher, B. (2015). DNA repair mechanisms in cancer development and therapy. *Front Genet* 6. doi: 10.3389/fgene.2015.00157.
194. Türkoğlu A., Sümeyye & Kockar, Feray. (2012). Expression Of Gapdh, B-Actin And B-2-Microglobulin Genes Under Chemically Induced Hypoxic Conditions In Hep3b And Pc3 Cells. *Journal of Applied Biological Sciences*.
195. Valery, P. C., Laversanne, M., and Bray, F. (2015). Bone cancer incidence by morphological subtype: a global assessment. *Cancer Causes and Control* 26, 1127–1139. doi: 10.1007/s10552-015-0607-3.

196. Van Assendefft, O. W., Meek, G. A., and Zijlstra, W. G. (1973) International System of Units (SI) in Physiology.
197. Van Der Toom, E. E., Verdone, J. E., Gorin, M. A., and Pienta, K. J. (2016). Technical challenges in the isolation and analysis of circulating tumor cells. Available at: www.impactjournals.com/oncotarget.
198. Vito, A., El-Sayes, N., and Mossman, K. (2020). Hypoxia-Driven Immune Escape in the Tumor Microenvironment. *Cells* 9. doi: 10.3390/cells9040992.
199. Walcher, L., Kistenmacher, A. K., Suo, H., Kitte, R., Dluczek, S., Strauß, A., Blandszun AR., Yevsa T., Fricke S., Klossatz-Boehlert U. (2020). Cancer Stem Cells—Origins and Biomarkers: Perspectives for Targeted Personalized Therapies. *Front Immunol* 11. doi: 10.3389/fimmu.2020.01280.
200. Wang, H., Jiang, H., Van De Gucht, M., and De Ridder, M. (2019). Hypoxic radioresistance: Can ROS be the key to overcome it? *Cancers (Basel)* 11. doi: 10.3390/cancers11010112.
201. Wang, L., Zuo, X., Xie, K., and Wei, D. (2018). “The role of CD44 and cancer stem cells,” in *Methods in Molecular Biology* (Humana Press Inc.), 31–42. doi: 10.1007/978-1-4939-7401-6_3.
202. Wang, W. C., Zhang, X. F., Peng, J., Li, X. F., Wang, A. L., Bie, Y. Q., Shi LH., Lin MB., Zhang XF. (2018). Survival mechanisms and influence factors of circulating tumor cells. *Biomed Res Int* 2018. doi: 10.1155/2018/6304701.
203. Wang YN, Zeng ZL, Lu J, Wang Y, Liu ZX, He MM, Zhao Q, Wang ZX, Li T, Lu YX, Wu QN, Yu K, Wang F, Pu HY, Li B, Jia WH, Shi M, Xie D, Kang TB, Huang P, Ju HQ, Xu RH.(2018). CPT1A-mediated fatty acid oxidation promotes colorectal cancer cell metastasis by inhibiting anoikis. *Oncogene*. 2018 Nov;37(46):6025-6040. doi: 10.1038/s41388-018-0384-z. Epub 2018 Jul 11. PMID: 29995871.
204. Wardman, P. (2009). The importance of radiation chemistry to radiation and free radical biology (the 2008 silvanus thompson memorial lecture). *British Journal of Radiology* 82, 89–104. doi: 10.1259/bjr/60186130.

205. Wiechec, E., Matic, N., Ali, A., and Roberg, K. (2022). Hypoxia induces radioresistance, epithelial-mesenchymal transition, cancer stem cell-like phenotype and changes in genes possessing multiple biological functions in head and neck squamous cell carcinoma. *Oncol Rep* 47. doi: 10.3892/or.2022.8269.
206. Wirtz, D., Konstantopoulos, K., and Searson, P. C. (2011). The physics of cancer: The role of physical interactions and mechanical forces in metastasis. *Nat Rev Cancer* 11, 512–522. doi: 10.1038/nrc3080.
207. Wozny AS, Gauthier A, Alphonse G, Malésys C, Varoclier V, Beuve M, Brichart-Vernos D, Magné N, Vial N, Ardail D, Nakajima T, Rodriguez-Lafrasse C. (2021). Involvement of HIF-1 α in the Detection, Signaling, and Repair of DNA Double-Strand Breaks after Photon and Carbon-Ion Irradiation. *Cancers (Basel)*. 2021 Jul 30;13(15):3833. doi: 10.3390/cancers13153833.
208. Wu, Q., You, L., Nepovimova, E., Heger, Z., Wu, W., Kuca, K., Adam V. (2022). Hypoxia-inducible factors: master regulators of hypoxic tumor immune escape. *J Hematol Oncol* 15. doi: 10.1186/s13045-022-01292-6.
209. Xu, W., Yang, Z., and Lu, N. (2015). A new role for the PI3K/Akt signaling pathway in the epithelial-mesenchymal transition. *Cell Adh Migr* 9, 317–324. doi: 10.1080/19336918.2015.1016686.
210. Yang, C., Tian, Y., Zhao, F., Chen, Z., Su, P., Li, Y., Qian A.. (2020). Bone microenvironment and osteosarcoma metastasis. *Int J Mol Sci* 21, 1–17. doi: 10.3390/ijms21196985.
211. Yang J, Antin P, Berx G, Blanpain C, Brabletz T, Bronner M, Campbell K, Cano A, Casanova J, Christofori G, Dedhar S, Derynck R, Ford HL, Fuxe J, García de Herreros A, Goodall GJ, Hadjantonakis AK, Huang RYJ, Kalchauer C, Kalluri R, Kang Y, Khew-Goodall Y, Levine H, Liu J, Longmore GD, Mani SA, Massagué J, Mayor R, McClay D, Mostov KE, Newgreen DF, Nieto MA, Puisieux A, Runyan R, Savagner P, Stanger B, Stemmler MP, Takahashi Y, Takeichi M, Theveneau E, Thiery JP, Thompson EW, Weinberg RA, Williams ED, Xing J, Zhou BP, Sheng G. (2020). Guidelines and definitions for research on epithelial-mesenchymal transition. *Nat Rev Mol Cell Biol*.

2020 Jun;21(6):341-352. doi: 10.1038/s41580-020-0237-9. Epub 2020 Apr 16. Erratum in: *Nat Rev Mol Cell Biol.* 2021 Dec;22(12):834. PMID: 32300252; PMCID: PMC7250738.

212.

213. Yang, M. H., Imrali, A., and Heeschen, C. (2015). Circulating cancer stem cells: The importance to select. *Chinese Journal of Cancer Research* 27, 437–449. doi: 10.3978/j.issn.1000-9604.2015.04.08.

214. Yoon, C., Lu, J., Yi, B. C., Chang, K. K., Simon, M. C., Ryeom, S., Yoon SS. (2021). PI3K/Akt pathway and Nanog maintain cancer stem cells in sarcomas. *Oncogenesis* 10. doi: 10.1038/s41389-020-00300-z.

215. Yu, Z., Pestell, T. G., Lisanti, M. P., and Pestell, R. G. (2012). Cancer stem cells. *International Journal of Biochemistry and Cell Biology* 44, 2144–2151. doi: 10.1016/j.biocel.2012.08.022.

216. Yuan, Y., Ye, H. Q., and Ren, Q. C. (2018). Proliferative role of BDNF/TrkB signaling is associated with anoikis resistance in cervical cancer. *Oncol Rep* 40, 621–634. doi: 10.3892/or.2018.6515.

217. Yuan, Y., Ye, H. Q., and Ren, Q. C. (2018). Upregulation of the BDNF/TrkB pathway promotes epithelial-mesenchymal transition, as well as the migration and invasion of cervical cancer. *Int J Oncol* 52, 461–472. doi: 10.3892/ijo.2017.4230.

218. Yun, Z., and Lin, Q. (2014). Hypoxia and regulation of cancer cell stemness. in *Advances in Experimental Medicine and Biology* (Springer New York LLC), 41–53. doi: 10.1007/978-1-4614-5915-6_2.

219. Zhang, G., Zhang, K., Zhao, Y., Yang, Q., and Lv, X. (2022). A novel stemness-hypoxia-related signature for prognostic stratification and immunotherapy response in hepatocellular carcinoma. *BMC Cancer* 22. doi: 10.1186/s12885-022-10195-1.

220. Zhang, H., Lu, H., Xiang, L., Bullen, J. W., Zhang, C., Samanta, D., Gilkes DM., He J., Semenza GL. (2015). HIF-1 regulates CD47 expression in breast cancer cells to promote evasion of

phagocytosis and maintenance of cancer stem cells. *Proc Natl Acad Sci U S A* 112, E6215–E6223. doi: 10.1073/pnas.1520032112.

221. Zhang, Q., Han, Z., Zhu, Y., Chen, J., and Li, W. (2021). Role of hypoxia inducible factor-1 in cancer stem cells (Review). *Mol Med Rep* 23. doi: 10.3892/mmr.2020.11655.

222. Zhang, Q., Lou, Y., Zhang, J., Fu, Q., Wei, T., Sun, X., Chen Q., Yang J., Bai X., Liang T. (2017). Hypoxia-inducible factor-2 α promotes tumor progression and has crosstalk with Wnt/ β -catenin signaling in pancreatic cancer. *Mol Cancer* 16. doi: 10.1186/s12943-017-0689-5.

223. Zhao, Y., Peng, J., Zhang, E., Jiang, N., Li, J., Zhang, Q., Zhang X., Niu Y. (2016). CD133 expression may be useful as a prognostic indicator in colorectal cancer, a tool for optimizing therapy and supportive evidence for the cancer stem cell hypothesis: a meta-analysis. Available at: www.impactjournals.com/oncotarget.

224. Zhao L, Song J, Sun Y, Ju Q, Mu H, Dong X, Ding J, Liu Y, Wang X, Sun L, Wu J, Jiao Y, Lu S, Zhao X. (2023). Tumor-derived proliferative CTCs and CTC clusters predict aggressiveness and early recurrence in hepatocellular carcinoma patients. *Cancer Med*. 2023 Jul;12(13):13912-13927. doi: 10.1002/cam4.5946. Epub 2023 Jun 19. PMID: 37337648; PMCID: PMC10358265.

225. Ziesenis, A. (2014). Hypoxia and the modulation of the actin cytoskeleton. *Hypoxia*, 11. doi: 10.2147/hp.s53575.

226. Zijl F, Krupitza G, Mikulits W. (2011). Initial steps of metastasis: cell invasion and endothelial transmigration. *Mutat Res*. 2011 Jul-Oct;728(1-2):23-34. doi: 10.1016/j.mrrev.2011.05.002. Epub 2011 May 12. PMID: 21605699; PMCID: PMC4028085.

Curriculum Vitae

Personal Data

Name Martina Quartieri
Address Schöffersstraße 2, 64295, Darmstadt
Date of birth 30.05.1993
Place of birth La Spezia
Nationality Italian

Education and Work Experience

2007-2012 High School in Classical Studies
07.07.2012 High School Diploma
2012-2016 Bachelor studies in Biotechnology at University of Pisa, Italy
18.07.2016 Bachelor Degree In Biotechnology, University of Pisa, Italy
2016-2018 Master studies in Cellular and Molecular Biotechnology, University of Trento, Italy
19.12.2018 Master Degree in Cellular and Molecular Biotechnology, Cancer Biology curriculum, University of Trento, Italy
02.2019-07.2019 Post-graduation Internship with Erasmus+, University of Nottingham, United Kingdom
Since 10.2019 Ph.D studies in biology at GSI Helmholtzzentrum für Schwerionenforschung, Darmstadt, and Technische Universität Darmstadt
Supervisor: Prof. Dr. Marco Durante

Acknowledgements

This PhD study has been performed at the biophysics department of GSI Helmholtzzentrum für Schwerionenforschung in Darmstadt, Germany and Technische Universität Darmstadt from October 2019 until April 2023. The work was supported by the graduate school HGS-HIRE.

First of all, I would like to thank Prof. Marco Durante for giving me the opportunity to perform my PhD thesis in the Biophysics department under his supervision.

I cordially thank Prof. Gerhard Thiel, my second supervisor from the TUD, for his availability and support and advices during the PhD meetings.

A very special thanks goes to Dr. Walter Tinganelli, Dr. Anggraeini Puspitasari, Dr. Olga Sokol from the Clinical Radiobiology group, for the stimulating discussions, the help and the support during the entire course of my PhD studies, and to Dr. Charlot Vandevoorde for the advices and help in particular during my final period at GSI.

I would like to thank Julius for the support, the help in the lab, and for being my office mate throughout these years, and Tamara for helping me during the experiments and for being one of the best lab colleagues I've ever had.

Thanks to Cristina, my 'little sister', for the support over the years and for always believing in me and in my potentials, for the laughs, the continuous support even in the most difficult moments, and for making me feel at home even if I am far away.

Thanks to Chiara, for the moments of freaking out together, for laughing even in times of work despair, for always believing in me and supporting me, for our evening talks and for always making me see things from a different perspective.

Thanks to Francesca, for the constant listening, support and backing, for the evenings full of laughs, the fantastic parties at her house, for the lasagne evening and the insect dinner, which is actually the moment when we first met.

Cristina, Chiara and Francesca, my 'banane', thank you for all the amazing evenings together, thank you for teaching me that everything can be overcome, even the most difficult moments, and for making me feel at home even though I am miles away.

Thanks to Gaia, the purest and simplest person I have ever met. Thank you for always listening and supporting me during these months, for the smiles and for making me feel like in a 'bubble', far away from thoughts and worries, every time I talk to you.

A special thanks to my friends Federica and Carlo, for all the parties, dinners and evenings that we spent together, for all the talks, the laughs and the Moscow Mules. You also are part of my family here, and you made my days happier and lighter all the times.

Thanks to all of my friends from GSI, Cosimo, Daria, Enrico, Niccolò, Gianmarco, Laura, Moritz, Timino, Warisara, Ha, Amelia, for all the coffee breaks, the evenings together and the laughs throughout these years. GSI would be very much different without you all.

Thanks to Chiara, Nicole and Arianna, my ‘far away’ friends from Italy, on whose support I could always count.

Lastly, I would like to express my enormous gratitude to my family, especially my parents. Without your support I would not have been able to study or do my doctorate. Thank you with all my heart!

Ehrenwörtliche Erklärung

Ich erkläre hiermit, dass ich die vorliegende Arbeit entsprechend den Regeln guter wissenschaftlicher Praxis selbstständig und ohne unzulässige Hilfe Dritter angefertigt habe. Sämtliche aus fremden Quellen direkt oder indirekt übernommenen Gedanken sowie sämtliche von Anderen direkt oder indirekt übernommenen Daten, Techniken und Materialien sind als solche kenntlich gemacht. Die Arbeit wurde bisher bei keiner anderen Hochschule zu Prüfungszwecken eingereicht. Die eingereichte elektronische Version stimmt mit der schriftlichen Version überein.

Darmstadt, den 15.09.2023